AD-A174 907 THREE-DIMENSIONAL FINITE ELEMENT ANALYSIS OF A SLAB ON STRESS DEPENDENT E..(U) ILLINOIS UNIV AT URBANA DEPT OF CIVIL ENGINEERING A M IOANNIDES ET AL. 31 OCT 86 1/3

UNCLASSIFIED AFOSR-TR-86-2108 AFOSR-82-0143 F/G 13/13 NL

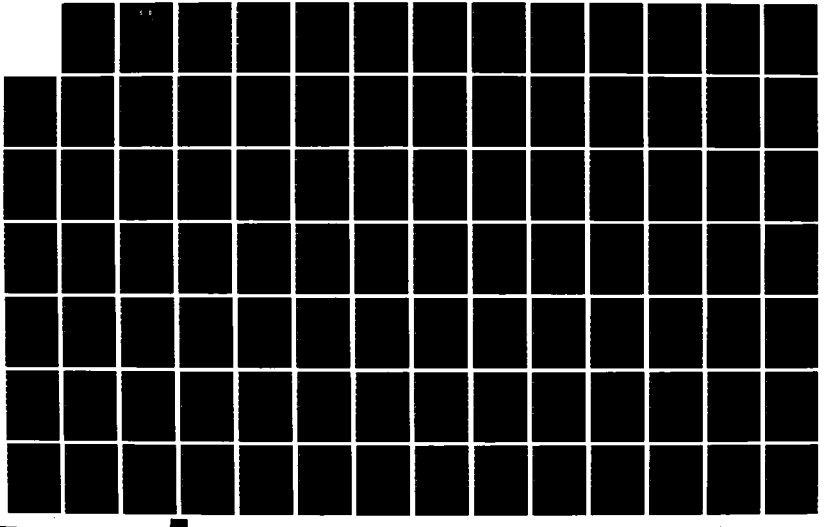

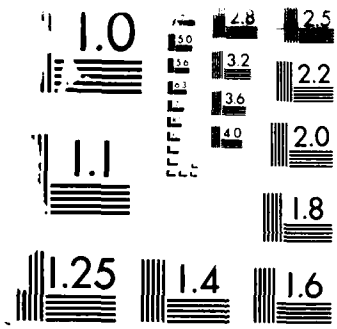
1.0
1.1
1.25
1.4
1.6
1.8
2.0
2.2
2.5
2.8
3.2
3.6
4.0

AFOSR-TR- 86-2108

THREE-DIMENSIONAL FINITE ELEMENT ANALYSIS OF A SLAB ON STRESS DEPENDENT ELASTIC SOLID FOUNDATION

Submitted to

Air Force Office of Scientific Research (AFOSR)
Air Force Systems Command
United States Air Force
Bolling AFB, DC 20332

by

TRANSPORTATION RESEARCH LABORATORY
DEPARTMENT OF CIVIL ENGINEERING
ENGINEERING EXPERIMENT STATION
UNIVERSITY OF ILLINOIS AT URBANA-CHAMPAIGN

Report Preparation by

Dr. A. M. Ioannides
Dr. M. R. Thompson
J. Donnelly
Dr. E. J. Barenberg

Program Manager:

Lt. Col. L. D. Hokanson

UNIVERSITY OF ILLINOIS
URBANA, ILLINOIS

OCTOBER, 1986

UNCLASSIFIED

SECURITY CLASSIFICATION OF THIS PAGE

REPORT DOCUMENTATION PAGE

1a REPORT SECURITY CLASSIFICATION: UNCLASSIFIED A174987	1b RESTRICTIVE MARKINGS
2a SECURITY CLASSIFICATION AUTHORITY	3 DISTRIBUTION/AVAILABILITY OF REPORT: Approved for Public Release; Distribution Unlimited.
2b DECLASSIFICATION/DOWNGRADING SCHEDULE	
4 PERFORMING ORGANIZATION REPORT NUMBER(S)	5. MONITORING ORGANIZATION REPORT NUMBER(S): AFOSR-TR- 86-2108
6a NAME OF PERFORMING ORGANIZATION: UNIVERSITY OF ILLINOIS AT URBANA-CHAMPAIGN; 6b. OFFICE SYMBOL (If applicable)	7a NAME OF MONITORING ORGANIZATION: AFOSR
6c. ADDRESS (City, State and ZIP Code): DEPARTMENT OF CIVIL ENGINEERING, URBANA, IL 61801	7b. ADDRESS (City, State and ZIP Code): Bld 410, BAFB D.C. 20332
8a. NAME OF FUNDING/SPONSORING ORGANIZATION AIR FORCE OFFICE OF SCIENTIFIC RESEARCH; 8b. OFFICE SYMBOL (If applicable) AFOSR/NA	9. PROCUREMENT INSTRUMENT IDENTIFICATION NUMBER: AFSOR-82-0143
8c. ADDRESS (City, State and ZIP Code): BOLLING AFB, DC 20332, Bld 410	10 SOURCE OF FUNDING NOS: PROGRAM ELEMENT NO. 61102F; PROJECT NO. 2307; TASK NO. C1; WORK UNIT NO.
11. TITLE (Include Security Classification): THREE-DIMENSIONAL FINITE ELEMENT ANALYSIS OF A-SLAB ON STRESS DEPENDENT ELASTIC SOLID FOUNDATION	
12. PERSONAL AUTHOR(S): IOANNIDES, A. M., DONNELLY, J., THOMPSON, M. R., BARENBERG, E. J.	
13a. TYPE OF REPORT: FINAL; 13b. TIME COVERED: FROM 21 Aug 84 TO 20 June 86	14. DATE OF REPORT (Yr., Mo., Day): 1986, October 31; 15. PAGE COUNT: 198
16. SUPPLEMENTARY NOTATION	

17. COSATI CODES		
FIELD	GROUP	SUB GR.

18. SUBJECT TERMS (Continue on reverse if necessary and identify by block number)

PAVEMENTS; PAVEMENT ANALYSIS; SLAB MODEL; SUBGRADE SUPPORT; FINITE ELEMENT SLAB MODEL; THREE-DIMENSIONAL ANALYSIS

19. ABSTRACT (Continue on reverse if necessary and identify by block number)

Research described in this Report comprises the final stage of a multi-component project, which examined current computerized analysis techniques for slabs-on-grade. The focus of investigations presented is the application of the three-dimensional finite element program GEOSYS for the analysis of a slab, resting on a stress dependent elastic solid foundation. This model can be used to establish baseline structural response data, representative of complex boundary and support conditions, thereby validating conclusions reached on the basis of two-dimensional analysis.

In the first part of the study, many computer runs were conducted to develop user guidelines for the fruitful utilization of the three-dimensional approach. Effects considered include mesh fineness and gradation, subgrade extent, boundary conditions, etc.

The three fundamental loading conditions, viz. interior, edge and corner, are examined in the second part of the Report. Two typical single- and multi-wheel U.S. Air Force aircraft are

(Continued)

20. DISTRIBUTION/AVAILABILITY OF ABSTRACT: UNCLASSIFIED/UNLIMITED ☒ SAME AS RPT. ☐ DTIC USERS ☐	21. ABSTRACT SECURITY CLASSIFICATION: UNCLASSIFIED
22a NAME OF RESPONSIBLE INDIVIDUAL: Lt. Col. Lawrence D. Hokanson	22b TELEPHONE NUMBER (Include Area Code): 202/767-4935; 22c. OFFICE SYMBOL: AFOSR/NA

DD FORM 1473, 83 APR EDITION OF 1 JAN 73 IS OBSOLETE UNCLASSIFIED

19. Continued

employed (F-15 and C-141). An iterative scheme is introduced to account for subgrade stress dependence. The effect of stress softening, typical of cohesive soils, is evaluated and discussed.

In addition, a number of interesting observations are made, and their bearing on current analysis and design approaches is considered. Two broad areas for future research are identified. The relevance and need of the GEOSYS model to future pavement research/development activities is established.

ACKNOWLEDGMENTS

This Report was prepared as part of a Project entitled, "VALIDATION OF A STRESS-DEPENDENT FINITE ELEMENT SLAB MODEL". The Project is sponsored (Grant No. AFOSR-82-0143) by the Air Force Office of Scientific Research (AFOSR), Air Force Systems Command, Bolling AFB, DC. Lt. Col. Lawrence D. Hokanson is the Program Manager.

DISCLAIMER

The contents of this Report reflect the views of the authors who are responsible for the facts and the accuracy of the data presented herein. The contents do not necessarily reflect the official views or policies of the U.S. Air Force. This Report does not constitute a standard, specification, or regulation.

(The reverse of this page is blank)

TABLE OF CONTENTS

CHAPTER Page

CHAPTER Page

LIST OF TABLES

LIST OF FIGURES

LIST OF SYMBOLS

a : radius of circular loaded area

2a : short side of finite element (plan view)

2b : long side of finite element (plan view)

c : side length of square loaded area

D : slab flexural stiffness [$= Eh^3/12(1 - \mu^2)$]

E : Young's modulus of slab

E_s : Young's modulus of elastic solid foundation

E_R : resilient modulus of foundation

E_R^* : average E_R for subgrade group

G_s : shear modulus of elastic solid foundation [$= E_s/2(1+\mu_s)$]

h : slab thickness

h_i : shape function for brick element

k : modulus of subgrade reaction (dense liquid foundation)

K_R : resilient modulus of subgrade reaction (stress dependent, resilient subgrade)

L : side length of square slab

ℓ : radius of relative stiffness for dense liquid foundation [$= \sqrt[4]{(D/k)}$]

ℓ_e : radius of relative stiffness for elastic solid foundation [$= \sqrt[3]{((1-\mu_s)D/G_s)}$]

NEL : number of elements belonging to a subgrade group

NCHNG : number of elements changing subgrade groups

NLAYER : number of slab layers

NLOWER : number of layers in upper subgrade portion

NMIDDLE : number of layers in middle subgrade portion

NUMEL : number of slab elements (plan view)

NUMELX : number of subgrade element columns (plan view)

NUMELZ : number of subgrade layers (cross-section)

NUPPER : number of layers in upper subgrade portion

P : applied load (force)

p : applied uniform pressure

q : (maximum value of) vertical subgrade pressure

q^*_c : surface subgrade stress under center of corner load

r : radial distance

u : generalized nodal displacement for brick element

X : subgrade lateral extent beyond slab edges

X_a : subgrade lateral extent beyond slab edges, adjacent to loaded edge

x : horizontal Cartesian coordinate

y : horizontal Cartesian coordinate

Z : total subgrade depth assumed in finite element model

z : vertical Cartesian coordinate

z_{cvs} : constant vertical strain depth

α : finite element aspect ratio (plan view) [= 2a/2b]

α_{ni} : coefficients of incompatible displacement functions

Δ : spacing in finite difference grid

Δ^*E_R : average change in E_R for elements changing subgrade groups

δ : (maximum value of) vertical deflection

ε : strain

ε_r : recoverable strain

ε_{cvs} : constant vertical strain

ζ : local orthogonal coordinate

η : local orthogonal coordinate

μ : Poisson's ratio for slab

μ_s : Poisson's ratio for elastic solid

ξ : local orthogonal coordinate

σ : (maximum value of) slab bending stress

σ_D : subgrade repeated deviator stress

σ_D^* : average σ_D for subgrade group

σ_1 : major principal stress

τ : shear stress

χ : mesh gradation (ratio of distance over which the mesh is fine and consists of square elements to size of the loaded area, c)

Subscripts

c : pertaining to corner loading

e : pertaining to edge loading

i : pertaining to interior loading

max : maximum value of

min : minimum value of

CHAPTER 1

INTRODUCTION

1.1 PROBLEM STATEMENT

Ever since the publication of Westergaard's pioneering works in the 1920's [1], the problem of slabs-on-grade has been investigated by pavement and other engineers, as one involving a plate on elastic foundation. In a recent Report for the U.S. Air Force Office of Scientific Research (AFOSR) [2], an exhaustive examination was presented of existing and/or potential tools that may be applied to the analysis of slab-on-grade pavement systems, within the context of two-dimensional plate theory. Several computer codes were developed, improved or expanded to analyze such pavement systems, using any of the commonly employed subgrade models, viz. the dense liquid (Winkler [3]), the elastic solid (Boussinesq [4]), and the two-parameter (Vlasov [5]) foundations, for any of the three fundamental loading conditions: interior, edge or corner [6; 7; 8; 9]. Furthermore, existing closed-form solutions for the same problem were collected and their accurate form was conclusively established [10].

Findings and results from earlier research clearly indicated that no current procedure can model fully the behavior of a slab of finite size, supported by a stress dependent fine-grained subgrade, extending beyond the slab edges. Consequently, it is sometimes difficult to establish

the accuracy and adequacy of two-dimensional slab-on-grade models, routinely used in engineering practice.

This Report describes the final stage of a multi-component project, which examined current computerized analysis techniques for slabs-on-grade. To conclude the investigations, an existing three-dimensional finite element model was adopted to provide a more realistic representation of the slab-on-grade problem. The model can be used to establish baseline structural response data, representative of complex slab boundary and foundation support conditions, thereby validating and reinforcing conclusions drawn on the basis of two-dimensional analysis. A brief account of the major accomplishments of earlier research under this Project is presented below.

1.2 PREVIOUS RESEARCH ACCOMPLISHMENTS

Research conducted under Grant No. AFOSR-82-0143 has been concerned primarily with analytical and numerical procedures applied to rigid pavements, treated as a plate on an elastic foundation. The major goal of this study has been to explore all existing or potential tools that may be applied to the analysis of slab-on-grade pavement systems. Within the context of two-dimensional plate theory, this was achieved to a large extent with the publication of AFOSR Report No. TR-85-0083 [2].

There are, in general, two methods of modeling subgrade support in a pavement system: the dense liquid (Winkler [3]), or the elastic solid (Boussinesq [4]). The initial thrust of the investigations was

collecting, evaluating and improving available methods of analysis involving both these models. Beginning with Westergaard's ground-breaking work in the 1920's [1], the technical literature contains several important contributions in this field which have remained largely unappreciated or even forgotten. Some have even been misquoted or misapplied in subsequent publications, while others, plagued by the complexity of mathematical vigor, never became popular with engineers. The automated digital computer has now replaced the slide-rule, and offers a unique possibility of taking full advantage of the work of such respectable investigators as Pickett, Ray, Bergstrom, Losberg, etc. Mathematical calculations of prohibitive volume a few decades ago, now become a routine exercise -- with much improved accuracy, too.

In the first year of this study, existing analyses employing the dense liquid foundation were examined. This included an exhaustive re-examination of Westergaard's work, which revealed the following [10]:

(i) Several equations ascribed to Westergaard in the literature are erroneous, usually through a series of typographical errors or misapplications. The correct form of these equations and their limitations have now been conclusively established.

(ii) Westergaard's original (1926) equation for the edge stress [1] is incorrect. The long ignored equation given in his 1948 paper [11] should be used instead.

(iii) An improved expression for the corner stress has been developed.

The Finite Element Method (F.E.M.) as applied to a plate on a Winkler subgrade was reviewed, and a number of recommendations for its proper use were formulated. The major single product of this effort is the revised and expanded version of ILLI-SLAB [6], a general description of which is given in section 1.3, below. This computer program has been found to be a versatile, user friendly, multi-purpose and accurate tool, if used correctly. Several modifications made during this study have enhanced its easy and error-free application, as well as the appreciation of its results.

To account for the stress dependent behavior of soils and their increased stiffness rapidly moving loads, the concept of the Resilient Modulus of Subgrade Reaction, K_R, was developed [12; 13]. Algorithms relating K_R and the level of vertical deflection, w, were established for four broad categories of cohesive soils. These have been incorporated into ILLI-SLAB through an iterative scheme: at the end of each iteration, nodal deflections are checked and the values of K_R updated, if necessary, to retain compatibility between modulus and deflection, as prescribed by the algorithms developed [14].

Work during the second year of this study, focused on elastic solid analyses of the same problem. This was dictated by the need to investigate further the following two effects:

(i) The effect of pavement system characteristics, as expressed by the radius of relative stiffness, on the relation between deflection and subgrade stress, i.e. the extent to which, if at all, the subgrade modulus, k, is an intrinsic soil property.

(ii) Load placement effects, i.e. interior, edge or corner loading conditions.

The investigation of the problem of a plate on an elastic solid foundation conducted is, perhaps, the most exhaustive to date. Computer programs have been developed during this research for considering the problem using four different approaches. Independent verification and mutual reinforcement of each program's results is, therefore, feasible. Each of these programs is particularly suitable for a given set of applications, and between them they cover most practical possibilities.

Since closed-form solutions for the response of an infinite plate on an elastic solid foundation have only been available for interior loading, programs developed have been used to derive similar predictive expressions for the edge and corner load conditions. Thus, Pickett's chart for the edge stress in a slab on an elastic solid foundation was re-calculated using computerized numerical integration [8]. The result was incorporated into an expanded version of H51, a program for the determination of the edge stress under multi-wheel loads. The new version is called H51ES and includes the elastic solid foundation option, while originally only the dense liquid subgrade was available. This exercise also provided a chance to re-examine the basic assumptions, limitations and applicability of such charts.

In addition, three other formulations were developed for the analysis of a finite-sized plate resting on an elastic solid foundation:

(i) A method based on the concept of "concordant deflections" for axisymmetric, circular plates (computer program CFES) [7].

(ii) A finite difference approach for rectangular plates (computer program FIDIES) [9].

(iii) A finite element solution for rectangular plates (computer program ILLI-SLAB - BOUSSINESQ option) [6].

Both (ii) and (iii) can handle any number of loads at any location. Comparative analyses conducted established the limits of applicability of these methods, following which load placement effects were evaluated.

An additional subgrade formulation was derived for the finite element analysis of a plate resting on a two-parameter Vlasov foundation [5]. This has also been included in ILLI-SLAB, to bridge the gap between the dense liquid and elastic solid solutions [6]. Thus, ILLI-SLAB is currently the first and only computer code that allows these multiple foundation options. In view of its importance for research conducted, a more detailed description of this program is appropriate.

1.3 ILLI-SLAB

ILLI-SLAB was first developed at the University of Illinois in the late 1970's for structural analysis of jointed, one- or two-layer concrete pavements with load transfer systems at the joints [15]. The original ILLI-SLAB model is based on the classical theory of a medium-thick plate on a Winkler foundation [16], and can evaluate the structural response of a concrete pavement system with joints and/or cracks. It employs the 4-noded plate bending element (ACM or RPB12)

which has 3 degrees-of-freedom per node [17]. The Winkler type subgrade is modeled as a uniform, distributed subgrade through an equivalent mass formulation [18]. This is a more realistic representation than the four concentrated spring elements used in other programs. A work equivalent load vector is used [17].

Assumptions regarding the concrete slab, stabilized base, overlay, subgrade, dowel bar, keyway, and aggregate interlock applicable to the original (dense liquid) ILLI-SLAB model can be summarized briefly as follows:

(i) Small deformation theory of an elastic, homogeneous medium-thick plate is employed for the concrete slab, stabilized base and overlay. Such a plate is thick enough to carry transverse load by flexure, rather than in-plane force (as would be the case for a thin membrane), yet is not so thick that transverse shear deformation becomes important. In this theory, it is assumed that lines normal to the middle surface in the undeformed plate remain straight, unstretched and normal to the middle surface of the deformed plate; each lamina parallel to the middle surface is in a state of plane stress; and no axial or in-plane shear stress develops due to loading.

(ii) The subgrade behaves as a Winkler foundation.

(iii) In case of a bonded stabilized base or overlay, full strain compatibility exists at the interface; in the unbonded case, shear stresses at the interface are neglected.

(iv) Dowel bars at joints are linearly elastic, and are located at the neutral axis of the slab.

(v) When aggregate interlock or a keyway is used for load transfer, load is transferred from one slab to an adjacent slab by shear. With dowel bars, some moment as well as shear may be transferred across the joints.

Various types of load transfer systems, such as dowel bars, aggregate interlock, keyways, or a combination of these can be considered at pavement joints. The model can also accommodate the effect of a stabilized base or an overlay, either with perfect bond or no bond. Thus, ILLI-SLAB provides several options that can be used in analyzing the following problem types:

1. Jointed concrete pavements with load transfer systems.
2. Jointed reinforced concrete pavements with cracks having reinforcement steel.
3. Continuously reinforced concrete pavements.
4. Concrete shoulders with or without tie bars.
5. Pavement slabs with a stabilized base or overlay, assuming either perfect bond or no bond between the two layers.
6. Concrete slabs of varying thicknesses and moduli of elasticity, and subgrades with varying moduli of support.

The program inputs are:

(a) Geometry of the slab, including type of base or overlay, load transfer system, subgrade, and slab dimensions.

(b) Elastic properties of concrete, stabilized base or overlay, load transfer system, and subgrade.

(c) Loading.

The outputs given by the program are:

(a) Nodal stresses in the slab, and stabilized base or overlay.

(b) Vertical reactions at the subgrade surface.

(c) Nodal deflections and rotations.

(d) Reactions on the dowel bars.

(e) Shear stresses at the joint for aggregate interlock and keyed joint systems.

The model has been verified by comparison with available theoretical solutions and results from experimental studies [19; 20; 10; 12].

As mentioned earlier, the revised and expanded version of ILLI-SLAB [2; 6] incorporates the elastic solid, resilient subgrade and two-parameter foundation idealizations, in addition to the original Winkler formulation. Comparative analyses are greatly facilitated, and the whole spectrum of possible subgrade idealizations can be examined, from the entirely discontinuous dense liquid, to the totally continuous elastic solid. The efficient and fruitful utilization of ILLI-SLAB is ensured by adherence to guidelines established during several convergence studies.

Despite the wide applicability of ILLI-SLAB, it is highly desirable to develop a three-dimensional finite element model to represent the slab-on-grade problem in more detail. Several very important processes can be modeled adequately only when such a model is

employed. For example, the response of the slab and the subgrade to loading, temperature and moisture changes etc. ideally requires a three-dimensional model for accurate simulation. Furthermore, theoretical analyses involving three-dimensional models can be very useful, not only in the investigation of those aspects that simply cannot be handled by a two-dimensional approach, but also in providing helpful insight for the improvement and better interpretation of results from two-dimensional analyses. The selection of an existing three-dimensional finite element model for the purposes of this study is described below.

1.4 THREE-DIMENSIONAL COMPUTER PROGRAM CHOICE

The following features were considered necessary in selecting a three-dimensional finite element model for the analysis of a slab on an elastic solid foundation:

1. Ease of Application: The program must require a minimum amount of input data, thus eliminating potential user pitfalls. It is very frustrating to have such a sophisticated model, but be unable to use it effectively due to the length of data preparation time required.

2. Meaningful Output: The large amount of information generated by such a program must be presented in a way to facilitate interpretation. Methods proven very helpful with the two-dimensional models may be adapted for use here as well.

3. Flexibility: Although this requirement is tempered by the complexity of the numerical solution, the three-dimensional model envisaged should be capable of analyzing a pavement system consisting of a slab and base, supported by a uniform or multi-layered elastic solid foundation. Any number of loads should be allowed at any location on the slab.

4. Stress Dependence: Stress dependent subgrade moduli can be accommodated through an iterative process similar to that currently used in ILLI-PAVE [21]. Values of the deviator stress, σ_D , for each element should be checked for compatibility against the resilient modulus, E_R, versus deviator stress algorithms developed by Thompson and Robnett [22]. If necessary, element values of E_R should be updated and a new iteration performed, until the convergence criteria are satisfied.

5. Effective Machine Implementation: It is apparent from the authors' two-dimensional investigations, that accurate and meaningful results require a fairly fine finite element mesh, i.e. a large number of elements. This creates a severe problem with respect to computer storage, particularly in the case of the proposed three-dimensional model. Efficient memory core allocation, in- and out-of-core operations, use of virtual memory and other advanced techniques are absolutely essential. The primary objective is to increase the number of elements that can be accommodated, although this will inevitably prolong execution time. In this day of personal computer networks, the latter problem is becoming less important. As far as possible, the model developed should be adapted for implementation on such a network.

Two programs with three-dimensional analysis capabilities are currently available at the University of Illinois: FINITE [23] and GEOSYS [24]. Both are multipurpose programs, i.e. they include libraries of one-, two- and three-dimensional elements. FINITE is primarily designed as a tool for the structural engineer, while GEOSYS is geared more toward geotechnical problems. The structure of both these programs is highly advanced and their performance is excellent. Indeed, their data management systems, for example, are among the most efficient to date. The utilization of such techniques in slab-on-grade analysis would eliminate several problems now experienced with respect to computer storage requirements. Unfortunately, due to their general nature, neither program is practical for routine analysis of pavement slabs. The major problems are:

1. A tremendous quantity of input data is required, even for the simplest slab-on-grade three-dimensional analysis.
2. Execution times are prolonged. This translates to prohibitive costs when implemented on a main-frame system.

For the purpose of this study, the GEOSYS finite element program was selected, primarily because its smaller code was freely accessible. This allowed its installation on the HARRIS 800-2 virtual memory computer at the Department of Civil Engineering, University of Illinois, Urbana. Programs currently executing on this machine are allowed up to a total of 48 megabytes of virtual space. Although the HARRIS is considerably slower than a main-frame machine, e.g. the CDC-CYBER, project costs for the HARRIS are much lower. Furthermore, since the GEOSYS source code

was available, this could be modified to suit the needs of the present investigation. Thus, both of the deficiencies mentioned above could be addressed in a satisfactory manner. Since GEOSYS has been the major tool for this research, a more detailed description of it will be presented below. Emphasis will be placed on those features of the program used in this study, and the modifications introduced to facilitate its use for slab-on-grade analysis.

1.5 GEOSYS

GEOSYS was developed in the early 1970's by a group of engineers, members of the technical staff of Agbabian Associates, El Segundo, California [24]. Dr Jeremy Isenberg served as Principal Investigator. The project was sponsored by the Advanced Research Projects Agency (ARPA) of the U.S. Department of Defense and was monitored by the U.S. Bureau of Mines. Its objective was to combine a number of recent advances in finite element theory and computer technology into a computer program for analyzing rock-structure interaction. This program applies to general two- and three-dimensional problems and can accommodate time dependent loading, gravity loading, and staged excavation or construction, using a wide variety of material property characteristics. To reduce the time spent in input data preparation, sophisticated mesh generators and a bandwidth reducer are employed. Multibuffering techniques allow accessing peripheral storage units, thereby reducing computer run time for large, out-of-core problems. The

element library contains several element types, including beam, rod, plane quad, brick and shell elements.

GEOSYS has many features that are not required in a typical slab-on-grade problem. Therefore, to make it more efficient for this study's needs, unnecessary portions of the code have been removed. This eliminated all unused subroutines, with the exception of three error routines useful in debugging operations. The capabilities taken out include mesh plotting, gravity and time dependent loading, bandwidth reduction, inelastic and anisotropic materials, simulation of sequential excavation and construction, two-dimensional geometry, and all element types except for one.

For the purpose of this study, the linear, isoparametric, three-dimensional hexahedral brick element was retained. This has eight nodes with three degrees-of-freedom per node (the displacements in each of the x, y and z directions). The assumed displacement approximations for this element are shown in Fig. 1.1. The first eight are the standard compatible interpolation functions. The other three are incompatible and are associated with linear shear and normal strains. The nine incompatible modes are eliminated at the element stiffness level by static condensation.

The resulting version of GEOSYS used for slab-on-grade analysis consists of about 53% of the original code. Tests using this "slimmer" version indicate that execution times are reduced by about 30% compared to the original version. Taking advantage of the program's symmetry capability, reduces execution times further when considering interior or

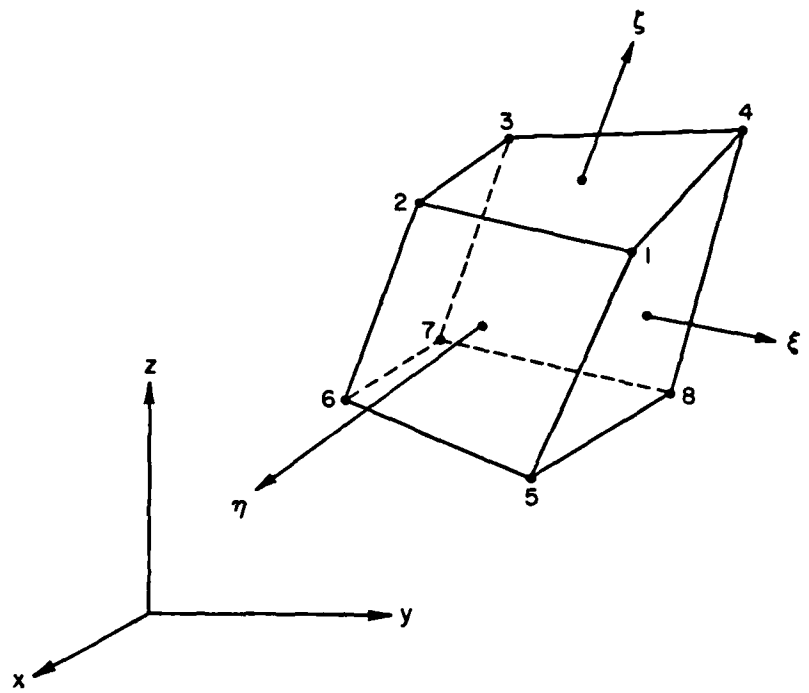

Assumed displacement approximations:

$$u_x = \sum_{i=1}^{8} h_i\, u_{xi} + h_9\, \alpha_{x1} + h_{10}\, \alpha_{x2} + h_{11}\, \alpha_{x3}$$

$$u_y = \sum_{i=1}^{8} h_i\, u_{yi} + h_9\, \alpha_{y1} + h_{10}\, \alpha_{y2} + h_{11}\, \alpha_{y3}$$

$$u_z = \sum_{i=1}^{8} h_i\, u_{zi} + h_9\, \alpha_{z1} + h_{10}\, \alpha_{z2} + h_{11}\, \alpha_{z3}$$

where:

$h_1 = 1/8\ (1+\xi)\ (1+\eta)\ (1+\zeta)$

$h_2 = 1/8\ (1-\xi)\ (1+\eta)\ (1+\zeta)$

$h_3 = 1/8\ (1-\xi)\ (1-\eta)\ (1+\zeta)$

$h_4 = 1/8\ (1+\xi)\ (1-\eta)\ (1+\zeta)$

$h_5 = 1/8\ (1+\xi)\ (1+\eta)\ (1-\zeta)$

$h_6 = 1/8\ (1-\xi)\ (1+\eta)\ (1-\zeta)$

$h_7 = 1/8\ (1-\xi)\ (1-\eta)\ (1-\zeta)$

$h_8 = 1/8\ (1+\xi)\ (1-\eta)\ (1-\zeta)$

$h_9 = (1-\xi^2)$

$h_{10} = (1-\eta^2)$

$h_{11} = (1-\zeta^2)$

Fig. 1.1 Linear, Three-Dimensional, Isoparametric Brick Element

edge loading. This permits using a finer mesh with correspondingly improved accuracy.

1.6 PRE- AND POST-PROCESSORS

A typical input file for GEOSYS consists of several hundred lines, each formatted according to a strict pattern. Since data for different slab-on-grade analysis runs are generally similar in structure, a pre-processor called "GEZIN" (GEOSYS Easy INput) was coded early in this study. This automatically prepares the data in the required format. Input for GEZIN includes fewer than 10 data cards, the format of which is similar to the one used for ILLI-SLAB [2]. Thus, mesh coordinates are only specified along the coordinate axes; loaded areas are prescribed in terms of the global (slab) coordinate system and are independent of the mesh used; work equivalent nodal loads are generated automatically from the applied distributed loads for the given mesh used; material properties are specified in terms of the more familiar Young's modulus and Poisson's ratio, rather than the bulk and shear moduli required by GEOSYS. This reduces data preparation to an almost trivial task and practically eliminates the possibility of errors during this stage.

Several post-processing programs were also coded during this investigation, to assist interpretation of computer results. These post-processors are used in conjunction with an iterative scheme introduced to account for the stress dependent behavior of typical fine-

grained soils. Thus, using calculated values of deviator stress in the foundation, material properties are updated for individual elements as required and a new input file is prepared. Additional execution cycles may then be initiated, until satisfactory closure is achieved. This iterative procedure is similar to that used for two-dimensional ILLI-SLAB analysis [12; 14]. User intervention between consecutive GEOSYS iterations is, therefore, unnecessary. Execution of the program is a fully automated process controlled by the user through the editing of a simple procedure file. Another program, called "COMPARE", may be used to perform a statistical analysis, comparing results from successive GEOSYS cycles. This enables the user to monitor the changes in system response, produced by the introduction of a stress dependent subgrade.

1.7 REPORT ORGANIZATION

Research reported herein focusses on the application of the three-dimensional finite element program GEOSYS [24] to the solution of the slab-on-grade problem. Studies conducted can be divided into two major parts:

(a) Preliminary mesh investigations, described in Chapter 2; and

(b) Examination of the three fundamental loading conditions, viz. interior, edge and corner. These are discussed in Chapters 3, 4 and 5.

Results from a total of 108 three-dimensional finite element runs are presented and interpreted in Chapter 2. An index of these runs is

given in the Appendix. Guidelines for the fruitful utilization of the GEOSYS model are developed to account for such effects as the sensitivity of the model to mesh fineness and gradation, subgrade extent, boundary conditions, etc. The requirement for a fairly large computer memory core is reiterated through numerous convergence studies.

In the runs described in Chapters 3, 4 and 5, typical single- and multi-wheel U.S. Air Force aircraft are employed (F-15 and C-141). An iterative scheme is introduced to account for subgrade stress dependence. The effect of stress softening, typical of cohesive soils, is evaluated and discussed.

In the final Chapter, a summary of the main conclusions reached and guidelines established is provided. In addition, a number of interesting observations are made, and their bearing on current analysis and design approaches is considered. Two broad areas for future research are identified, and the relevance of the GEOSYS model in these and other directions is illustrated.

CHAPTER 2

PRELIMINARY MESH INVESTIGATIONS

2.1 SCOPE OF STUDIES

The problem of a slab-on-grade may be investigated in three-dimensions using a finite element mesh similar to the one shown in Fig. 2.1. In this Figure, the slab is resting on a cube of soil, carved out of the Boussinesq half-space and maintained intact by the assumption of boundary conditions on the four vertical sides and on the base. The implication is that if these boundaries are far enough from the critical locations of response, they will have no effect on the behavior of the system. It is, therefore, necessary to determine at the beginning, the required lateral and vertical extents of the subgrade, dictated by each of the available boundary condition choices.

In addition, two-dimensional studies have shown that finite element results may not be very useful unless due consideration is given to the effect of mesh fineness and gradation, as well as element aspect ratios [2; 6]. Within the slab, these attributes can be quantified using several simple ratios. Thus, mesh fineness may be expressed in terms of (2a/h), where 2a is the side length of a square element (or of the plan view of a brick element), and h is the slab thickness; gradation, χ, can be defined as the ratio of the distance over which the mesh is fine and consists of square elements to the side length, c, of the applied (square) load; and finally, element aspect ratio may be denoted by α and

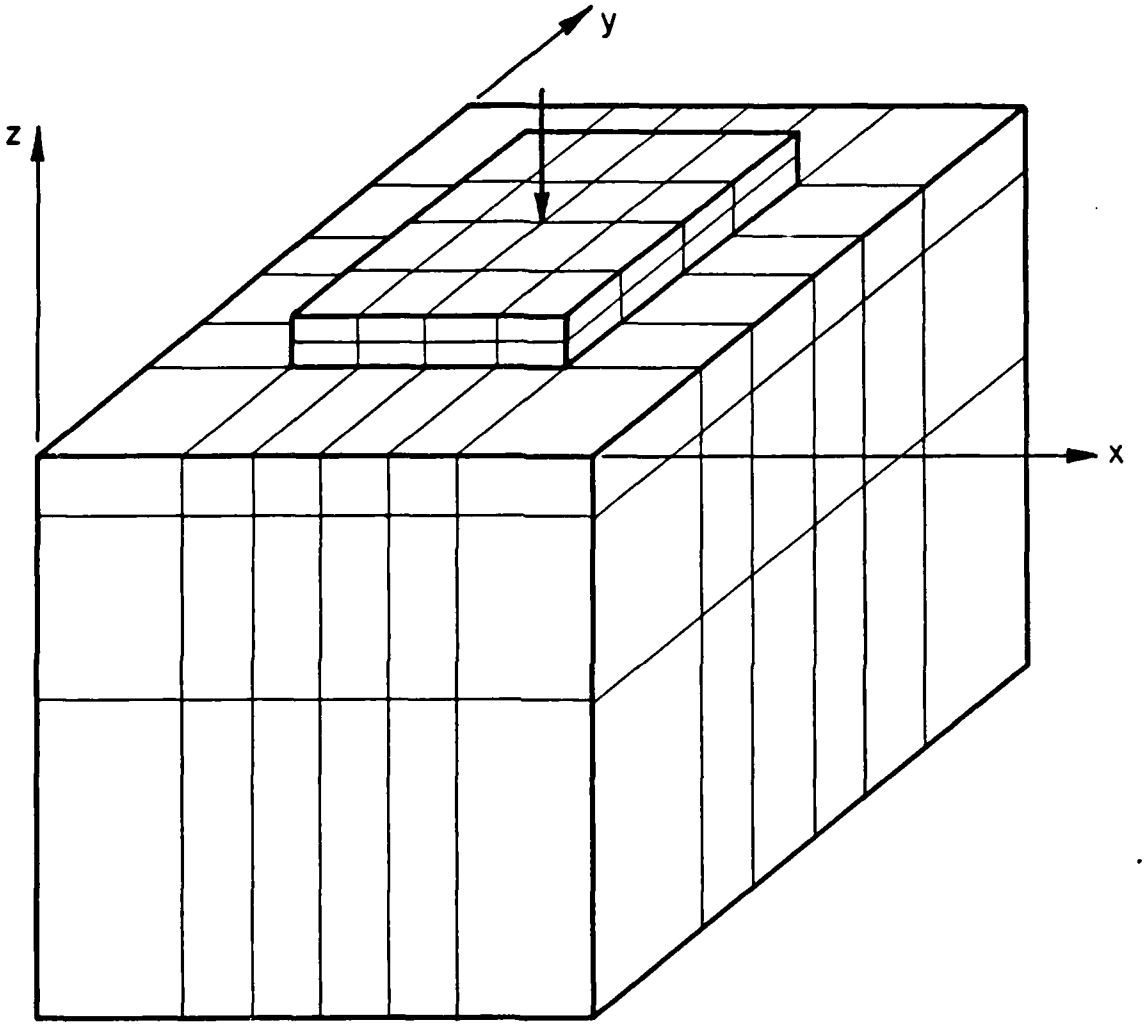

Fig. 2.1 Typical Three-Dimensional Finite Element Mesh for Slab-On-Grade

is the ratio of the long element side divided by the short element side (for the brick element, the plan view is considered). Two-dimensional results indicate that for good results, (2a/h) must be 0.8 or less, χ about 3.0 or more, and α should be less than 3.0 [2; 6]. Note that the mesh fineness guideline was only developed for square elements. The values may not necessarily hold for the three-dimensional problem, but they provide a starting point for a similar investigation. An examination of these mesh characteristics is rendered much more complex in three dimensions. Results presented below are inevitably not exhaustive, but may still be used to establish some guidelines for designing the finite element mesh.

Finally, the method of extrapolating finite element results to obtain, for instance, maximum stress values, needs to be investigated. This factor will be considered first, since maximum responses will be used below as primary indicators of performance, and since they are fairly sensitive to the extrapolation method adopted.

2.2 SELECTION OF STRESS EXTRAPOLATION METHOD

For the linear solid (brick) element used in GEOSYS (see Fig. 1.1), displacements are calculated at each of the eight nodal points, but stresses (and strains) are determined only at the centroid of the element ($\xi = \eta = \zeta = 0$). This location can be shown to be the optimal stress point for the brick element at which "stresses may be almost as accurate as nodal displacements" [25]. In most slab-on-grade

applications, however, critical stress values may occur at the corner or edge of an element, in the slab or in the subgrade, or at their interface. It is, therefore, necessary to extrapolate from calculated values to obtain the required stresses at the critical locations. Such an extrapolation will inevitably involve at least some loss of accuracy, and dictates a careful choice of the extrapolation method to be used.

Unfortunately, there is no unique answer to the question which extrapolation procedure is the best. There are numerous possible choices, each involving a different amount of computational effort and having both advantages and disadvantages. All of them, however, are essentially ad-hoc approximations lacking a rigorous mathematical basis. The basic problem is that in extrapolating, more information is demanded from the finite element results than is actually available. The limitations of any answer must always be borne in mind, therefore, when evaluating extrapolated results.

Now, the choice of a particular method depends on the anticipated behavior of the structure. Thus, a sound selection can only be made after considerable experience has been gained with such finite element applications, coupled with some engineering intuition. A given method may sometimes work better, and at other times worse than another. This will depend on the problem solved, the structure characteristics (e.g. slab and subgrade material properties, loading, etc.), as well as the finite element mesh attributes (e.g. fineness, gradation, element aspect ratios, etc.). In fact, mesh fineness is one of the most important factors affecting the choice of extrapolation method. All reasonable

choices may be expected to give very similar results as the mesh is made finer. In such a case, closed-form solutions, if available, may be used to evaluate the methods.

To illustrate these comments, the case of a slab loaded by a point load at its interior may be considered. This problem will be the test-case for most of the analyses in this Chapter. Taking advantage of symmetry, only one-quarter of the slab needs to be modeled (Fig. 2.2). This means that, although the point load is applied at the central node, the closest estimate of the maximum bending stress (developing under this node) will be that for the centroid of the element on which the load is applied. Extrapolation is needed to obtain the stress under the load. Table 2.1 shows a comparison between values of the maximum bending stress under the load, determined by three different extrapolation schemes, using results from five GEOSYS runs. The finite element mesh used in Run 5 is shown in Fig. 2.2, while for the other four runs a different number of elements were employed within the slab.

The 12-in. slab was modeled by two 6-in. layers, in which a linear stress distribution with depth may be assumed. The justification for this assumption will be discussed later. Thus, the stress σ_x or σ_y at the bottom of the slab beneath each element centroid may be determined by linear extrapolation using the corresponding values for the two slab layers from the computer outputs. Having done this for all elements in the vicinity of the load, the problem reduces to that of two-dimensional extrapolation. Figure 2.3 is a schematic illustration of the three methods compared in Table 2.1.

TABLE 2.1

COMPARISON OF THREE EXTRAPOLATION METHODS

RUN	SLAB MESH	MAX. BENDING STRESS, σ_i (psi) ORTHOGONAL	DIAGONAL	QUADRATIC
2	2x2	17.17	13.83	-
3	3x3	24.79	19.45	22.82
4	4x4	29.99	23.85	27.42
5	5x5	33.80	27.23	30.77
6	6x6	36.96	29.94	33.43

Notes:

Slab: 15 ft x 15 ft x 1 ft
Soil: 30 ft x 30 ft x 30 ft
$E = 4 \times 10^6$ psi; $\mu = 0.15$
$E_s = 1 \times 10^4$ psi; $\mu_s = 0.45$
$\ell_e = 45.5$ in.
Load, P = 3600 lbs (interior; point load)
Mesh : See Fig. 2.2 (Run 5)

Equations Used:

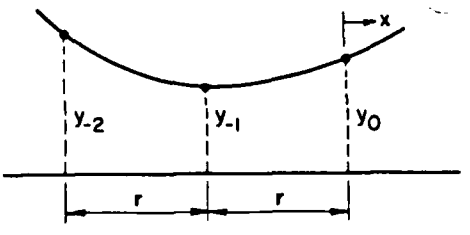

Orthogonal, Diagonal:

$$y = y_o + (y_o - y_{-1})\, x/r$$

Quadratic:

$$y = y_o + (y_{-2} - 4y_{-1} + 3y_o)\, x/2r + (y_{-2} - 2y_{-1} + y_o)\, x^2/2r^2$$

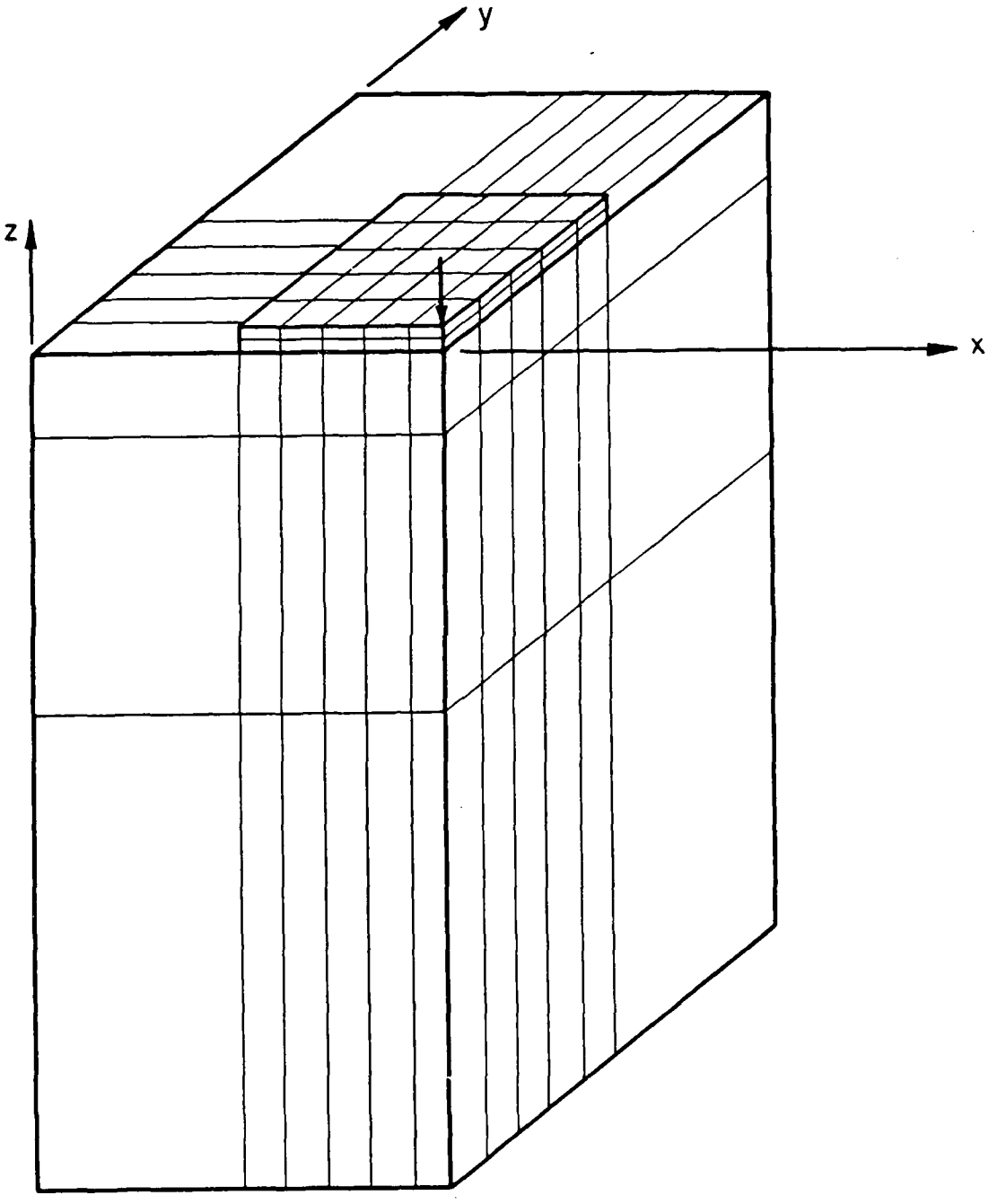

Fig. 2.2 Three-Dimensional Finite Element Mesh for Run 5

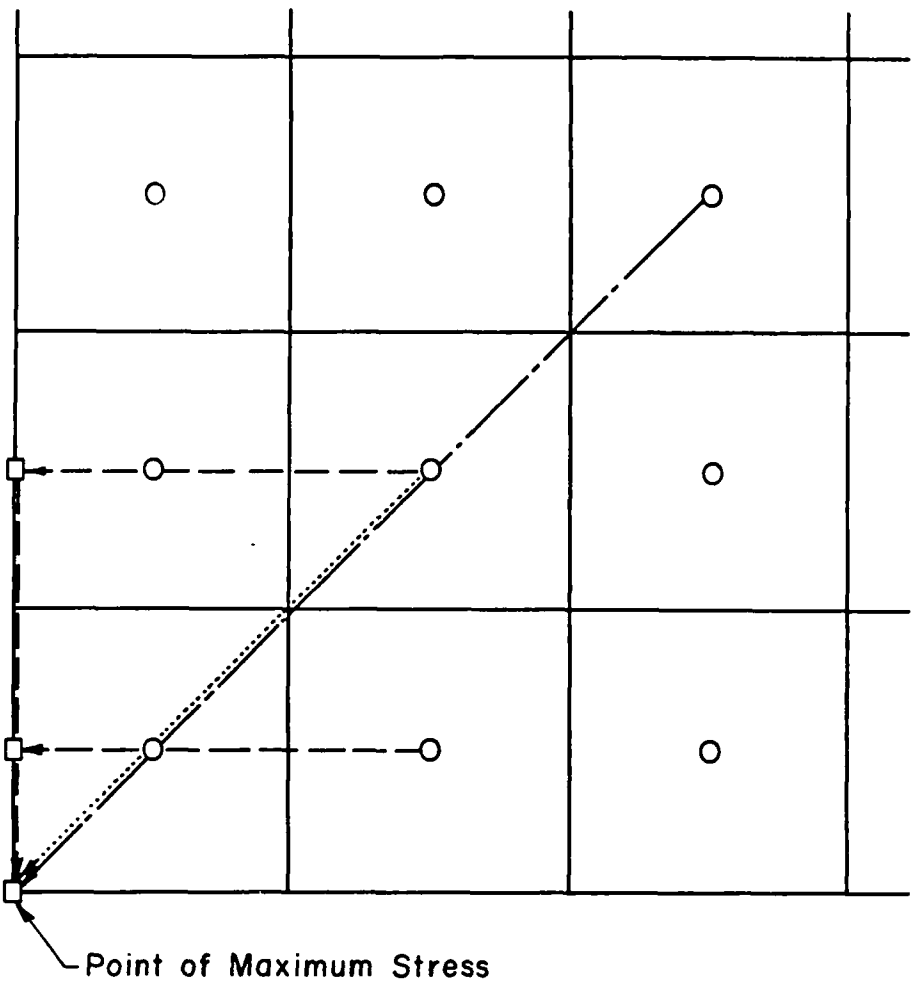

Fig. 2.3 Schematic Illustration of Extrapolation Methods Considered

Orthogonal linear extrapolation requires four nodes with known stresses at the bottom of the slab. Three linear extrapolations are involved in this method. The first two establish the necessary values for the third. As shown in Fig. 2.3, this is done first parallel to the x-axis, followed by the last extrapolation parallel to the y-axis. Extrapolating first in the y- and then in the x-direction will, of course, lead to the same result. In fact, one could first extrapolate in the horizontal plane using values from the computer output, and then project to the bottom of the slab, without affecting the result.

Diagonal linear extrapolation employs only two locations of known stress values at the bottom of the slab. For the cases considered in Table 2.1, this method gives a maximum bending stress value about 80% of that from orthogonal linear extrapolation.

Finally, quadratic diagonal extrapolation needs three known stress points in order to determine the value at the fourth. Application of this method to the cases considered in Table 2.1, yields maximum stresses near 90% compared to orthogonal linear extrapolation.

Theoretically, maximum interior bending stress, σ_i, tends to infinity as the radius of the applied loaded area, a, tends to zero [26]. Application of the closed-form equation, however, indicates that usually the increase in σ_i is not that drastic. For the total applied load considered here, for example, a uniform pressure, p, of 100 psi (a = 3.39 in.) yields σ_i equal to 44 psi. Increasing p to 1×10^9 psi (a = 0.001 in.) causes σ_i to rise to only 55 psi. Nonetheless, it can be concluded that the orthogonal linear extrapolation method gives best

results for this example. This procedure involves more computations, but takes into account a larger number of computer results. Thus, the individual error in any one of these will have a lesser effect on the extrapolated value. On the other hand, diagonal linear and quadratic extrapolations are faster, but suffer a penalty in accuracy. Since they employ fewer data points, they are more sensitive to errors in the individual element stresses. Furthermore, a larger portion of the data used in the latter two methods is further away from the point of maximum stress than for the orthogonal linear extrapolation. Note that the relative performance of the three methods in Table 2.1 is insensitive to mesh fineness, probably because the theoretical solution tends to infinity.

Unless otherwise indicated, orthogonal linear extrapolation will be used in analyzing bending stress results in the remainder of this Report. This method may also be used with subgrade stress data. When the stress state is known to be axisymmetric, however, diagonal linear or quadratic extrapolations are more appropriate. An example is the subgrade stress due to an interior load. In such cases, diagonal linear extrapolation is used below.

2.3 VERTICAL SUBGRADE EXTENT

In three-dimensional finite element modeling of a slab-on-grade, a cube of soil is carved out of the semi-infinite Boussinesq half-space (see Fig. 2.1). The dimensions of this cube must be large enough so

that end effects are minimized. On the other hand, the finite size of computer memory and of other resources, dictate the use of a rather small subgrade idealization. The next question to be answered then, is how deep should the foundation extend so that both these conflicting requirements are adequately satisfied. Two series of runs were performed to provide some guidelines in this respect.

Series A comprised seven runs. These considered the effect of increasing the subgrade depth, Z, on the behavior of the slab in Run 5 (Fig. 2.2) under an interior point load. Pertinent model details are given in Table 2.1, with the exception that the soil was divided in this case into a number of layers, NUMELZ, each 5-ft thick. Figure 2.4 shows the mesh for Run 10.

Results from these runs are tabulated in Table 2.2. It is observed that both maximum bending and subgrade stresses (σ_i and q_i) converge to a constant value fairly quickly. Increasing the subgrade depth beyond 20 to 25 ft (or 5 to 7 times the radius of relative stiffness, ℓ_e) will have no effect on these stresses. Also note that σ_i converges from below, while q_i seems to converge from above.

The behavior of deflection, however, requires more attention. Maximum deflection, δ_i, increases with subgrade depth as expected, but does not converge to a constant value, even for a depth of 35 ft (9 ℓ_e). An additional 0.044 mils of deflection is accumulated for every additional 5 ft of subgrade beyond 20 ft. This is due to the presence of lateral boundaries at a finite distance, X, from the slab edges, which in this case was 7.5 ft (2 ℓ_e). As a result, vertical strains in

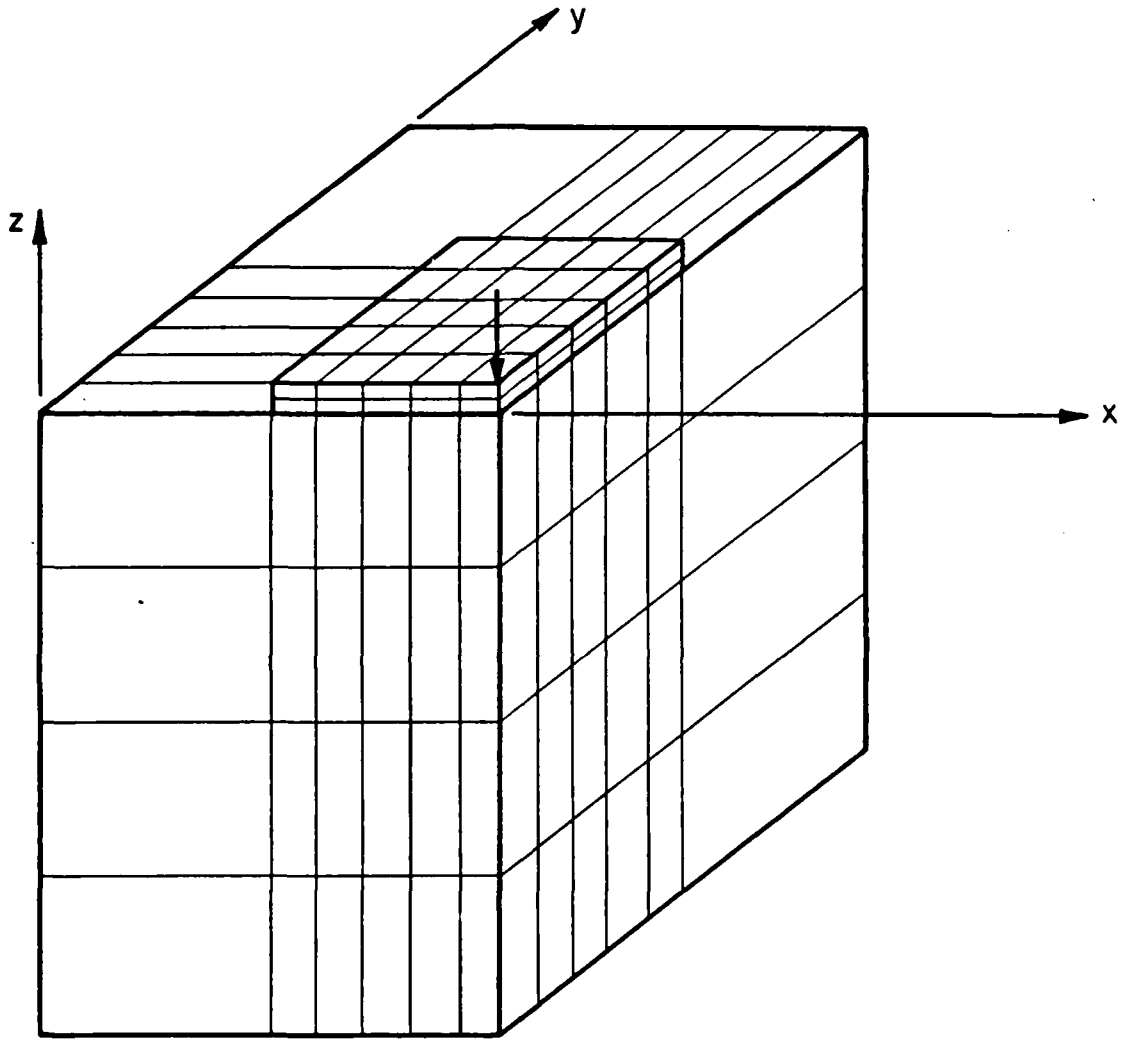

Fig. 2.4 Three-Dimensional Finite Element Mesh for Run 10

TABLE 2.2

EFFECT OF SUBGRADE VERTICAL EXTENT -- SERIES A

RUN	SUBGRADE DEPTH, Z (ft)	δ_i		q_i		σ_i	
		mils	%	psi	%	psi	%
7	5	1.334	69.05	(0.3012)	(105.28)	32.73	96.67
8	10	1.643	85.04	0.2840	99.27	33.79	99.79
9	15	1.750	90.58	0.2864	100.10	33.85	99.97
10	20	1.799	93.12	0.2861	100.00	33.86	100.00
11	25	1.844	95.45	0.2864	100.10	33.86	100.00
12	30	1.888	97.72	0.2861	100.00	33.86	100.00
13	35	1.932	100	0.2861	100	33.86	100

Notes:

-See Table 2.1 for problem specifications, and Fig. 2.4 for typical mesh.

-Subgrade is divided into 5-ft thick layers.

-Maximum deflection, δ_i, under interior point load, at top of slab.

-Maximum subgrade stress, q_i, under interior point load, at top of subgrade, by diagonal linear extrapolation (except for Run 7, q_i at z=2.5 ft).

-Maximum bending stress, σ_i, under interior point load, at bottom of slab, by orthogonal linear extrapolation.

-Responses expressed as a percentage of the values for Run 13.

the subgrade reach a level where they remain constant, rather than decrease as in a truly semi-infinite elastic solid, since they are not allowed to be distributed beyond the model boundaries.

To investigate this phenomenon further, Series B - consisting of seven additional runs - was conducted. These runs were similar to those in Series A. The lateral subgrade extent, X, beyond the slab edges, however, was increased to 35 ft (9 ℓ_e), and an additional vertical nodal plane was introduced at 5 ft from the slab edge. Furthermore, the NUMELZ subgrade layers consisted of two 1-ft layers at the top, followed by (NUMELZ-2) 7-ft layers to the required total subgrade depth, Z. The finite element mesh for one of these runs is shown in Fig. 2.5.

Table 2.3 presents a summary of maximum responses obtained from Series B. A plot of these is shown in Fig. 2.6. Trends exhibited by these results are similar to those observed with Series A data. Again, deflection increases slowly, and even at significant depths a small but finite vertical strain persists. This is illustrated in Fig. 2.7, in which vertical strain appears to attain a constant value at a depth of about 40 ft (10.5 ℓ_e). Beyond this depth, 0.0016 mils of additional deflection is accumulated for each extra foot of subgrade.

Comparison with Series A indicates that the depth at which vertical strain decreases to a constant value, as well as this value itself, are both influenced by the lateral extent of the subgrade. Therefore, for a given lateral subgrade extent, the finite element model will overestimate vertical deformation, if the subgrade extends vertically beyond the constant vertical strain depth, z_{cvs}. Although this is

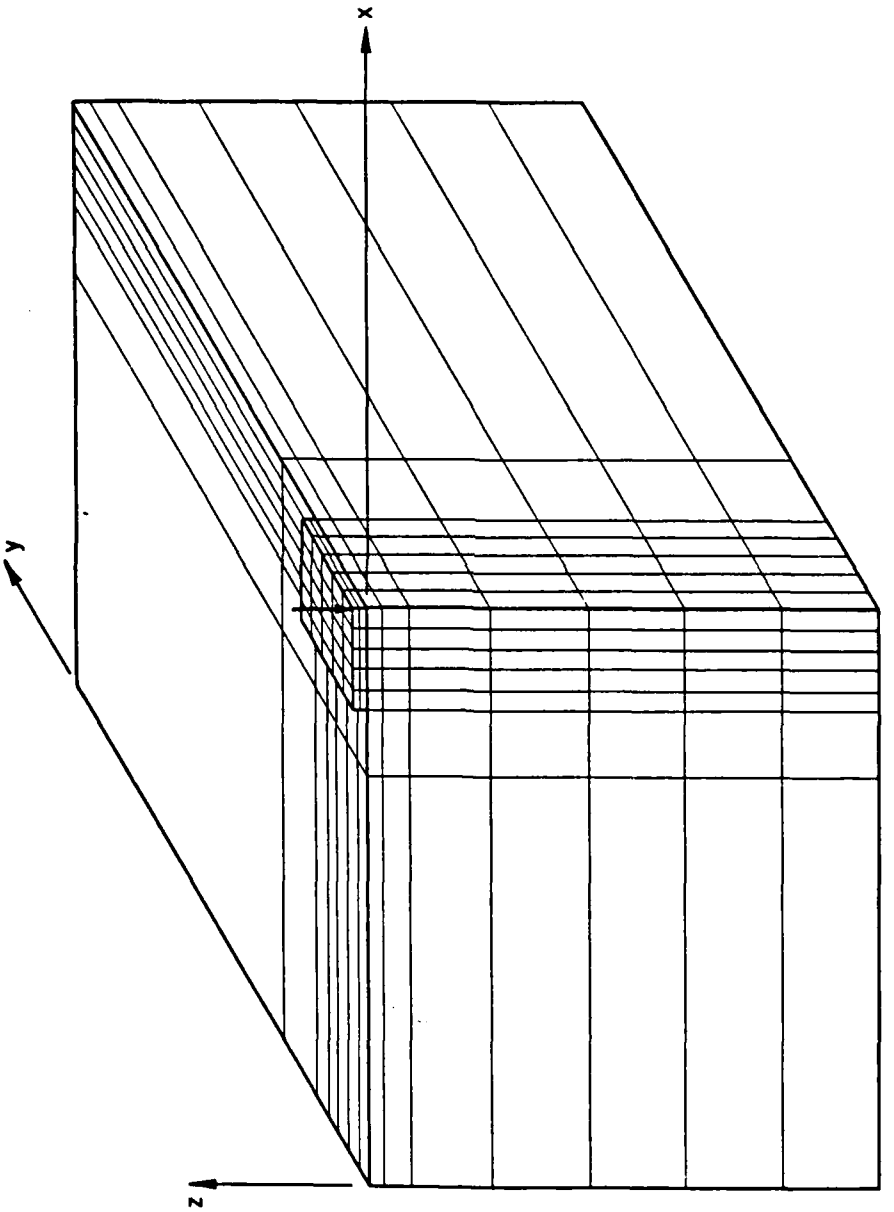

Fig. 2.5 Three-Dimensional Finite Element Mesh for Run 56

TABLE 2.3

EFFECT OF SUBGRADE VERTICAL EXTENT -- SERIES B

RUN	SUBGRADE DEPTH, Z	Δ_i		q_i		σ_i	
		mils	%	psi	%	psi	%
				0.3412	103.0	34.06	99.62
				0.3341	100.8	34.18	99.97
				0.3321	100.2	34.16	99.91
				0.3315	100.0	34.18	99.97
				0.3316	100.1	34.19	100.00
				0.3314	100.0	34.19	100.00
				0.3314	100	34.19	100

Notes:

-See Table 2.1 for test section specifications, and Fig. 2.5 for typical mesh.

-Subgrade consists of two 2 ft layers at the top, followed by a number of 2-ft layers to the total subgrade depth, Z.

-For location of interpolated method for maximum responses, see Table 2.2.

-Responses expressed as a percentage of the values for Run 101.

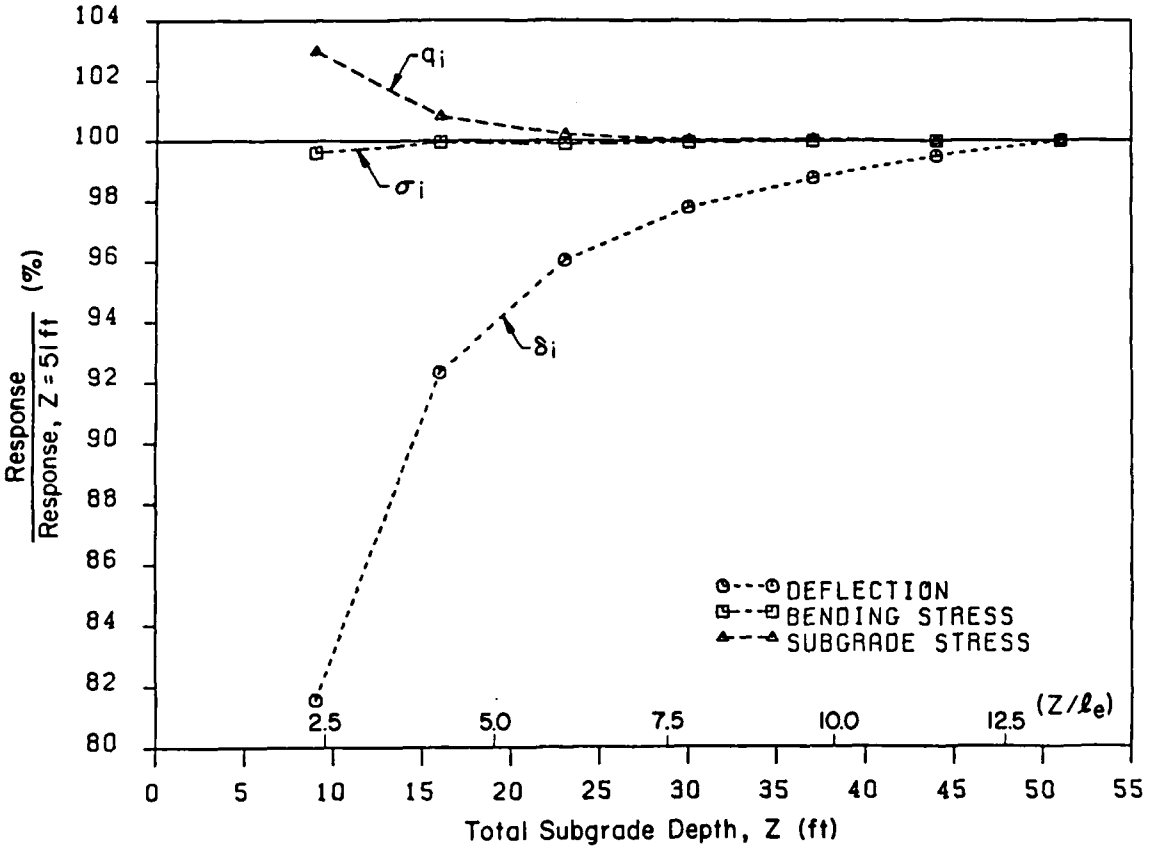

Fig. 2.6 Effect of Subgrade Vertical Extent -- Series B

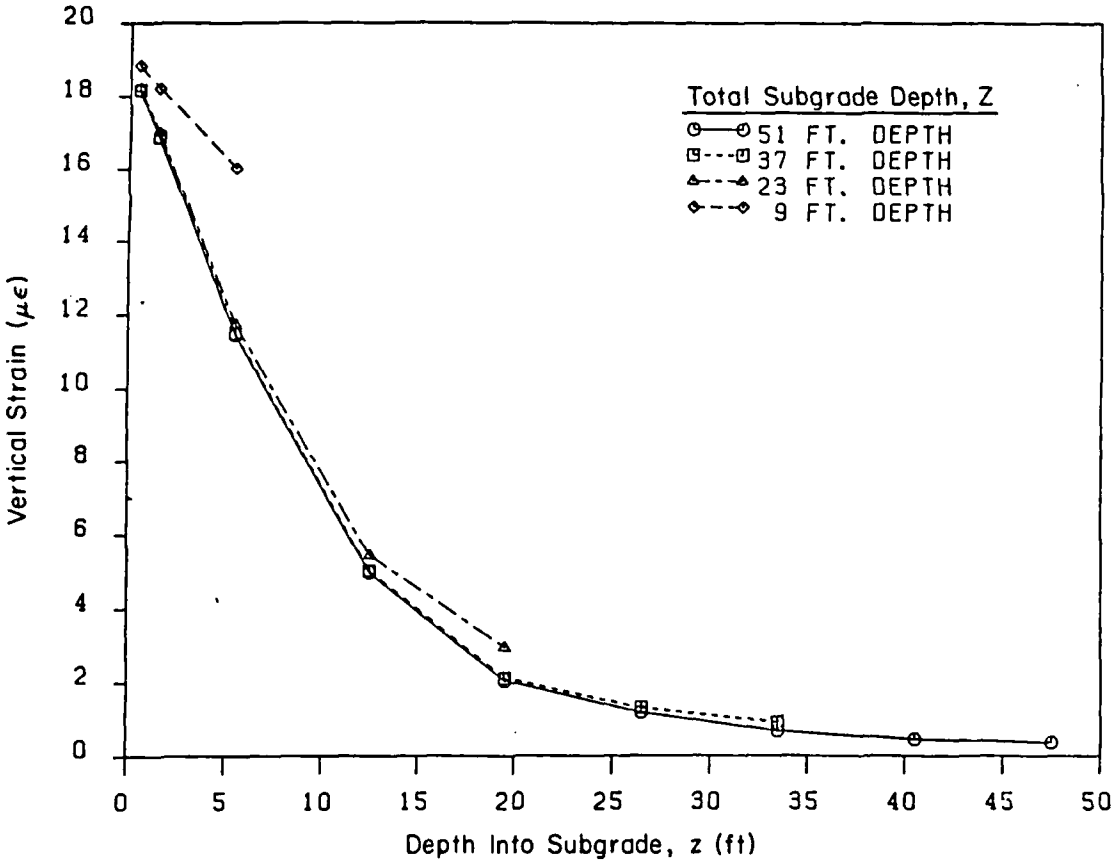

Fig. 2.7 Variation of Compressive Vertical Strain, ε_{zz}, in the Subgrade With Depth (Under Point Load, by Diagonal Extrapolation)

influenced by the lateral extent of the subgrade, a subgrade depth of about 40 ft (10 ℓ_e) may be used as a typical value. For this depth, strain and stress profiles are nearly identical to those obtained for deeper subgrades (see, for example, Fig. 2.7). Furthermore, q_i and σ_i converge to their final values much earlier (see Fig. 2.6). In a similar layered elastic solution using ELP15 [27] for a semi-infinite half-space, only 0.039% of the total vertical deformation in the subgrade occurred below the 40-ft depth. Thus, modeling the subgrade to this depth is an appropriate method of representing a semi-infinite elastic solid in the three-dimensional finite element solution.

2.4 LATERAL SUBGRADE EXTENT

It was indicated in the preceding section, that the size of the soil model cube in the horizontal direction can affect significantly the maximum deflection, δ_i, of a slab-on-grade. This observation was examined more closely by another set of seven runs, the results from which are presented in Table 2.4. These runs are variations of the model used in Run 5 (see Table 2.1 and Fig. 2.2), in which different extents of subgrade were used beyond the slab edges. This extent, X, was divided in each case into NUMELX elements of equal width. Figure 2.8 shows the finite element mesh for Run 18. Results are plotted in a normalized fashion in Fig. 2.9.

Maximum bending and subgrade stresses are not significantly affected by lateral subgrade extent, but deflection can be grossly

TABLE 2.4

EFFECT OF SUBGRADE LATERAL EXTENT BEYOND SLAB EDGES

RUN	NUMELX	LATERAL EXTENT, X (ft)	δ_i		q_i		σ_i	
			mils	%	psi	%	psi	%
16	1	4.0	1.837	84.50	0.3010	102.70	33.55	98.73
17	2	7.5	1.906	87.67	0.2990	102.01	33.78	99.41
18	3	12.0	2.005	92.23	0.2976	101.54	33.90	99.76
26	3	18.0	2.096	96.41	0.2961	101.02	33.93	99.85
29	3	24.0	2.148	98.80	0.2948	100.58	33.96	99.94
37	3	30.0	2.170	99.82	0.2940	100.30	33.96	99.94
51	3	36.0	2.174	100	0.2931	100	33.98	100

Notes:

-See Table 2.1 for problem specifications, and Fig. 2.8 for typical mesh.

-Subgrade extends X ft beyond slab edges, and is divided into NUMELX elements of equal width;
Total Depth of Subgrade, Z = 30 ft.

-For location of and extrapolation method for maximum responses, see Table 2.2.

-Responses expressed as a percentage of the values for Run 51.

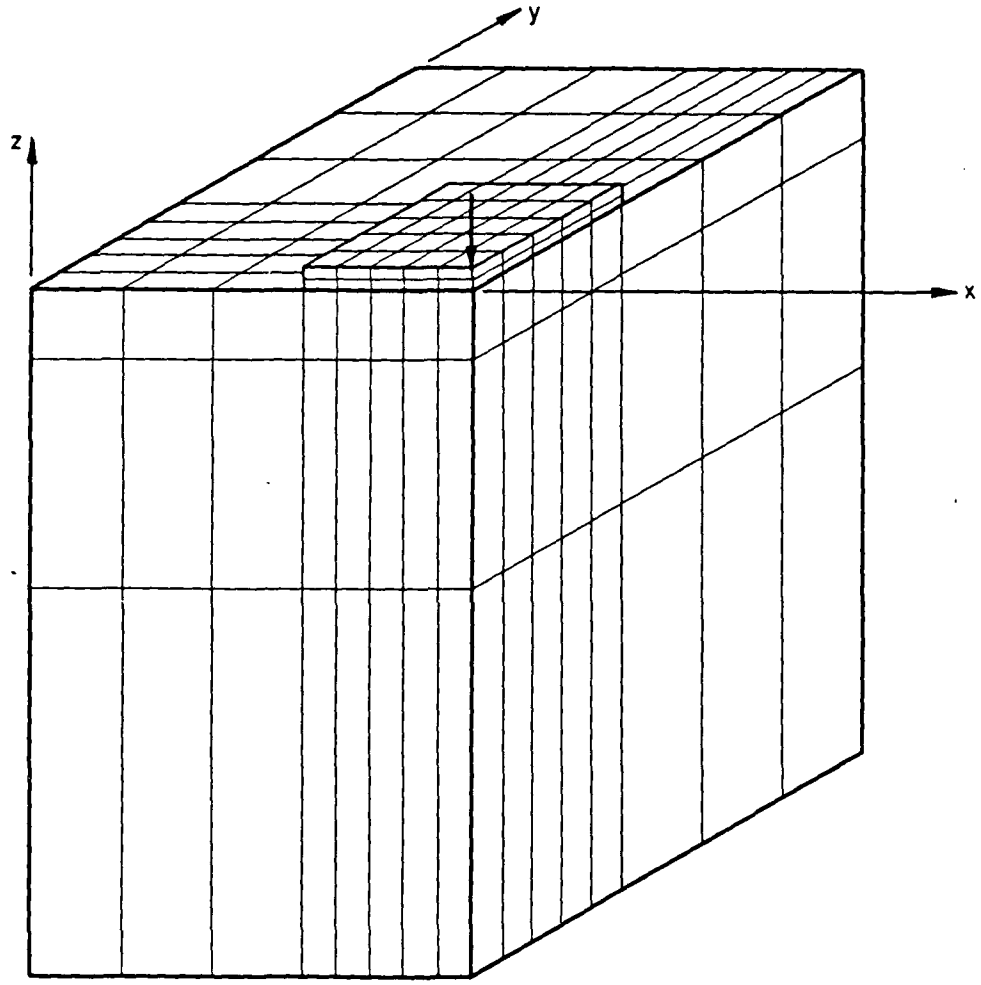

Fig. 2.8 Three-Dimensional Finite Element Mesh for Run 18

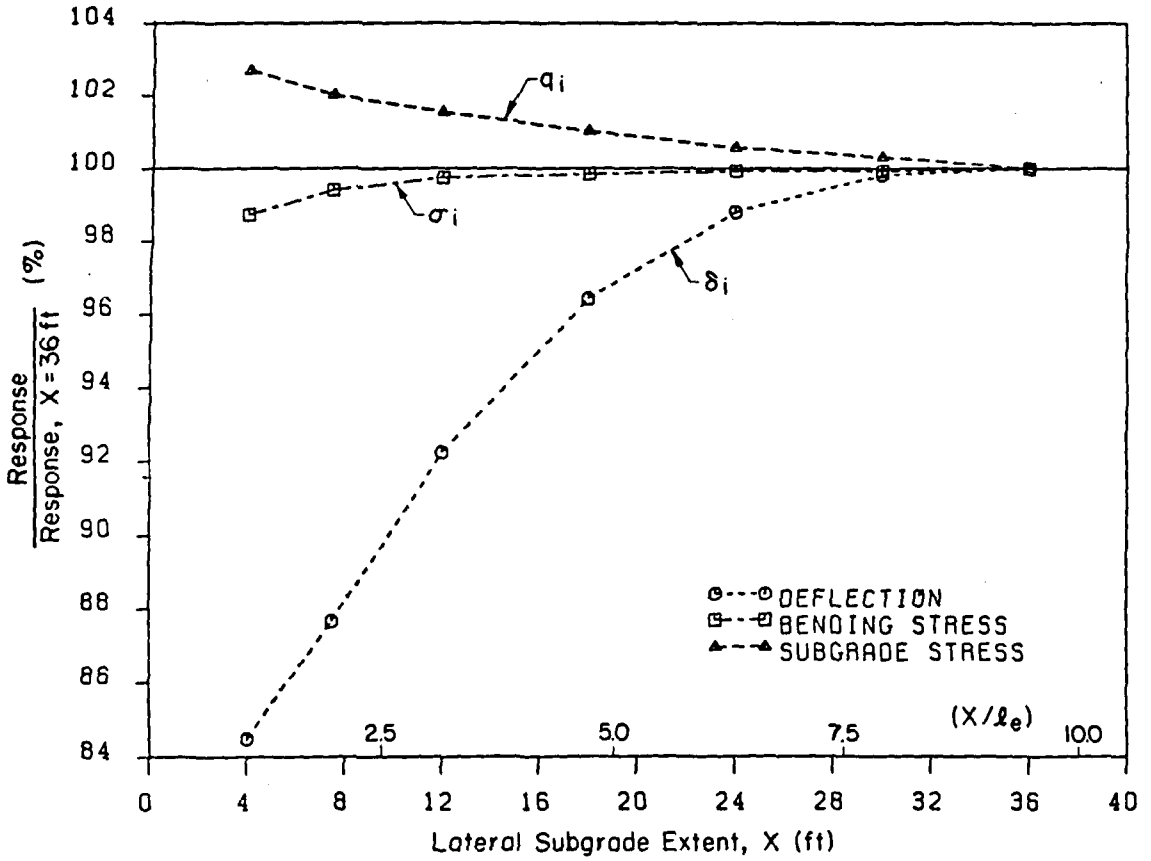

Fig. 2.9 Effect of Subgrade Lateral Extent Beyond Slab Edges

underestimated. The trends in Fig. 2.9 confirm the observations made in the previous section. Since the total depth of the subgrade, Z, is kept constant at 30 ft (8 ℓ_e) in these runs, the effect of increasing the subgrade lateral extent, X, is to increase the depth at which vertical strain becomes a constant, and to decrease the value of this constant vertical strain itself.

The total calculated deflection will, in general, consist of two parts:

(a) The contribution of the subgrade layers above the constant vertical strain depth, z_{cvs}; and

(b) The contribution of the layers below this depth.

The strain in part (b) is, of course, smaller than in part (a). As X (or Z) increases, the relative significance of part (a) increases. The relative significance of part (b) is diminished further by the fact that the value of the constant vertical strain ε_{cvs} decreases, as X (or Z) increases. Both these effects lead to higher calculated deflections.

Table 2.4 shows that major improvement in the value of δ_i is achieved even when X is only 24 ft (6 ℓ_e). Therefore, lateral extents between 25 and 35 ft (or 7-10 ℓ_e) should be used. This assertion is reinforced further by the radial strain distributions shown in Fig. 2.10. These are practically indistinguishable for X = 24 ft (6 ℓ_e) and X = 30 ft (8 ℓ_e). Similar plots (not included in this Report) for numerous other relevant responses indicate a similar trend. This implies that the model as a whole, not just the maximum responses, will converge at the suggested lateral extent.

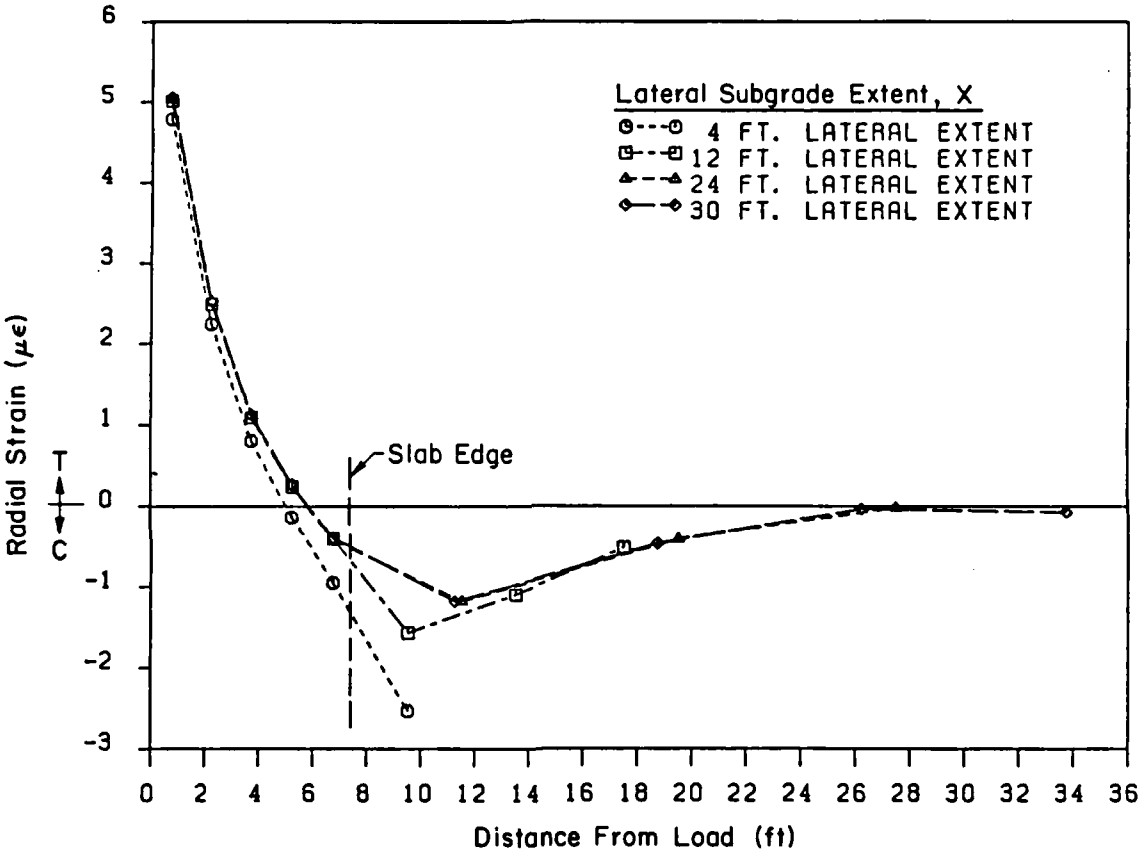

Fig. 2.10 Radial Strain, ε_{yy}, Distributions Along Slab y-Axis of Symmetry, at 1.5 ft Below Subgrade Surface: Effect of Subgrade Lateral Extent Beyond Slab Edges

As an additional check on the adequacy of a selected value of X, the following relative measure of convergence is proposed: the compressive radial strains near the lateral boundaries should be less than about 1% of the (maximum) tensile radial strain in the subgrade, which occurs underneath the load. This will ensure that the effect of the boundaries is negligible.

2.5 BOUNDARY CONDITIONS

In the runs presented thus far, lateral and bottom boundaries have been assumed to be on rollers, which allow displacements in the plane of the boundary concerned, but restrain displacement perpendicular to this plane. In GEOSYS, this boundary condition also applies to a plane of symmetry, since the linear solid element employed has only three displacement degrees-of-freedom at each node. In this section, selection of boundary conditions for three-dimensional finite element analysis of a slab-on-grade will be discussed, and the choices made in the previous runs justified.

Several different boundary condition options exist for the problem examined in this study. The primary consideration in selecting one from among these, is the simple observation that at an infinite distance from the load, a subgrade boundary will experience neither displacements nor stresses. This suggests that any boundary condition (e.g. fixed, free, or on rollers) will be adequate, if the soil extends to infinity. As the boundaries move closer to the load, either or both the stress-free

and displacement-free conditions will inevitably be violated, introducing an error into the solution.

Carrier and Christian [28] discussed the selection of boundary conditions for an axisymmetric (two-dimensional) finite element analysis of a plate on an elastic half-space. Their major conclusion was that the boundary condition must take into consideration the Poisson's ratio of the subgrade, μ_s. Thus, for an incompressible soil ($\mu_s = 0.5$), the most reliable results were obtained using an unrestrained (free) vertical side boundary, and a horizontal lower boundary that is free to move laterally (rollers). For a compressible soil, they indicated that either free or fixed boundary conditions could be used, assuming that the boundaries are located far enough from the load. In the present study, a Poisson's ratio value of 0.45 is used for the subgrade, implying only a small degree of compressibility. The recommendations made by Carrier and Christian [28] for an incompressible soil may provide a preliminary guideline for this study, as well.

If lateral displacements in the horizontal lower boundary are restrained, the model will be too stiff compared to the semi-infinite elastic half-space. On the other hand, a horizontal lower boundary that is free to move laterally allows the elements to distribute their load by deforming. Therefore, a smooth base should be assumed. For the vertical lateral boundaries, vertical displacements should be permitted, being similar to the lateral displacements on the horizontal base. Both free and roller-type boundaries would allow such displacements.

In order to examine the behavior of these two types of lateral boundaries (i.e. free, or on rollers), results from four runs are compared in Table 2.5. Two of these runs, Run 5 and Run 37, have also been presented above (see Tables 2.1 and 2.4). The two new runs (Run 57 and Run 58, respectively) are identical to these runs, except that free rather than roller-type lateral boundaries are assumed.

Table 2.5 confirms that maximum responses are more sensitive to the boundary conditions used when the lateral boundaries are closer to the load. Furthermore, maximum deflection, δ_i, is once again affected much more significantly than the other two responses. Complete distributions of deflection for the four cases considered are shown in Fig. 2.11. As expected, a stiffer response (lower deflection) is obtained with the roller-type, compared to the free boundaries. The two curves for boundaries at 37.5 ft (10 ℓe) from the load are fairly close to each other. They may be assumed to provide a better approximation to the elastic half-space response than the curves for boundaries at 15 ft (4 ℓ_e) from the load. When the lateral boundaries are this close, neither boundary condition appears to have an advantage over the other, since one underestimates while the other overestimates the half-space response by approximately the same amount.

Finally, Fig. 2.12 presents the variation of radial strain in the surface subgrade layer. This shows that of the two curves for boundaries at 15 ft (4 ℓ_e) from the load, the one with the roller-type boundary condition is closer to the curves for boundaries at 37.5 ft (10

TABLE 2.5

COMPARISON OF FREE AND ROLLER-TYPE LATERAL BOUNDARIES

RUN	Distance of Boundaries from Load (ft)	Lateral Boundary Conditions	δ_i		q_i		σ_i	
			mils	%	psi	%	psi	%
5	15.0	ROLLERS	1.869	100	0.2975	100	33.80	100
57		FREE	2.690	144	0.3005	101	33.93	100
37	37.5	ROLLERS	2.170	100	0.2940	100	33.96	100
58		FREE	2.317	107	0.2946	100	33.97	100

Notes:

-See Table 2.1 for problem specifications, and Fig. 2.2 for typical mesh.

-For location of and extrapolation method for maximum responses, see Table 2.2.

-Responses expressed as a percentage of the values for Runs 5 and 37.

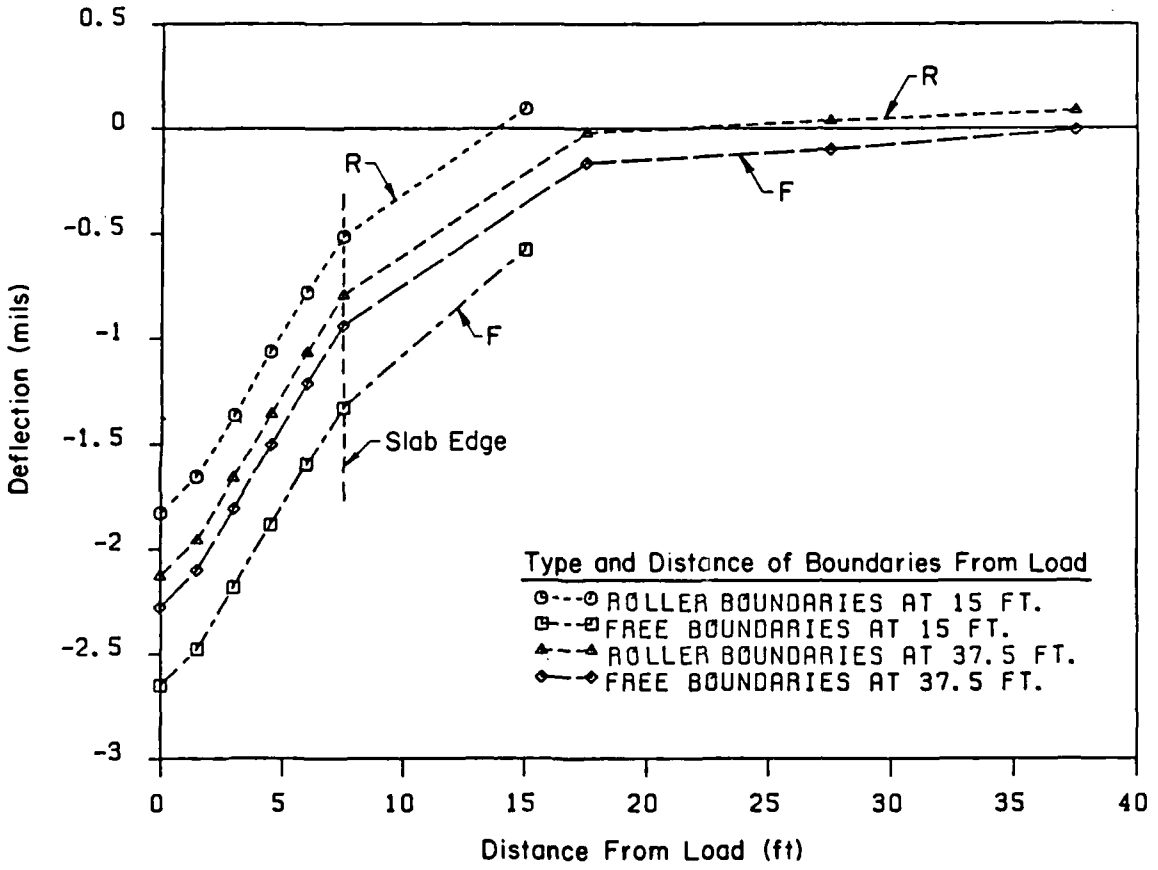

Fig. 2.11 Effect of Boundary Conditions on Subgrade Surface Deflection Profile

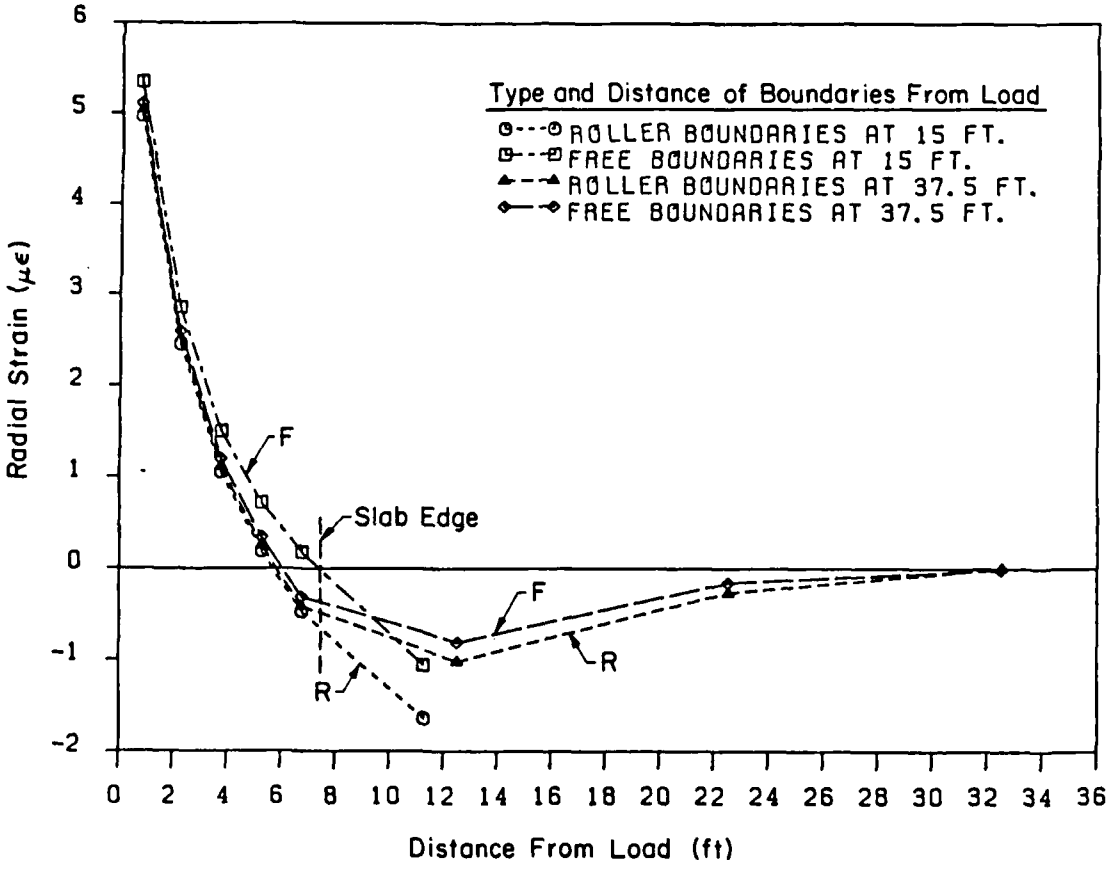

Fig. 2.12 Radial Strain, ε_{yy}, Distributions Along Slab y-Axis of Symmetry, at 1.5 ft Below Subgrade Surface: Effect of Boundary Conditions

ℓ_e) from the load. For these reasons, roller-type lateral boundaries are used in this study.

2.6 NUMBER OF SLAB LAYERS

Another choice made in the preceding runs which needs to be justified, is the use of only two 6-in. layers in modeling the 12-in. thick concrete slab. Using just one layer would yield a bending stress close to zero for all slab elements. The calculated stress point for the linear brick element is at its center, and this would be on or very near to the neutral axis (N.A.). Therefore, the minimum number of slab layers required for bending stress calculation is two. The critical value of this stress typically occurs in the extreme fiber of slab (at the top or at the bottom), which calls for an extrapolation from the calculated stress point values.

In medium-thick plate theory, a linear distribution of strain within the slab thickness is assumed, with the neutral axis at mid-depth. To check the validity of this assumption for three-dimensional slab-on-grade analyses using the linear brick element, Run 5 (see Table 2.1 and Fig. 2.2) was repeated using an increasing number of slab layers (NLAYER). Table 2.6 shows a comparison of the maximum responses from these runs. Figure 2.13 is a graphical presentation of the same results, normalized with respect to the responses obtained using the greatest number of slab layers (NLAYER = 6).

TABLE 2.6

EFFECT OF NUMBER OF SLAB LAYERS

RUN	NLAYER	δ_i		q_i		σ_i	
		mils	%	psi	%	psi	%
5	2	1.869	99.47	0.2975	100.03	33.80	99.73
14	3	1.875	99.79	0.2974	100.00	32.94	97.20
15	4	1.877	99.89	0.2974	100.00	33.33	98.35
25	5	1.878	99.95	0.2974	100.00	33.70	99.44
28	6	1.879	100	0.2974	100	33.89	100

Notes:

-See Table 2.1 for problem specifications, and Fig. 2.2 for typical mesh.

-For location of and extrapolation method for maximum responses, see Table 2.2 (σ_i extrapolation uses lower two slab layers).

-Responses expressed as a percentage of the values for Run 28.

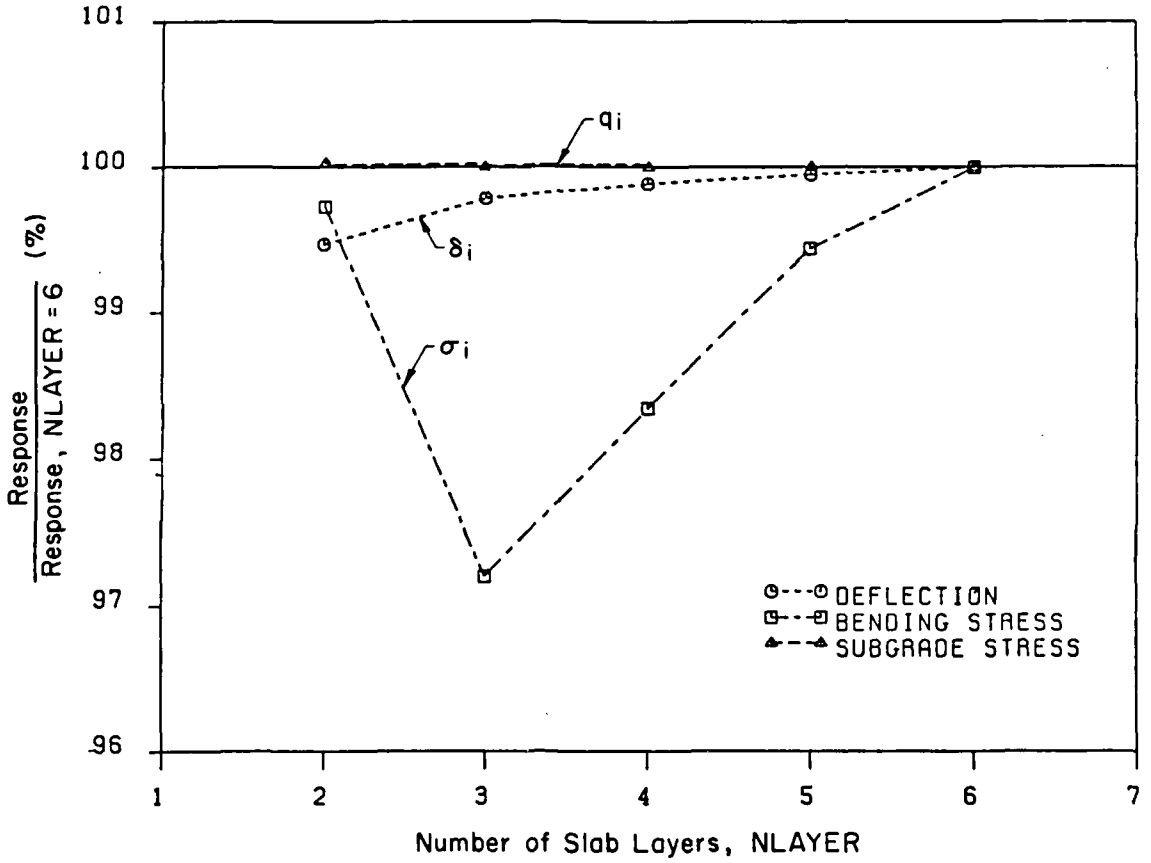

Fig. 2.13 Effect of Number of Slab Layers

It is observed that although there is a slight improvement in the results as the number of layers increases, maximum deflection and subgrade stress can be determined fairly accurately with any number of layers. Maximum bending stress, however, is slightly more sensitive to this effect. According to the extrapolation method adopted (see section 2.2), only values from the lower two slab layers are used in calculating the maximum bending stress. This probably explains the good performance of the two-layer slab, which is the only case involving a calculated stress point above the neutral axis. As a result, the two-layer slab gives results very close to those obtained using five or six layers, which makes it a very attractive option.

Figure 2.14 shows the variation of bending stress within the slab depth for the runs in Table 2.6. The element nearest to the load is considered here, but similar plots may be obtained at other locations. The figure confirms that the distribution is nearly linear as assumed by classical plate theory for any number of slab layers. The choice of a two-layer slab model is, therefore, seen to be justified.

2.7 VERTICAL DIVISION OF SUBGRADE

In most of the preceding runs, the soil cube has been divided into three layers, by horizontal nodal planes located at depth, z, values of 0, -3, -13 and -30 ft. This follows from an arbitrary but intuitive assumption, that the total depth of the subgrade may be divided into an upper, a middle and a lower portion. Any number of layers may be

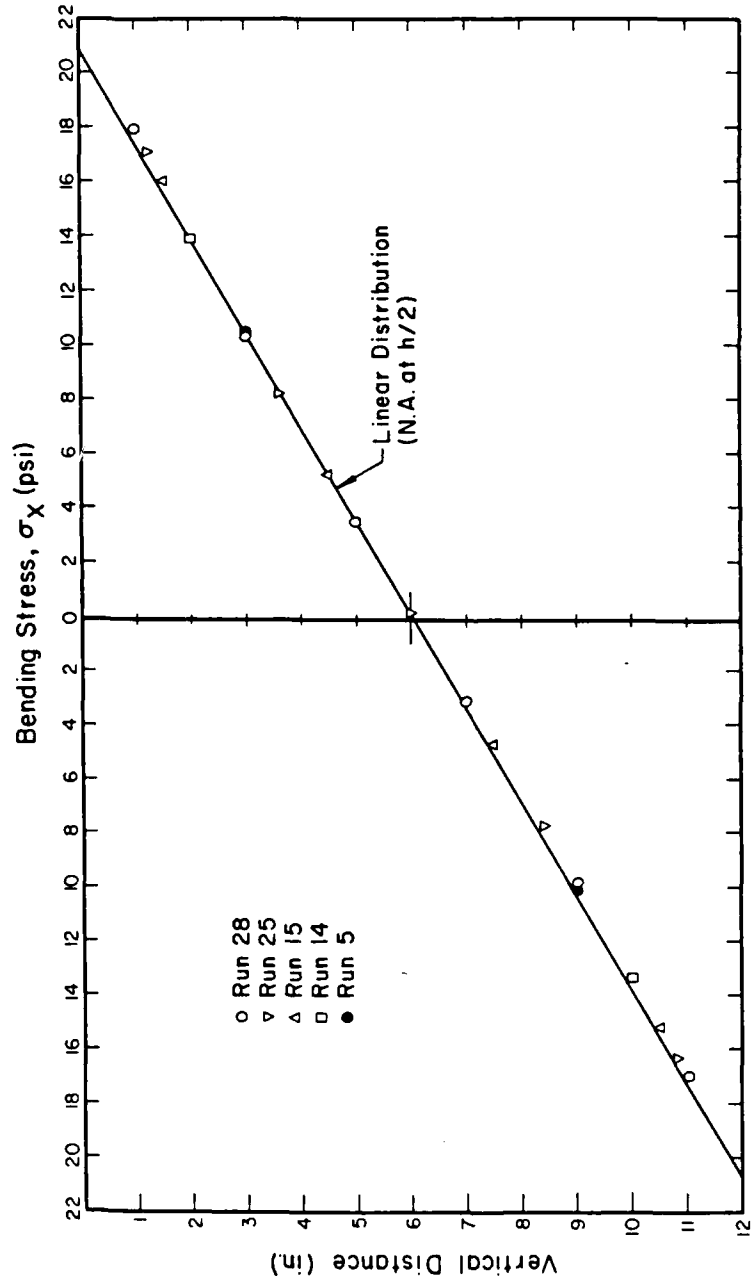

Fig. 2.14 Bending Stress Distribution Within Slab Thickness

ascribed to each of these three portions. In the runs above, one layer per portion was used for simplicity. In this section the effect of the number of layers used in the subgrade will be examined, with a view of developing some user guidelines for later runs.

Six series of runs were conducted to determine both the extent and the required fineness of the three arbitrary portions of the subgrade. In all these runs, the problem considered in Run 5 (see Table 2.1 and Fig. 2.2) was re-examined, using different discretizations of the subgrade in the vertical direction. In Series A, the subgrade was assumed to be 30 ft deep. Of these, the top 8 ft (2 ℓ_e) were considered to comprise the upper portion, the next 7 ft (2 ℓ_e) the middle, and the bottom 15 ft (4 ℓ_e) the lower portion. One layer was ascribed to each of the latter two, and the effect of varying the number of layers in the upper portion (NUPPER) was investigated. The results are shown in Table 2.7. These are also plotted in Fig. 2.15.

Maximum deflection and bending stress are only slightly sensitive to this effect. The subgrade stress, however, is significantly improved as the upper portion is divided into more layers. This is to be expected since the stress points, from which maximum subgrade stress is extrapolated, move closer to the surface (as the upper layers become thinner). The accuracy of the extrapolation is thereby improved. In fact, Fig. 2.15 suggests that further improvement is possible using a still finer upper portion. An alternative interpretation is that the assumed thickness of the upper portion (8 ft or 2 ℓ_e) was too large.

TABLE 2.7

EFFECT OF SUBGRADE UPPER PORTION FINENESS -- SERIES A

RUN	NUPPER	δ_i		q_i		σ_i	
		mils	%	psi	%	psi	%
21	2	1.887	99.47	0.2985	92.22	33.92	99.59
23	3	1.893	99.79	0.3131	96.73	34.00	99.82
24	4	1.893	99.79	0.3200	98.86	34.06	100.00
27	5	1.897	100	0.3237	100	34.06	100

Notes:

-See Table 2.1 for problem specifications, and Fig. 2.2 for typical mesh.

-Depth of Upper Portion = 8 ft (consists of NUPPER layers of equal thickness);
Depth of Middle Portion = 7 ft (consists of one layer);
Depth of Lower Portion = 15 ft (consists of one layer);
Total Depth of Subgrade, Z = 30 ft.

-For location of and extrapolation method for maximum responses, see Table 2.2.

-Responses expressed as a percentage of the values for Run 27.

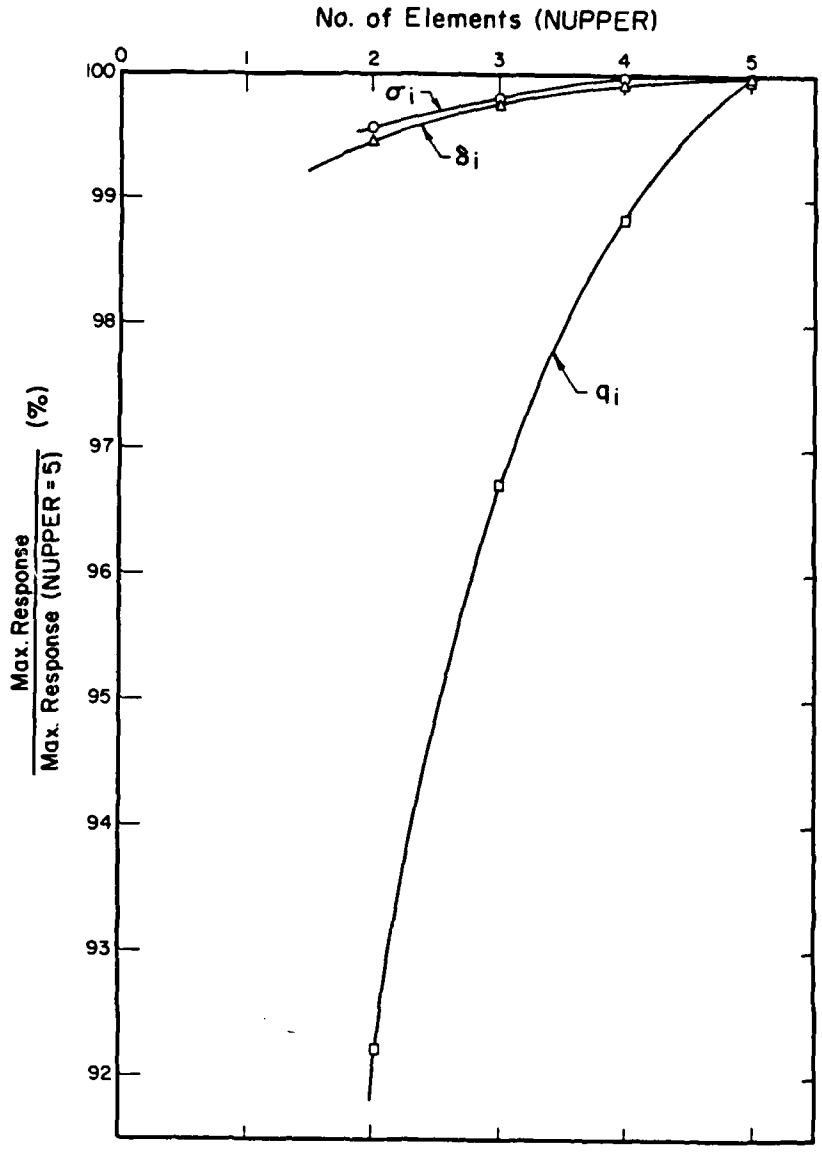

Fig. 2.15 Effect of Subgrade Upper Portion Fineness -- Series A

In Series B, the upper portion was considered to be only 4-ft thick, while the middle extended from 4 to 13 ft (1 to 3 ℓ_e), leaving the last 17 ft (4 ℓ_e) to the lower portion. The latter two portions were again ascribed one layer each. Table 2.8 and Fig. 2.16 show that the sensitivity of responses is less pronounced for this Series than for Series A, suggesting that the choice of a shallower upper portion and correspondingly thinner upper layers is warranted. In addition, the thickness of the upper layers should be between 1 and 2 ft (0.25 to 0.5 ℓ_e) for better accuracy. On the other hand, results from Run 34 in Table 2.8 appear to be less accurate than those from Run 27 in Table 2.7, indicating that consideration must be paid to the extent and fineness of the other two portions as well. For this reason, two additional series of runs were conducted.

Series C examines the effect the lower portion fineness by assuming that the upper and middle portions are 4-ft thick each (1 ℓ_e), and consist of one layer each. The 22-ft (6 ℓ_e) thick lower portion is divided into an increasing number of layers, NLOWER, which become progressively thicker with depth. The maximum responses from these runs are presented in Table 2.9. The sensitivity of the results to lower portion fineness appears to be limited, provided the lower portion begins at a considerable depth, preferably below half the constant vertical strain depth, z_{cvs} (see Fig. 2.7). The distribution of subgrade stress with depth is also insensitive to the lower portion fineness under these conditions, as shown in Fig. 2.17.

TABLE 2.8

EFFECT OF SUBGRADE UPPER PORTION FINENESS -- SERIES B

RUN	NUPPER	δ_i		q_i		σ_i	
		mils	%	psi	%	psi	%
36	1	1.870	99.36	0.2853	86.12	33.77	99.35
32	2	1.879	99.84	0.3243	97.89	33.93	99.82
35	3	1.881	99.94	0.3292	99.37	33.99	100.00
34	4	1.882	100	0.3313	100	33.99	100

Notes:

-See Table 2.1 for problem specifications, and Fig. 2.2 for typical mesh.

-Depth of Upper Portion = 4 ft (consists of NUPPER layers of equal thickness);
Depth of Middle Portion = 9 ft (consists of one layer);
Depth of Lower Portion = 17 ft (consists of one layer);
Total Depth of Subgrade, Z = 30 ft.

-For location of and extrapolation method for maximum responses, see Table 2.2.

-Responses expressed as a percentage of the values for Run 34.

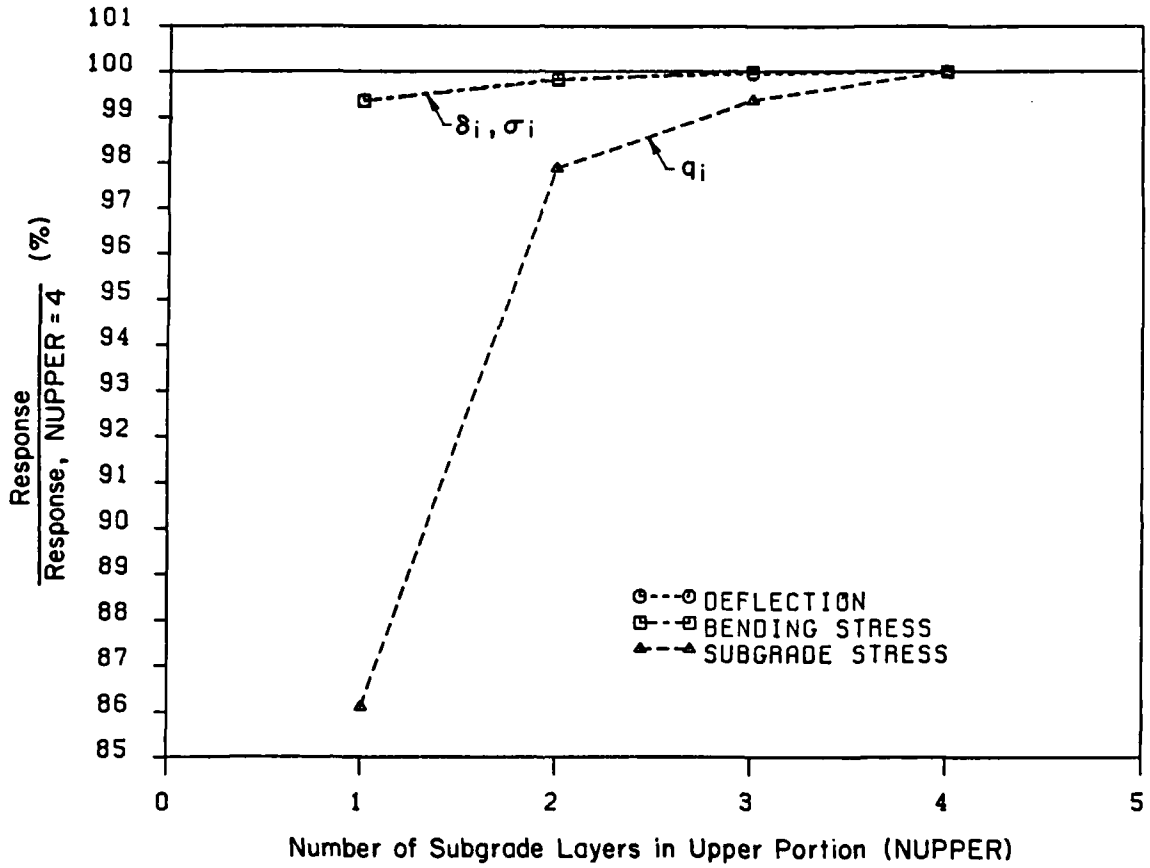

Fig. 2.16 Effect of Subgrade Upper Portion Fineness -- Series B

TABLE 2.9

EFFECT OF SUBGRADE LOWER PORTION FINENESS -- SERIES C

RUN	NLOWER	Divisions of Lower Portion (ft)	δ_i		q_i		σ_i	
			mils	%	psi	%	psi	%
22	1	8; 30	1.855	97.94	0.3060	102.93	33.73	99.38
21	2	8; 15; 30	1.887	99.63	0.2985	100.40	33.92	99.94
20	3	8; 11.7; 19.1; 30	1.892	99.89	0.2976	100.10	33.94	100.00
19	4	8; 10.5; 15; 21.5; 30	1.894	100	0.2973	100	33.94	100

Notes:

-See Table 2.1 for problem specifications, and Fig. 2.2 for typical mesh.

-Depth of Upper Portion = 4 ft (consists of one layer);
Depth of Middle Portion = 4 ft (consists of one layer);
Depth of Lower Portion = 22 ft;
Total Depth of Subgrade, Z = 30 ft.

-For location of and extrapolation method for maximum responses, see Table 2.2.

-Responses expressed as a percentage of the values for Run 19.

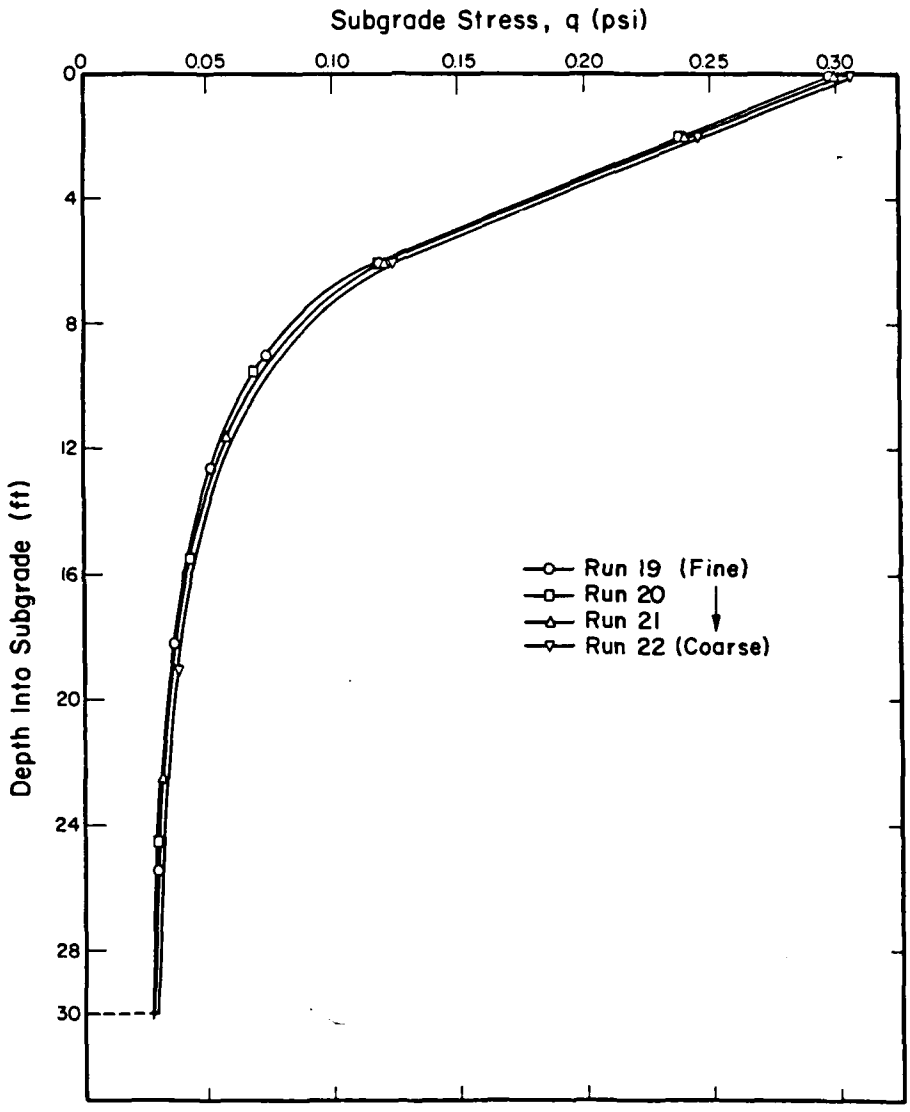

Fig. 2.17 Effect of Subgrade Lower Portion Fineness on Subgrade Stress Distribution with Depth (Under Point Load, by Diagonal Extrapolation)

Results from Series D confirm these assertions. In the runs tabulated in Table 2.10, the upper and middle portions are assumed to be 2-ft thick each (0.5 ℓ_e) and to consist of one layer each. Thus, the lower layer extends from 4 ft to 30 ft (1 ℓ_e to 7 ℓ_e). The sensitivity of maximum responses under these conditions is increased, suggesting that the extent and fineness of the middle portion also needs to be considered.

Series E runs investigate the effect of the middle portion fineness assuming an upper portion between 0 and 4 ft (0 to 1 ℓ_e), a middle portion between 4 and 15 ft (1 to 4 ℓ_e), and a lower portion from 15 to 40 ft (4 to 10 ℓ_e). Each of the upper and lower portions are divided into two layers of equal thickness. In these runs, therefore, the conclusions reached earlier in this section, as well as those in section 2.3 on the subgrade vertical extent, are incorporated. Maximum responses from this series are presented in Table 2.11. A normalized plot of these results is shown in Fig. 2.18. The sensitivity of the results to the fineness of the middle portion is less than for the upper portion, but greater than for the lower portion. Although one middle portion layer would be adequate for maximum response determination under these conditions, it is recommended that at least two layers be used for better results when considering distribution of stresses and displacements with depth.

As further confirmation of these suggestions, the runs in the last Series F were performed. In these, each of the upper and middle portions were assumed to consist of two layers of equal thickness. The

TABLE 2.10

EFFECT OF SUBGRADE LOWER PORTION FINENESS -- SERIES D

RUN	NLOWER	Divisions of Lower Portion (ft)	δ_i		q_i		σ_i	
			mils	%	psi	%	psi	%
33	1	4; 30	1.789	94.31	0.3470	108.40	33.31	97.80
32	2	4; 13; 30	1.879	99.05	0.3243	101.31	33.93	99.62
31	3	4; 9.1; 17.7; 30	1.893	99.79	0.3212	100.34	34.00	99.82
30	4	4; 7.5; 13; 20.5; 30	1.897	100	0.3201	100	34.06	100

Notes:

-See Table 2.1 for problem specifications, and Fig. 2.2 for typical mesh.

-Depth of Upper Portion = 2 ft (consists of one layer);
Depth of Middle Portion = 2 ft (consists of one layer);
Depth of Lower Portion = 26 ft;
Total Depth of Subgrade, Z = 30 ft.

-For location of and extrapolation method for maximum responses, see Table 2.2.

-Responses expressed as a percentage of the values for Run 30.

TABLE 2.11

EFFECT OF SUBGRADE MIDDLE PORTION FINENESS -- SERIES E

RUN	NMIDDLE	δ_i		q_i		σ_i	
		mils	%	psi	%	psi	%
105	1	2.194	99.32	0.3230	101.70	34.11	99.71
102	2	2.205	99.82	0.3191	100.47	34.21	100.00
103	3	2.208	99.95	0.3181	100.16	34.23	100.01
104	4	2.209	100	0.3176	100	34.21	100

Notes:

-See Table 2.1 for problem specifications, and Fig. 2.2 for typical mesh.

-Depth of Upper Portion = 4 ft (consists of two layers of equal thickness);
Depth of Middle Portion = 11 ft (consists of NMIDDLE layers of equal thickness);
Depth of Lower Portion = 25 ft (consists of two layers of equal thickness);
Total Depth of Subgrade, Z = 40 ft.

-For location of and extrapolation method for maximum responses, see Table 2.2.

-Responses expressed as a percentage of the values for Run 104.

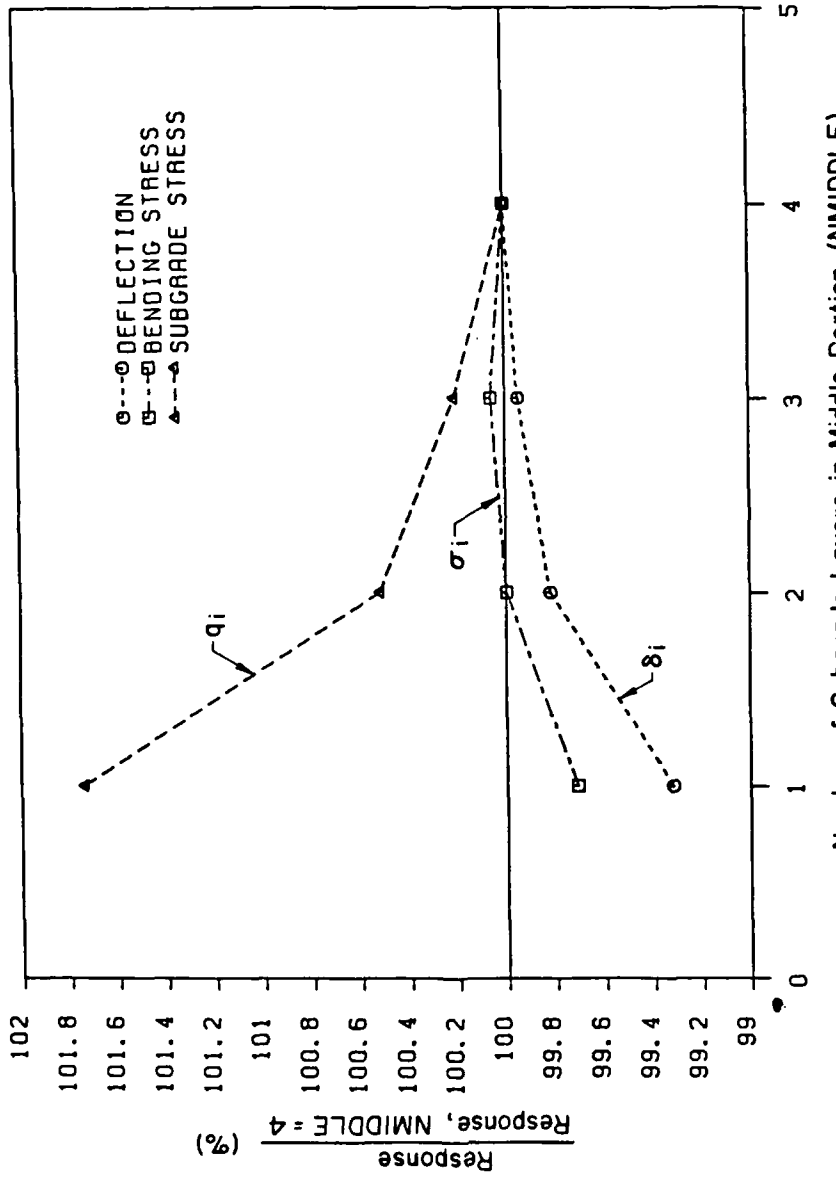

Fig. 2.18 Effect of Subgrade Middle Portion Fineness -- Series E

upper portion was 4-ft thick (1 ℓ_e), while the middle portion extended from 4 to 15 ft (1 to 4 ℓ_e). The number of layers, NLOWER, in the lower portion - which extended from 15 to 40 ft (4 to 10 ℓ_e) - varied as indicated in Table 2.12. The sensitivity of maximum responses is very small under these conditions and one layer in the lower portion appears to be adequate.

The preceding discussion has led to the following conclusions which can be used as guidelines in future runs. The subgrade may be divided into three portions in the vertical direction. The upper portion should extend from 0 to 4 ft (0 to 1 ℓ_e) and should consist of layers not more than 1 to 2-ft (0.25 to 0.5 ℓ_e) thick. The middle portion should extend from 4 to 15 ft (1 to 4 ℓ_e), or half the constant vertical strain depth, z_{cvs}, if known, and should be divided into at least 2 layers. Finally, the lower portion should cover the remainder of the soil cube, and may be divided into one or more layers.

2.8 HORIZONTAL SUBGRADE MESH FINENESS AND GRADATION

Mesh fineness in the horizontal plane has been identified as one of the most important factors influencing the accuracy of finite element results in earlier two-dimensional studies conducted at the University of Illinois [2; 6], and elsewhere. The investigation of this effect for the three-dimensional case was conducted in two stages. In this section, the horizontal mesh fineness in the region of the model between the slab edges and the vertical lateral boundaries is considered first.

TABLE 2.12

EFFECT OF SUBGRADE LOWER PORTION FINENESS -- SERIES F

RUN	NLOWER	δ_i		q_i		σ_i	
		mils	%	psi	%	psi	%
108	1	2.199	99.59	0.3196	100.19	34.17	99.85
102	2	2.205	99.86	0.3191	100.03	34.21	99.97
107	3	2.207	99.95	0.3190	100.00	34.22	100.00
106	4	2.208	100	0.3190	100	34.22	100

Notes:

-See Table 2.1 for problem specifications, and Fig. 2.2 for typical mesh.

-Depth of Upper Portion = 4 ft (consists of two layers of equal thickness);
Depth of Middle Portion = 11 ft (consists of two layers of equal thickness);
Depth of Lower Portion = 25 ft (consists of NLOWER layers of equal thickness);
Total Depth of Subgrade, Z = 40 ft.

-For location of and extrapolation method for maximum responses, see Table 2.2.

-Responses expressed as a percentage of the values for Run 108.

The extent of this region was discussed in section 2.4, above. Horizontal mesh fineness in the slab itself is considered in section 2.9.

Based on the conclusions reached in section 2.4, the lateral extent, X, of the subgrade beyond the slab edges, has been set to 30 ft (8 ℓ_e) in the runs below, for the horizontal subgrade mesh fineness investigation. The model used is identical to that in Run 5 (see Table 2.1 and Fig. 2.2), the major variable being the number of elements of equal size employed within X (NUMELX).

Maximum responses from these runs are shown in Table 2.13, and are plotted in a normalized form in Fig. 2.19. All three responses converge from below, and bending stress is not sensitive to this effect. For accurate subgrade stress and deflection values, however, a relatively fine mesh is needed. Naturally, this will be more demanding on computer storage requirements. An alternative was sought in the use of elements of unequal size.

The effect of the load applied on the slab diminishes with distance from the slab edges. Therefore, in modeling the subgrade, smaller elements are appropriate near the slab, while the mesh can become coarser closer to the vertical lateral boundaries. In investigating horizontal subgrade mesh gradation, it was decided that only two elements would be used within X. Table 2.14 shows a comparison between Run 40 - in which a 4-ft (1 ℓ_e) element was used next to the slab, followed by a 26-ft (7 ℓ_e) element to the lateral boundary - and two runs from Table 2.13. It is observed that the uneven division of X in

TABLE 2.13

INVESTIGATION OF HORIZONTAL SUBGRADE MESH FINENESS

RUN	NUMELX	δ_i		q_i		σ_i	
		mils	%	psi	%	psi	%
39	1	1.924	87.57	0.2874	97.36	33.93	99.94
38	2	2.109	95.99	0.2915	98.75	33.98	100.09
37	3	2.170	98.77	0.2940	99.59	33.96	100.02
61	4	2.197	100	0.2952	100	33.95	100

Notes:

-See Table 2.1 for problem specifications, and Fig. 2.2 for typical mesh.

-Subgrade Lateral Extent Beyond Slab Edges, X = 30 ft (consists of NUMELX elements of equal width).

-For location of and extrapolation method for maximum responses, see Table 2.2.

-Responses expressed as a percentage of the values for Run 61.

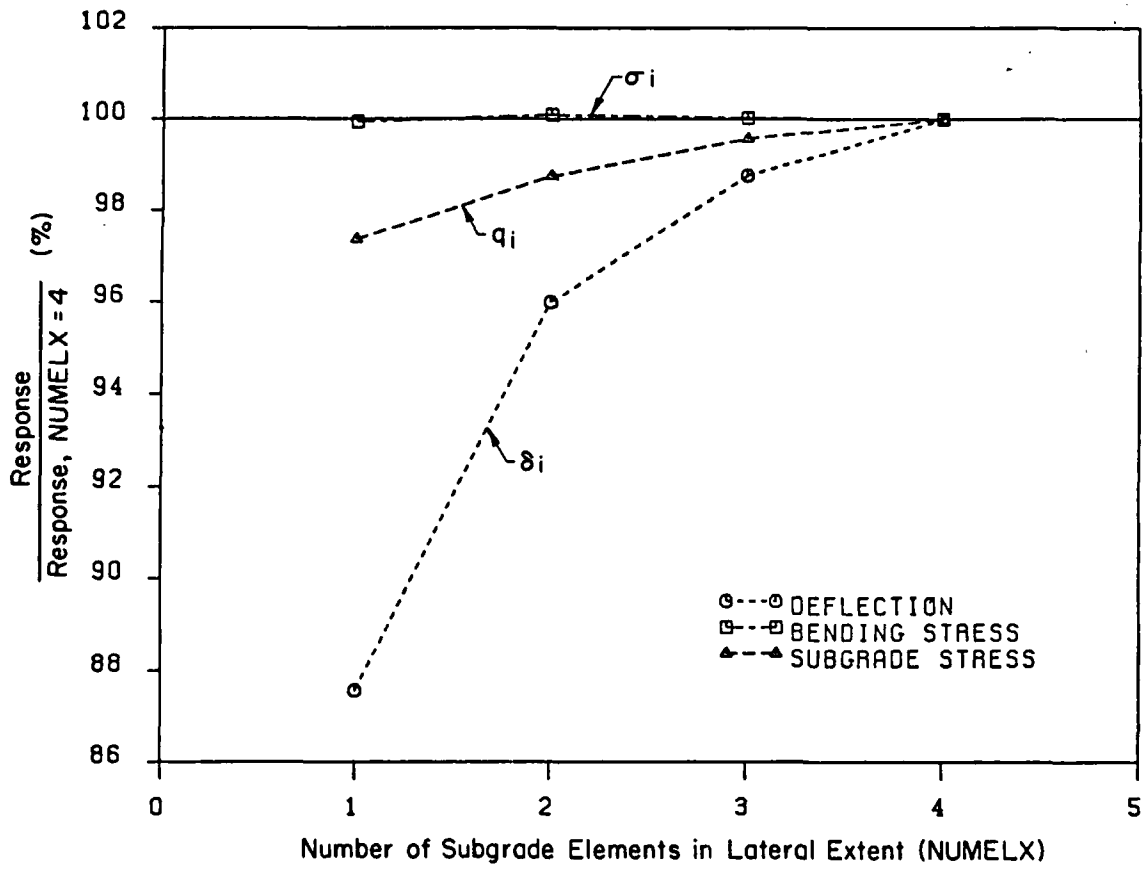

Fig. 2.19 Effect of Horizontal Subgrade Mesh Fineness

TABLE 2.14

EFFECT OF HORIZONTAL SUBGRADE MESH GRADATION

RUN	Divisions of X (ft)	δ_i		q_i		σ_i	
		mils	%	psi	%	psi	%
61	4 @ 7.5'	2.197	100	0.2952	100	33.95	100
38	2 @ 15'	2.109	95.99	0.2915	98.75	33.98	100.00
40	1 @ 4'; 1 @ 26'	2.136	97.22	0.2956	100.14	33.88	99.79

Notes:

-See Table 2.1 for problem specifications, and Fig. 2.2 for typical mesh.

-Subgrade Lateral Extent Beyond Slab Edges, X = 30 ft.

-For location of and extrapolation method for maximum responses, see Table 2.2.

-Responses expressed as a percentage of the values for Run 61.

Run 40 gives improved results over Run 38, in which the two elements were of equal size. Furthermore, comparing with Run 61, which employed the finest mesh in Table 2.13, leads to the conclusion that Run 40 gives results of adequate accuracy. It is, therefore, recommended that X be divided into two elements, one 4 ft in size near the slab (1 ℓ_e or 2a/h $\approx$ 4.0), and another 26 ft for the remainder (7 ℓ_e or 2a/h $\approx$ 26.0).

2.9 HORIZONTAL SLAB MESH FINENESS AND ELEMENT ASPECT RATIO

In this section, the investigation of the horizontal mesh fineness will be completed, by considering the finite element discretization within the slab itself. The importance of this factor cannot be overemphasized. Earlier two-dimensional studies [2] have shown that the mesh fineness required for good accuracy can be expressed in terms of the non-dimensional ratio (2a/h), where 2a is the length of a (square) element, and h is the slab thickness. A value of about 0.8 or less was recommended for use with ILLI-SLAB [6].

Three series of GEOSYS runs were conducted to examine the influence of horizontal slab mesh fineness on the response of the three-dimensional slab-on-grade. In Series A, the model was similar to that in Run 5, except that the number of elements (NUMEL) into which the 15-ft (4 ℓ_e) square slab was divided in the horizontal direction, was varied. Some runs in this Series have already been presented in section 2.2, in conjunction with the selection of stress extrapolation method. Results shown in Table 2.15 have been obtained - as always - using

TABLE 2.15

INVESTIGATION OF HORIZONTAL SLAB MESH FINENESS -- SERIES A

RUN	NUMEL	(2a/h)	δ_i		q_i		σ_i	
			mils	%	psi	%	psi	%
2	16	3.75	1.738	90.24	0.2675	90.40	17.17	41.42
3	36	2.5	1.807	93.82	0.2768	93.55	19.45	46.92
4	64	1.875	1.844	95.74	0.2922	98.75	29.99	72.35
5	100	1.5	1.869	97.04	0.2975	100.54	33.80	81.54
6	144	1.25	1.890	98.13	0.2985	100.88	36.96	89.17
59	196	1.07	1.908	99.06	0.2977	100.01	39.31	94.84
60	256	0.94	1.926	100	0.2959	100	41.45	100

Notes:

-See Table 2.1 for problem specifications, and Fig. 2.2 for typical mesh.

-Subgrade Lateral Extent Beyond Slab Edges, X = 7.5 ft (consists of one element); Total Depth of Subgrade, Z = 30 ft (consists of three layers).

-For location of and extrapolation method for maximum responses, see Table 2.2.

-Responses expressed as a percentage of the values for Run 60.

orthogonal linear extrapolation for the maximum bending stress, and diagonal linear extrapolation for the maximum subgrade stress, as per the recommendations formulated in section 2.2. The trends observed here are similar to those noted in earlier two-dimensional finite element studies [2; 6], inasmuch as all three maximum responses converge from below. Deflection and subgrade stress appear to be less sensitive to horizontal mesh fineness, and adequate accuracy may be expected as (2a/h) approaches the value of 0.8. This is the same value as determined from the two-dimensional studies [2; 6]. For the case analyzed in Series A, bending stress is more sensitive to this effect, perhaps requiring values of (2a/h) less than 0.8 for convergence.

To investigate the effect of maximum aspect ratio, α_{max}, three additional runs were conducted. The finite element meshes employed are variants of the one used for Run 6 (see Table 2.15). Two 1.25-ft elements (2a/h = 1.25) were retained near the load, while the remainder of the slab was divided uniformly into a number of larger rectangular elements. Table 2.16 summarizes maximum responses thus obtained. Although the solution deteriorates as α_{max} increases, the impact of this factor is limited, especially if α_{max} is kept below 3. This recommendation is similar to the one developed using the two-dimensional ILLI-SLAB model [2; 6].

In Series B of the horizontal slab mesh fineness investigation, the vertical and lateral extents of the subgrade were modified to correspond to the guidelines established in sections 2.3 and 2.4, above. Maximum

TABLE 2.16

INVESTIGATION OF MAXIMUM SLAB ELEMENT ASPECT RATIO

RUN	Slab Divisions	α_{max}	δ_i		q_i		σ_i	
			mils	%	psi	%	psi	%
6	6@1.25′	1.00	1.890	100	0.2985	100	36.96	100
63	3@1.67′; 2@1.25′	1.33	1.887	99.84	0.2976	99.70	36.78	99.51
64	2@2.25′; 2@1.25′	2.00	1.879	99.42	0.2948	98.76	36.80	99.57
65	1@5.00′; 2@1.25′	4.00	1.866	98.73	0.2796	93.67	36.04	97.51

Notes:

-See Table 2.1 for problem specifications, and Fig. 2.2 for typical mesh.

-Subgrade Lateral Extent Beyond Slab Edges, X = 7.5 ft (consists of one element); Total Depth of Subgrade, Z = 30 ft (consists of three layers).

-For location of and extrapolation method for maximum responses, see Table 2.2.

-Responses expressed as a percentage of the values for Run 6.

responses shown in Table 2.17 confirm the general trends and observations noted in Series A results.

The model in Series C is identical to that in Series B. The difference is that the loading, which was a point load, P = 3600 lbs, in Series B (and all preceding) runs, was applied as a 6-in. by 6-in. distributed load under 100 psi of pressure. In the finite element formulation, this is converted into four work equivalent nodal loads for each element on which the external load is applied. The results from Series C runs are given in Table 2.18. Also given in this Table, are the responses from a similar run of the two-dimensional finite element program ILLI-SLAB [6], using a mesh fineness ratio (2a/h) of 1.5. Figure 2.20 shows the GEOSYS responses normalized with respect to the corresponding ILLI-SLAB results. The value of (2a/h) of 0.8 suggested by earlier two-dimensional studies seems to be appropriate for GEOSYS runs as well, with bending stress being more sensitive to this effect than deflection and subgrade stress.

2.10 EFFECT OF SUBGRADE POISSON'S RATIO

Carrier and Christian [28] have pointed out that the selected value of the subgrade Poisson's ratio, μ_s, has a great bearing on other choices with respect to the finite element model, most notably the boundary conditions used. In section 2.5 above, recommendations were developed according to which roller-type lateral boundaries should be used in the three-dimensional GEOSYS model. The effect of the value of

TABLE 2.17

INVESTIGATION OF HORIZONTAL SLAB MESH FINENESS -- SERIES B

RUN	NUMEL	(∠a/h)	δ_i		q_i		σ_i	
			mils	%	psi	%	psi	%
43	36	2.5	2.109	95.39	0.2914	84.20	25.14	63.31
44	64	1.875	2.147	97.11	0.3171	91.62	30.34	76.40
45	100	1.5	2.172	98.24	0.3299	95.32	34.17	86.05
46	144	1.25	2.192	99.14	0.3398	98.18	37.20	93.68
94	196	1.07	2.211	100	0.3461	100	39.71	100

Notes:

-See Table 2.1 for problem specifications, and Fig. 2.2 for typical mesh.

-Subgrade Lateral Extent Beyond Slab Edges, X = 35 ft (consists of two elements); Total Depth of Subgrade, Z = 30 ft (consists of five layers).

-For location of and extrapolation method for maximum responses, see Table 2.2.

-Responses expressed as a percentage of the values for Run 94.

TABLE 2.18

INVESTIGATION OF HORIZONTAL SLAB MESH FINENESS -- SERIES C

RUN	NUMEL	(2a/h)	δ_i		q_i		σ_i	
			mils	%	psi	%	psi	%
99	36	2.5	2.077	80.16	0.2858	82.96	23.93	57.80
98	64	1.875	2.112	81.51	0.3105	90.13	28.56	68.98
97	100	1.5	2.135	82.40	0.3228	93.70	31.82	76.86
96	144	1.25	2.151	83.02	0.3321	96.40	34.28	82.80
95	196	1.07	2.165	83.56	0.3380	98.11	36.22	87.49
100	256	0.9375	2.177	84.02	0.3427	99.48	37.83	91.37
ILLI-SLAB		1.5	2.591	100	0.3445	100	41.40	100

Notes:

-See Table 2.1 for problem specifications, and Fig. 2.2 for typical mesh.

-Subgrade Lateral Extent Beyond Slab Edges, X = 35 ft (consists of two elements); Total Depth of Subgrade, Z = 30 ft (consists of five layers).

-Applied Load: 6-in. by 6-in. @ 100 psi.

-For location of and extrapolation method for maximum responses, see Table 2.2.

-Responses expressed as a percentage of the values for the ILLI-SLAB Run.

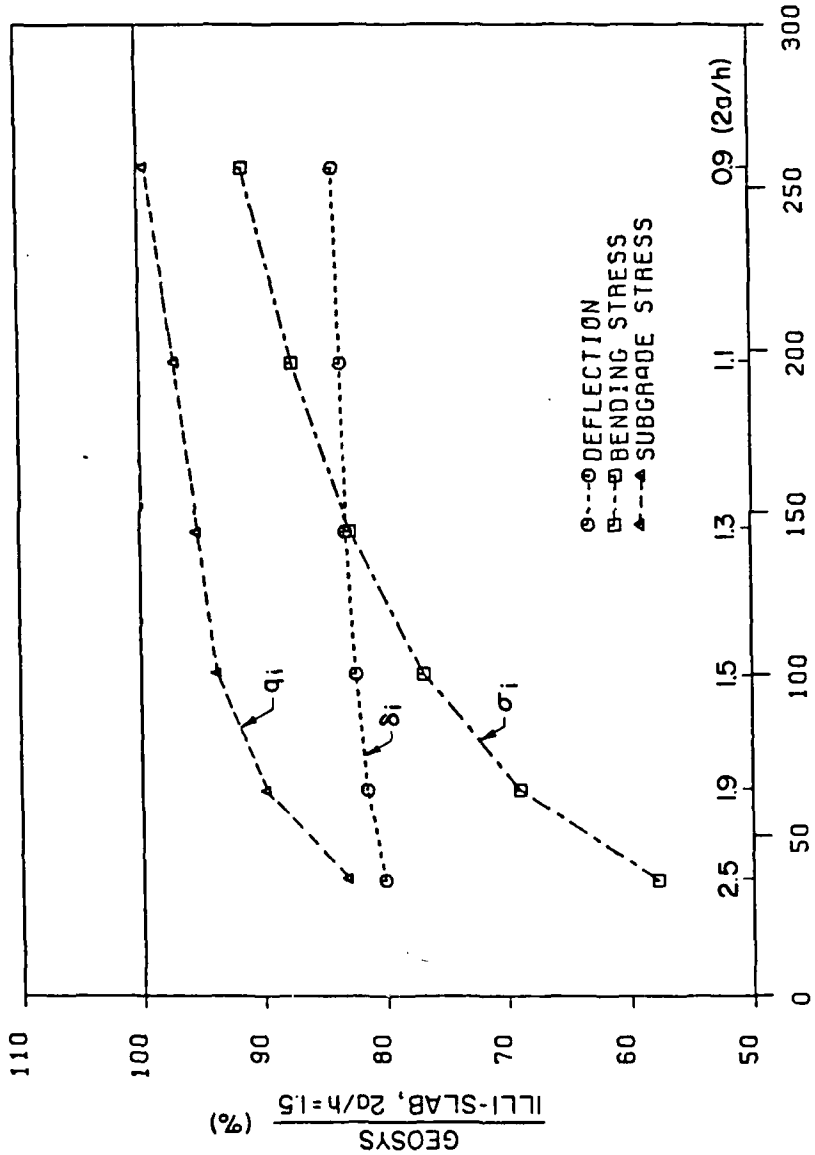

Fig. 2.20 Effect of Horizontal Slab Mesh Fineness (Interior Loading)

μ_s under these conditions is examined below using two series of runs. The model used is basically that in Run 5 (see Table 2.1 and Fig. 2.2), with some modifications as described below.

In Series A, the lateral boundaries are located at 30 ft (8 ℓ_e) beyond the slab, and the subgrade extends to a depth of 30 ft (8 ℓ_e). Maximum responses from these runs are presented in Table 2.19 and are plotted in a normalized fashion in Fig. 2.21. These show that deflection and subgrade stress are more sensitive to the value of μ_s than bending stress. Maximum deflection decreases with μ_s for values above about 0.3, while maximum subgrade stress increases by about the same amount under these conditions. Figure 2.22 shows the deflection profiles for the three runs in Table 2.19. It is observed that for the higher μ_s values, the subgrade behaves increasingly like an incompressible material, displacing upward in the region beyond the slab.

The runs in Series B are similar to those in Series A, with the exception that the lateral boundaries are only 7.5 ft (2 ℓ_e) beyond the slab, while the vertical extent of the subgrade is increased to 35 ft (9 ℓ_e). The trends in Table 2.20 are also very similar to those observed with Series A, above. Maximum deflection is significantly more sensitive to μ_s under these conditions.

TABLE 2.19

EFFECT OF SUBGRADE POISSON'S RATIO -- SERIES A

RUN	μ_s	δ_i		q_i		σ_i	
		mils	%	psi	%	psi	%
48	0.1	2.296	106	0.2758	94	33.22	98
47	0.3	2.318	107	0.2740	93	33.94	100
37	0.45	2.170	100	0.2940	100	33.96	100

Notes:

-See Table 2.1 for problem specifications, and Fig. 2.2 for typical mesh.

-Subgrade Lateral Extent Beyond Slab Edges, X = 30 ft; Total Depth of Subgrade, Z = 30 ft.

-For location of and extrapolation method for maximum responses, see Table 2.2.

-Responses expressed as a percentage of the values for Run 37.

AD-A174 987 THREE-DIMENSIONAL FINITE ELEMENT ANALYSIS OF A SLAB ON STRESS DEPENDENT E..(U) ILLINOIS UNIV AT URBANA DEPT OF CIVIL ENGINEERING A M IOANNIDES ET AL. 31 OCT 86 2/3

UNCLASSIFIED AFOSR-TR-86-2108 AFOSR-82-0143 F/G 13/13 NL

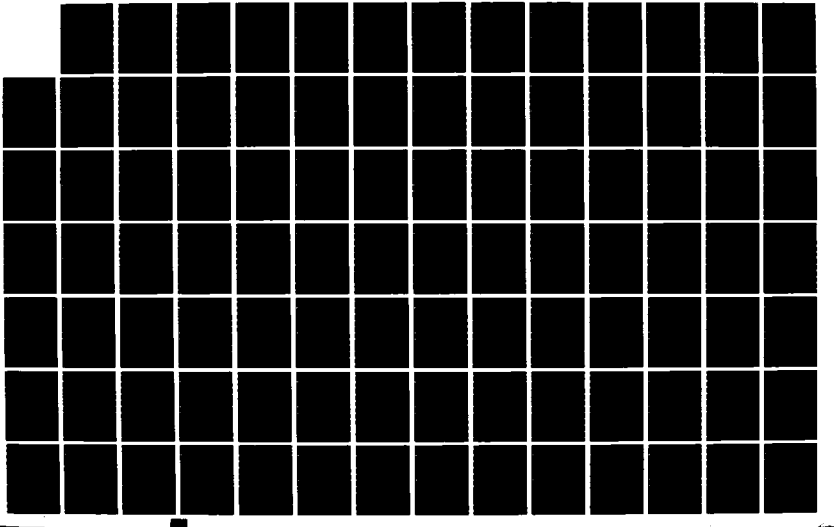

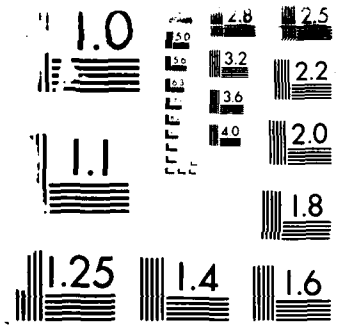
1.0
1.1
1.25
1.4
1.6
1.8
2.0
2.2
2.5
2.8
3.2
3.6
4.0

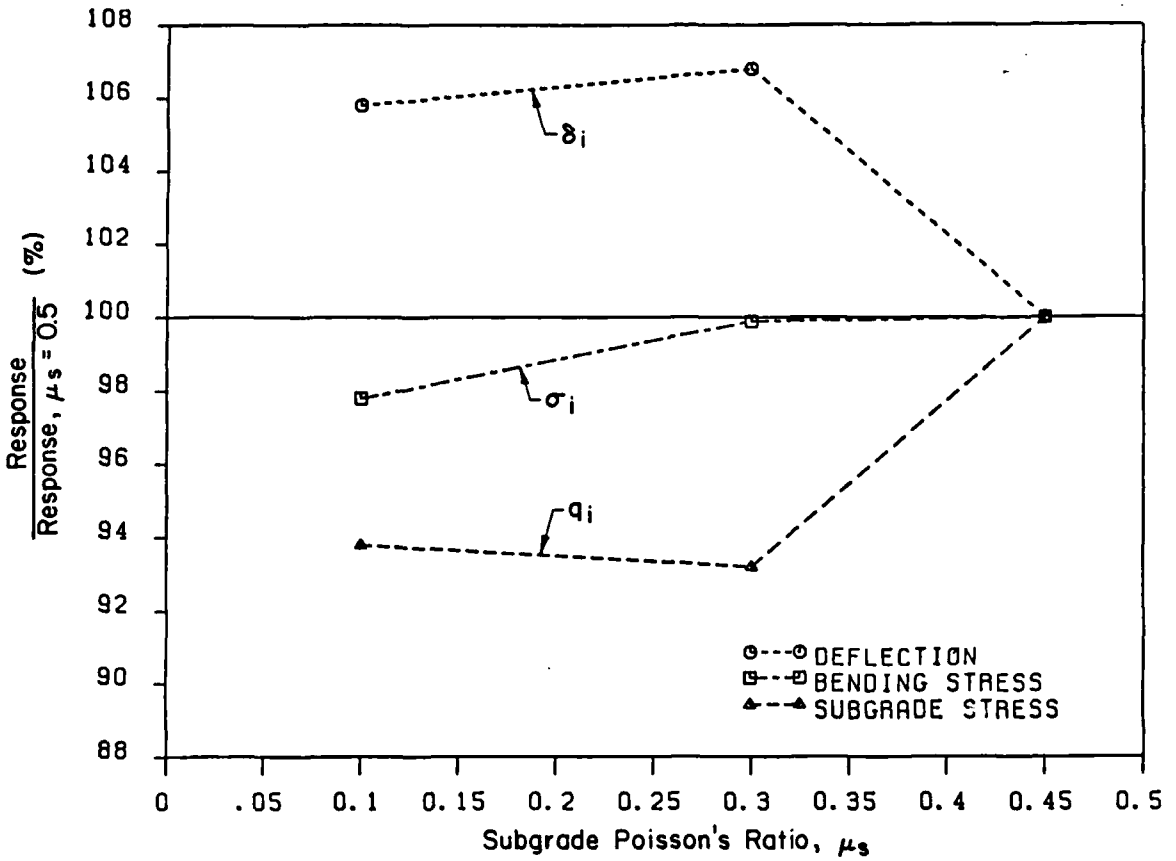

Fig. 2.21 Effect of Subgrade Poisson's Ratio on Maximum Responses

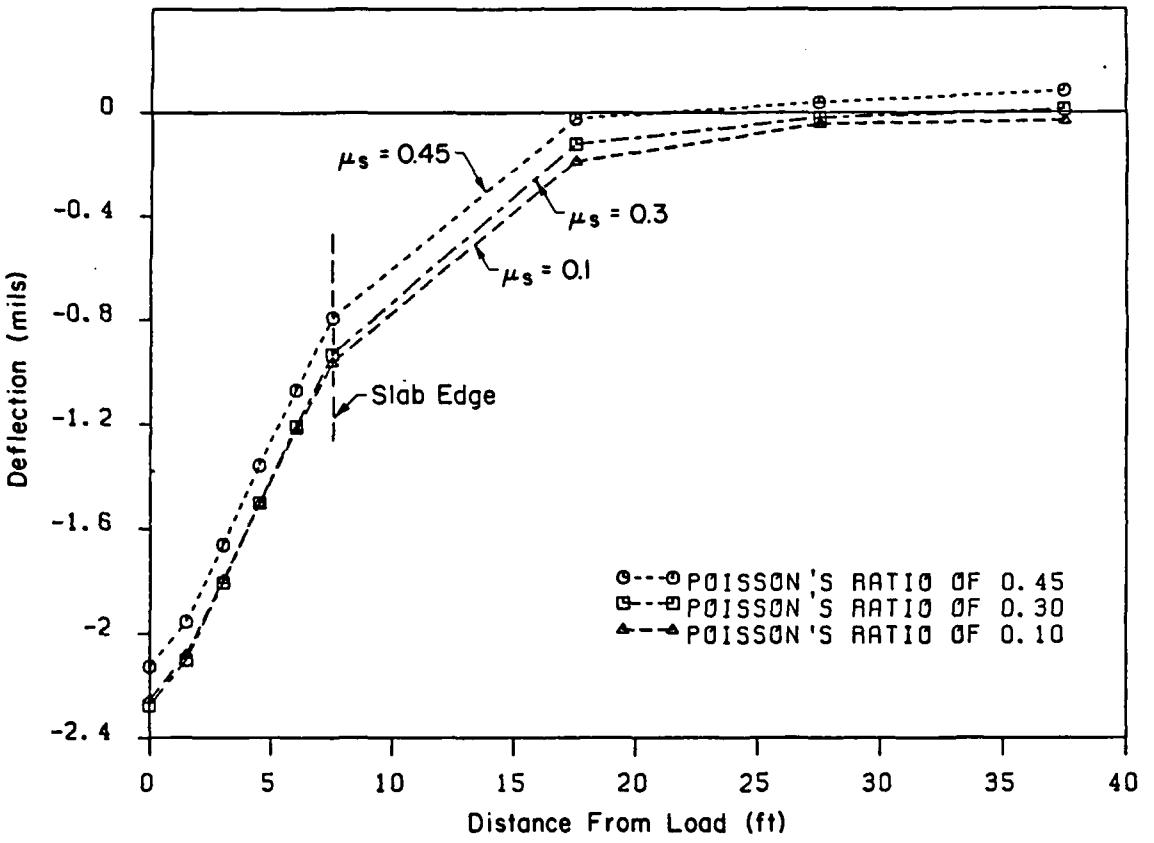

Fig. 2.22 Effect of Subgrade Poisson's Ratio on Subgrade Surface Deflection Profile

TABLE 2.20

EFFECT OF SUBGRADE POISSON'S RATIO -- SERIES B

RUN	μ_s	δ_i		q_i		σ_i	
		mils	%	psi	%	psi	%
50	0.10	2.173	140	0.2801	98	33.11	98
49	0.30	2.507	130	0.2749	96	33.79	100
13	0.45	1.932	100	0.2861	100	33.86	100

Notes:

-See Table 2.1 for problem specifications, and Fig. 2.2 for typical mesh.

-Subgrade Lateral Extent Beyond Slab Edges, X = 7.5 ft; Total Depth of Subgrade, Z = 35 ft.

-For location of and extrapolation method for maximum responses, see Table 2.2.

-Responses expressed as a percentage of the values for Run 13.

2.11 LATERAL SUBGRADE EXTENT FOR EDGE LOADING

The majority of the guidelines established above, for an adequate three-dimensional finite element model of a slab-on-grade under an interior load, may be applicable under the other two fundamental loading conditions, viz. edge and corner loading. Such guidelines include, for example, those pertaining to the vertical extent and mesh fineness for the subgrade, the division into layers of the slab, as well as the horizontal slab mesh fineness. It is considered, however, that for edge (and corner) loading, the area of subgrade immediately adjacent to the load becomes structurally more significant than under interior loading. For this reason, the conclusions reached in sections 2.4 and 2.8 with respect to the subgrade lateral extent and mesh fineness may not be adequate. In this section, the effect of the subgrade lateral extent under edge loading is investigated. The horizontal subgrade mesh fineness effect is considered in section 2.12, below.

The case considered here, is that of a point load applied at the edge of a square slab. This is symmetric and gives rise to three distinct subgrade areas, which can be considered separately. These are: the area adjacent to the loaded edge; the area adjacent to the edge at right angles to the loaded edge; and the area adjacent to the edge that is parallel to the loaded edge. Only results pertaining to the area adjacent to the load - which is the most critical - will be presented here. Additional data not included in this Report confirmed that the

guidelines established earlier may be considered to apply to the other two subgrade regions.

Two series of GEOSYS runs were performed for this investigation. Details of the parameters used are shown in Table 2.21. The main variable in the seven runs presented, is the lateral extent of the subgrade, X_a, adjacent to the loaded edge. The mesh for Run 72 is shown in Fig. 2.23. Maximum responses tabulated in Table 2.21 exhibit trends similar to those observed in section 2.4 for interior loading. Maximum bending stress seems largely insensitive to this effect, while maximum deflection and subgrade stress converge from below and from above, respectively.

To examine more closely the influence of the lateral extent in the region immediately adjacent to the loaded edge, runs in Series B were conducted. These employ three narrow elements in this region (2.5 ft each, compared to 10 ft or more in Series A). Results from these three runs are presented in Table 2.22. They indicate that performance is improved, and all three responses are practically independent of X_a.

Subgrade radial strain was shown earlier to correlate well with the effect of the lateral boundaries (see section 2.4). Therefore, a plot of radial strain, ε_{xx}, profiles beyond the loaded slab edge, for the three runs in Series B is presented in Fig. 2.24. These profiles are obtained at a depth of 1.5 ft below the subgrade surface (i.e. at the mid-depth of the first layer of subgrade elements), along the slab x-axis of symmetry by linear orthogonal extrapolation. All three profiles are very similar confirming the observations made with respect

TABLE 2.21

EFFECT OF LATERAL SUBGRADE EXTENT UNDER EDGE LOADING -- SERIES A

RUN	X_a (ft)	Divisions of X_a	δ_e mils	%	q_e psi	%	σ_e psi	%
68	20	2 @ 10'	3.492	95.86	0.7490	104.93	51.76	100.49
70	30	3 @ 10'	3.563	97.80	0.7329	102.68	51.66	100.29
71	35	2@12.5'; 1@10'	3.580	98.27	0.7221	101.16	51.61	100.19
72	40	2@15'; 1@10'	3.593	98.63	0.7139	100.01	51.51	100.00
73	45	2@17.5'; 1@10'	3.602	98.87	0.7076	99.13	51.43	99.84
76	50	3@13.3'; 1@10'	3.636	99.81	0.7193	100.77	51.54	100.06
77	55	3@15'; 1@10'	3.643	100	0.7138	100	51.51	100

Notes:

Slab: 15 ft x 15 ft x 1 ft
Soil: (X_a+15+7.5) ft x 30 ft x 30 ft
$E = 4 \times 10^6$ psi; $\mu = 0.15$
$E_s = 1 \times 10^4$ psi; $\mu_s = 0.45$
$\ell_e = 45.5$ in.
Load, P = 3600 lbs (edge; point load)
Mesh : See Fig. 2.23 (Run 72)

-Maximum deflection, δ_e, under edge point load, at top of slab.

-Maximum subgrade stress, q_e, under edge point load, at top of subgrade, by orthogonal linear extrapolation.

-Maximum bending stress, σ_e, under edge point load, at bottom of slab, by orthogonal linear extrapolation.

-Responses expressed as a percentage of the values for Run 77.

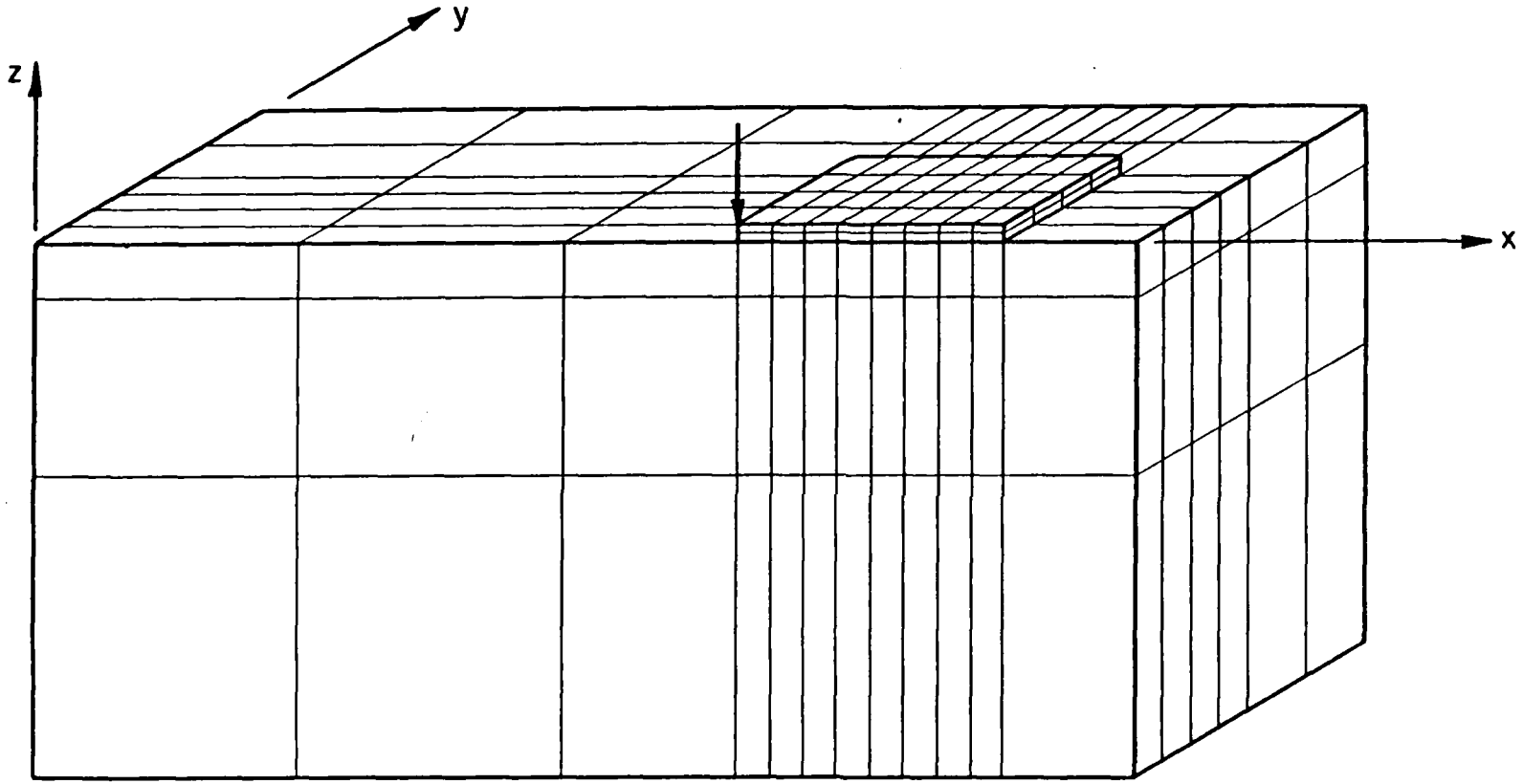

Fig. 2.23 Three-Dimensional Finite Element Mesh for Run 72

TABLE 2.22

EFFECT OF LATERAL SUBGRADE EXTENT UNDER EDGE LOADING -- SERIES B

RUN	X_a (ft)	Divisions of X_a	δ_e		q_e		σ_e	
			mils	%	psi	%	psi	%
81	30	2@11.25'; 3@2.5'	4.238	99.55	1.1552	99.69	57.57	100.09
80	40	2@16.25'; 3@2.5'	4.243	99.67	1.1558	99.74	57.52	100.00
83	50	3@14.16'; 3@2.5'	4.257	100	1.1588	100	57.52	100

Notes:

-See Table 2.21 for problem specifications, and Fig. 2.23 for typical mesh, except:
Soil: (X_a+15+20) ft x 85 ft x 30 ft.

-For location of and extrapolation method for maximum responses, see Table 2.21.

-Responses expressed as a percentage of the values for Run 83.

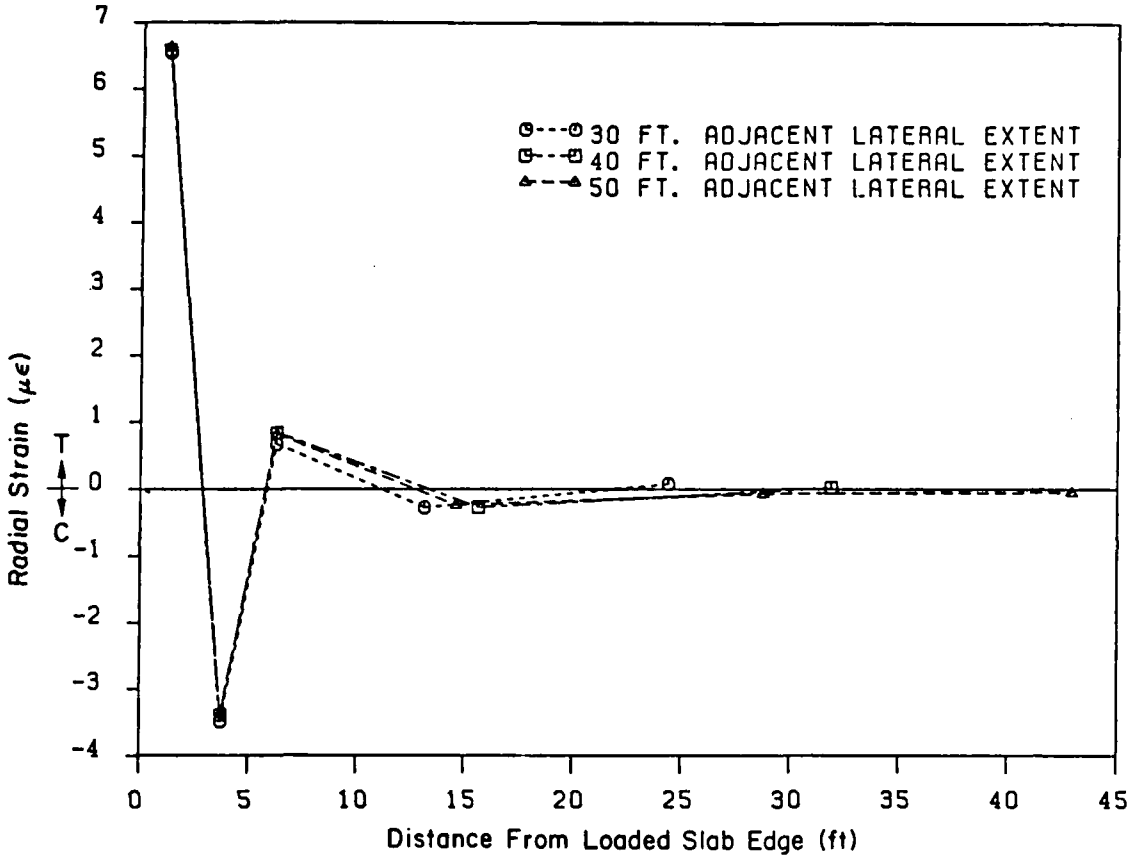

Fig. 2.24 Radial Strain, ε_{xx}, Distributions Along Slab x-Axis of Symmetry, at 1.5 ft Below Subgrade Surface (Beyond Slab, by Orthogonal Extrapolation): Effect of Adjacent Subgrade Lateral Extent

to maximum responses. Thus, provided the adjacent subgrade lateral extent beyond the slab edges, X_a, is about 40 ft (10 ℓ_e) or more, the fineness of the elements right next to the loaded edge is the overriding consideration. This factor is examined below.

2.12 HORIZONTAL SUBGRADE MESH FINENESS FOR EDGE LOADING

Following the same reasoning as in section 2.11, only the portion of the subgrade adjacent to the loaded edge will be considered here. For the remainder, the guidelines established using interior loading may be considered applicable.

This investigation was conducted in a manner similar to that employed in section 2.7 for the vertical division of the subgrade. Thus, the subgrade in the horizontal direction may be considered to consist of three portions: an inner region adjacent to the loaded edge, a transition portion, and an outer part beyond the transition zone to the lateral boundary. A total adjacent subgrade lateral extent beyond the slab edges, X_a, of 50 ft (13 ℓ_e) was assumed, with 42.5 ft (11 ℓ_e) constituting the outer portion, while the 7.5 ft (2 ℓ_e) next to the loaded slab edge made up the transition and inner regions. This division is suggested by Fig. 2.24.

The effect of the mesh fineness in the outer portion was considered first through the runs of Series A. Results from these are presented in Table 2.23. The only variable here is the number, NOUTER, of elements of equal width, covering the 42.5 ft of the outer region. The 7.5 ft of

TABLE 2.23

EFFECT OF HORIZONTAL SUBGRADE MESH FINENESS FOR EDGE LOADING -- SERIES A

RUN	NOUTER	δ_e		q_e		σ_e	
		mils	%	psi	%	psi	%
85	1	4.198	98.61	1.1589	100.27	57.46	99.90
86	2	4.245	99.72	1.1569	100.10	57.49	99.95
83	3	4.257	100	1.1558	100	57.52	100

Notes:

-See Table 2.21 for problem specifications, and Fig. 2.23 for typical mesh, except:
Soil: 95 ft x 100 ft x 30 ft.

-Width of Inner Portion = 5.0 ft (consists of two elements of equal width);
Width of Transition Portion = 2.5 ft (consists of one element);
Width of Outer Portion = 42.5 ft (consists of NOUTER elements of equal width);
Total Adjacent Lateral Extent of Subgrade Beyond Slab Edges, X_a = 50 ft.

-For location of and extrapolation method for maximum responses, see Table 2.21.

-Responses expressed as a percentage of the values for Run 83.

the transition and inner portions, were divided into three elements (each 2.5 ft wide) in all three runs. The first two of these elements constitute the inner region, and the third forms the transition portion. Maximum responses in Table 2.23 suggest that the system is fairly insensitive to this effect. Looking at the radial strain, ε_{xx}, profiles in Fig. 2.25, however, indicates that using only one element in the outer region may be inadequate. At least two elements should be used in the outer element range for best results.

The sensitivity of the inner region, assumed here to consist of the 5.0 ft adjacent to the loaded edge, may be expected to be higher. To investigate this, Series B consisting of four runs was conducted. One 22.5-ft element was used in each of the outer and transition portions. The only variable in these runs is the number, NINNER, of elements of equal width, covering the 5.0 ft of the inner range. Maximum responses are shown in Table 2.24, and are plotted in a normalized form in Fig. 2.26. Results confirm the higher sensitivity of the solution to this effect, especially of maximum subgrade stress. In fact, a value of (2a/h) below 1.0 appears to be necessary for the convergence of q_e. Further evidence for this is provided by the deflection profiles of the subgrade surface beyond the loaded edge for Series B runs, shown in Fig. 2.27. These suggest that within the first 3 ft (0.75 ℓ_e) from the slab, five or more elements should be provided ($2a/h \leq 1.0$), while from 3 to 5 ft (0.75 to 1.25 ℓ_e) only two elements can suffice ($2a/h \leq 2.5$).

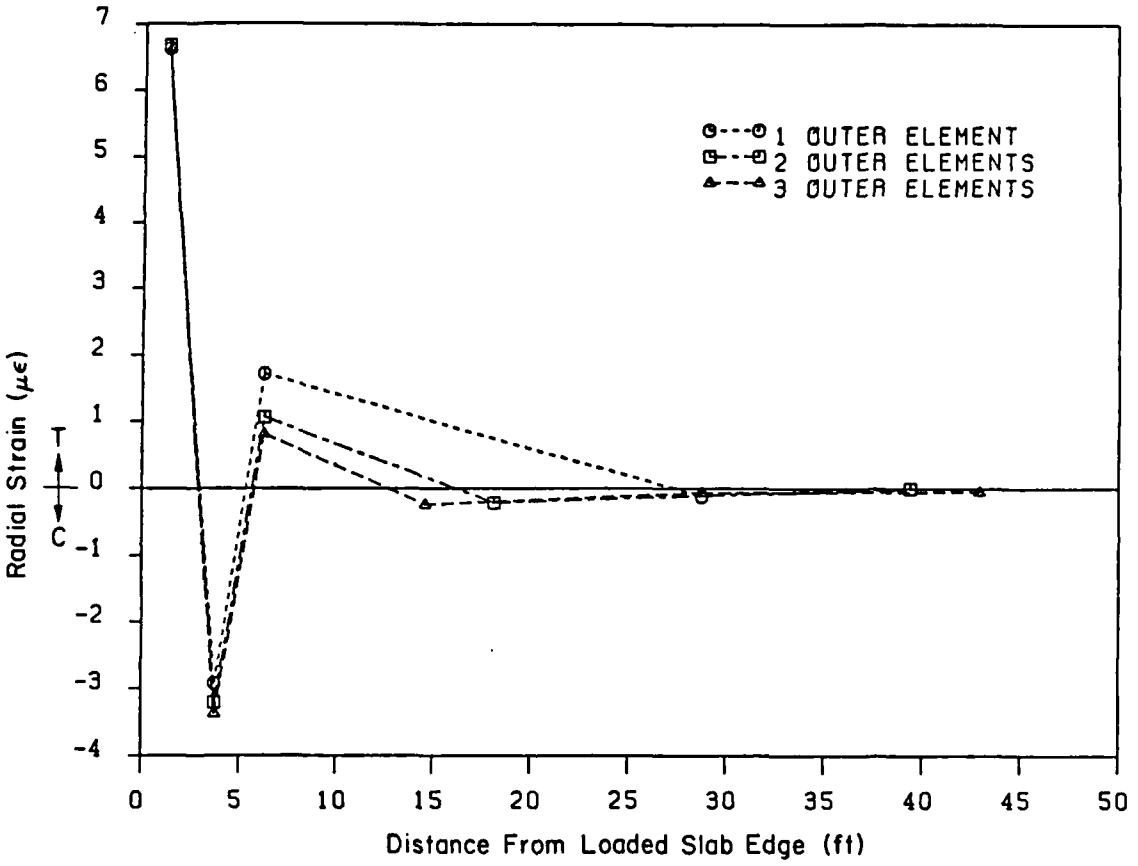

Fig. 2.25 Radial Strain, ε_{xx}, Distributions Along Slab x-Axis of Symmetry, at 1.5 ft Below Subgrade Surface (Beyond Slab, by Orthogonal Extrapolation): Effect of Subgrade Outer Portion Mesh Fineness

TABLE 2.24

EFFECT OF HORIZONTAL SUBGRADE MESH FINENESS FOR EDGE LOADING -- SERIES B

RUN	NINNER	δ_e		q_e		σ_e	
		mils	%	psi	%	psi	%
89	2	4.207	97.43	1.1581	88.65	57.39	98.34
87	3	4.275	99.00	1.2437	95.20	58.01	99.40
90	4	4.303	99.65	1.2842	98.30	58.25	99.81
91	5	4.318	100	1.3064	100	58.36	100

Notes:

-See Table 2.21 for problem specifications, and Fig. 2.23 for typical mesh, except:
Soil: 95 ft x 100 ft x 30 ft.

-Width of Inner Portion = 5.0 ft (consists of NINNER elements of equal width);
Width of Transition Portion = 22.5 ft (consists of one element);
Width of Outer Portion = 22.5 ft (consists of one element);
Total Adjacent Lateral Extent of Subgrade Beyond Slab Edges, X_a = 50 ft.

-For location of and extrapolation method for maximum responses, see Table 2.21.

-Responses expressed as a percentage of the values for Run 91.

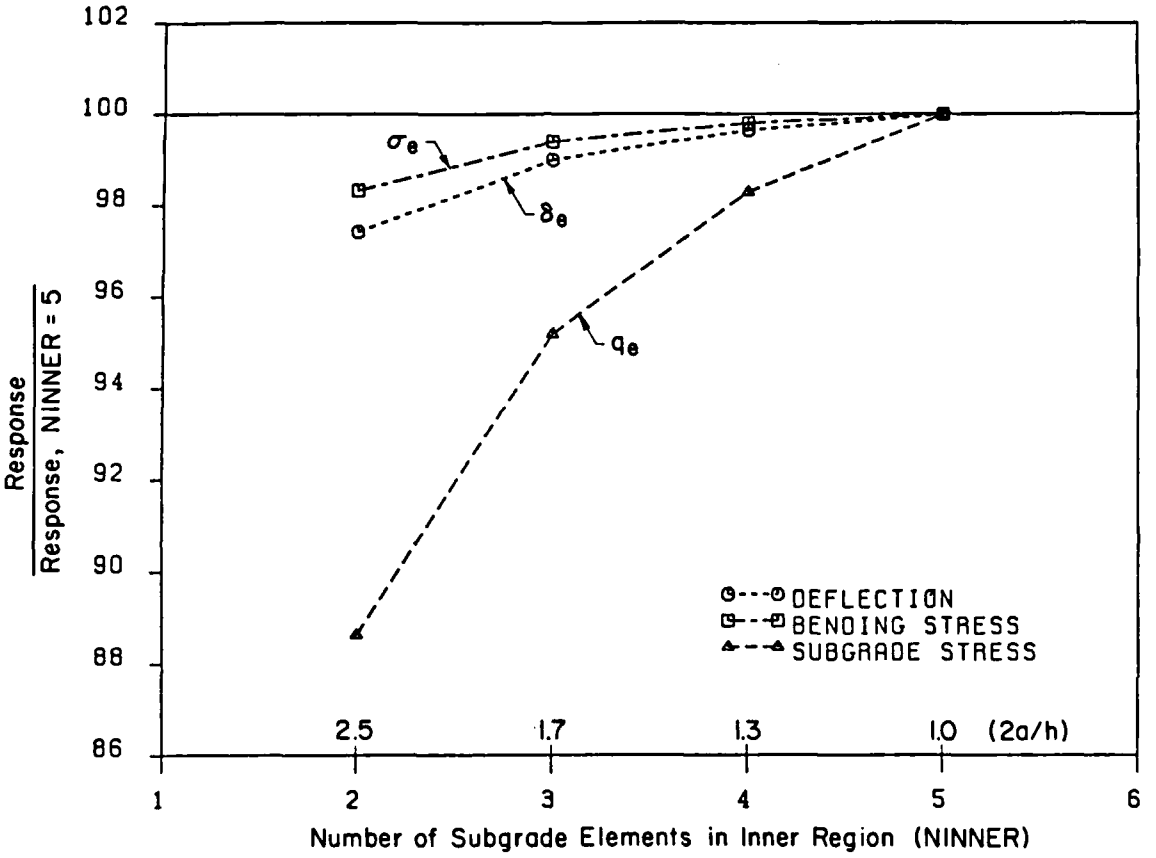

Fig. 2.26 Effect of Subgrade Inner Portion Mesh Fineness on Maximum Responses

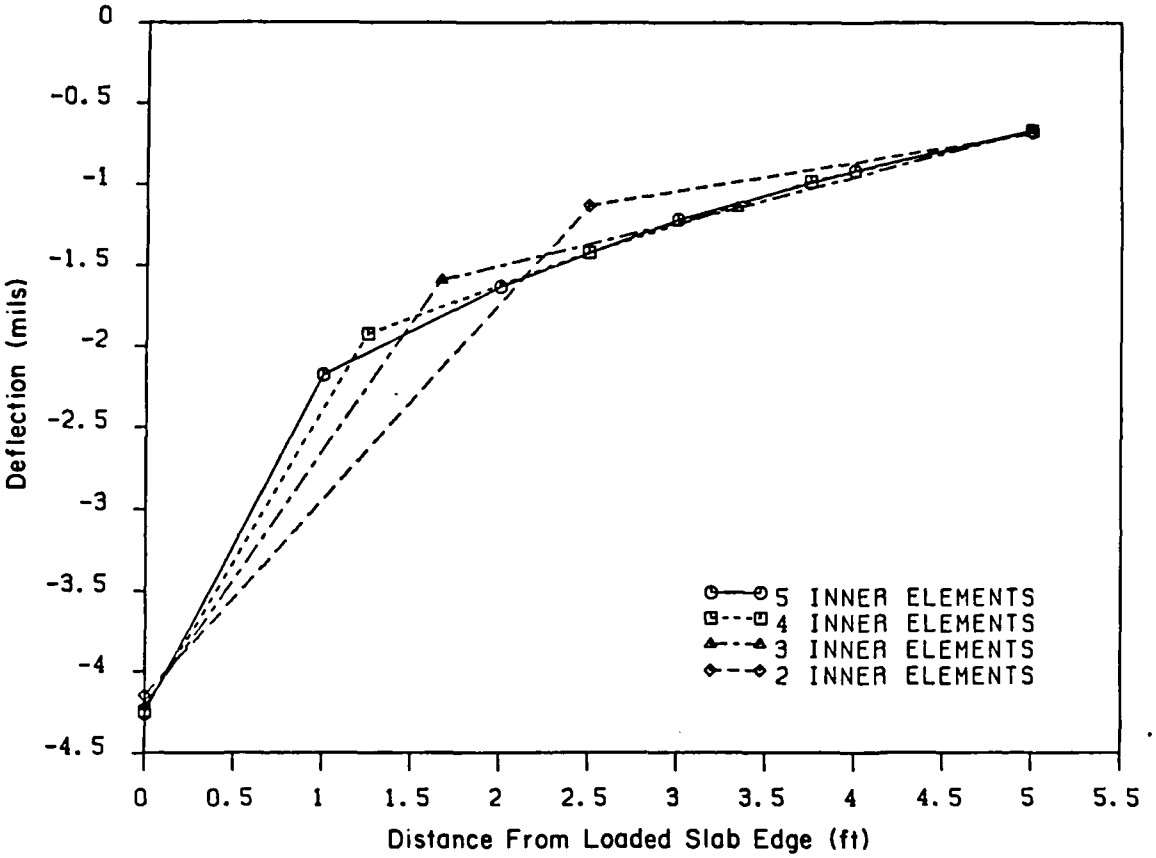

Fig. 2.27 Effect of Subgrade Inner Portion Mesh Fineness on Subgrade Surface Deflection Profile, Beyond Slab

2.13 HORIZONTAL SLAB MESH FINENESS FOR EDGE LOADING

Two-dimensional analyses of a slab-on-grade indicate that slab mesh fineness guidelines established for an interior load may be applicable to the other two loading conditions, i.e. edge and corner. The paramount importance of this factor, however, dictates an investigation of the requirements for accurate results under edge loading.

Four runs were performed using the mesh shown in Fig. 2.28, except that the number of elements used in the slab was varied. Maximum responses from these runs are presented in Table 2.25. Figure 2.29 is a normalized plot of the same results. The usual trend of convergence from below is observed once again, with subgrade and bending stresses being much more sensitive than deflection to mesh fineness. It appears that a value of (2a/h) below 1.5 is needed for convergence of maximum bending stress. The dramatic increase in execution costs, however, may preclude such an option, even if the memory capacity of the computer is not exceeded. A possible solution is to provide a graded mesh, i.e. use finer elements in the vicinity of the load, and provide for a smooth transition to coarser ones farther away. This technique proved very effective in two-dimensional studies, especially when element aspect ratios, were kept near or below 3. No attempt was made here to establish guidelines for gradation of the three-dimensional finite element mesh.

Alternatively, an estimate of the error in the solution using a coarse mesh can be obtained from Figures 2.20 and 2.29. For the

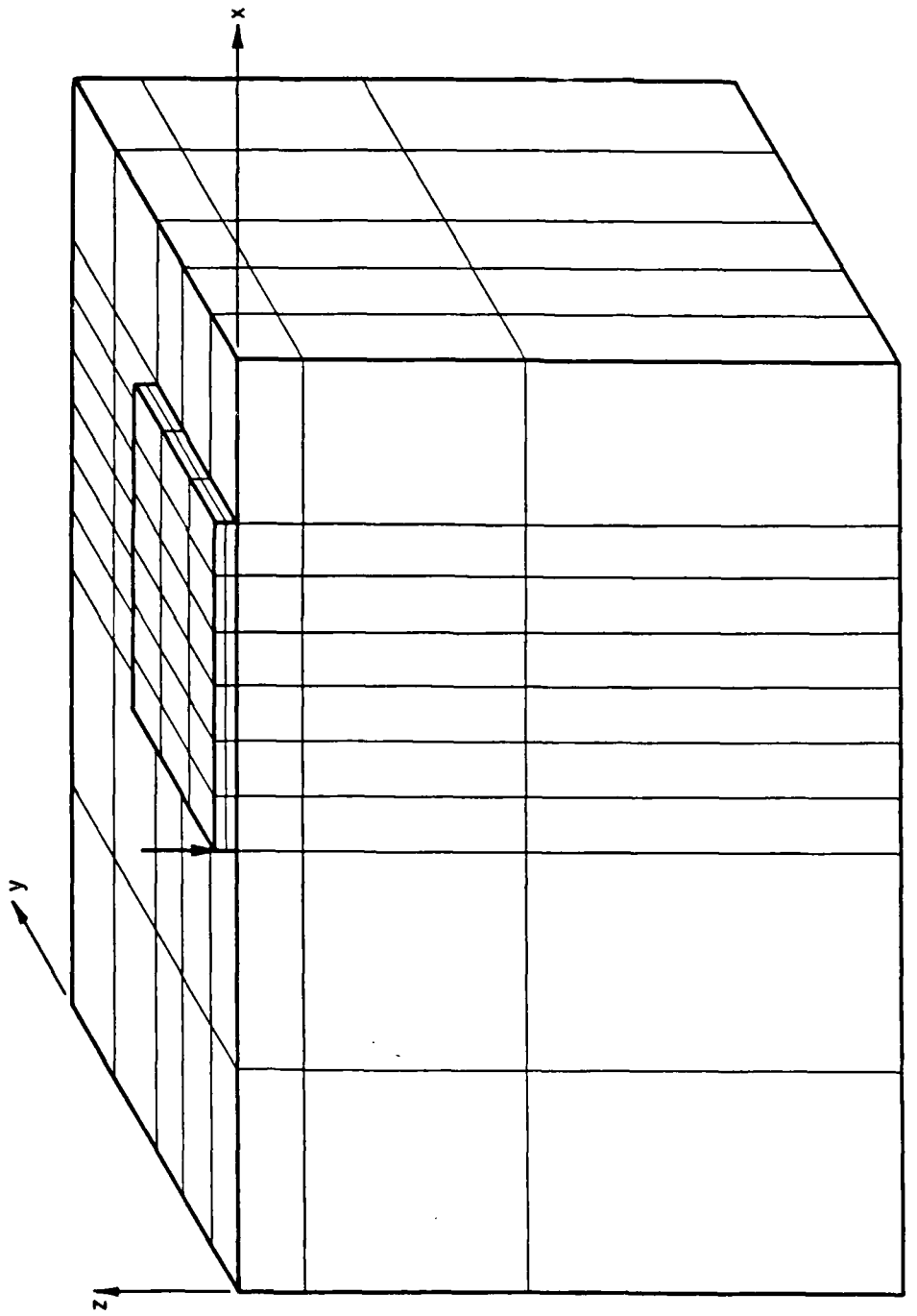

Fig. 2.28 Three-Dimensional Finite Element Mesh for Run 67

TABLE 2.25

EFFECT OF HORIZONTAL SLAB MESH FINENESS FOR EDGE LOADING

RUN	NUMEL	(2a/h)	CYBER Cost ($)	δ_e		q_e		σ_e	
				mils	%	psi	%	psi	%
66	16	3.75	6	3.167	88.84	0.5827	73.09	25.70	43.28
67	36	2.5	13	3.380	94.81	0.6704	84.09	38.08	64.13
68	64	1.875	31	3.492	97.95	0.7490	93.95	51.76	87.17
69	100	1.5	341	3.565	100	0.7972	100	59.38	100

Notes:

-See Table 2.21 for problem specifications, and Fig. 2.28 for typical mesh (Run 67), except:
Soil: 42.5 ft x 37.5 ft x 30 ft.

-For location of and extrapolation method for maximum responses, see Table 2.21.

-Responses expressed as a percentage of the values for Run 69.

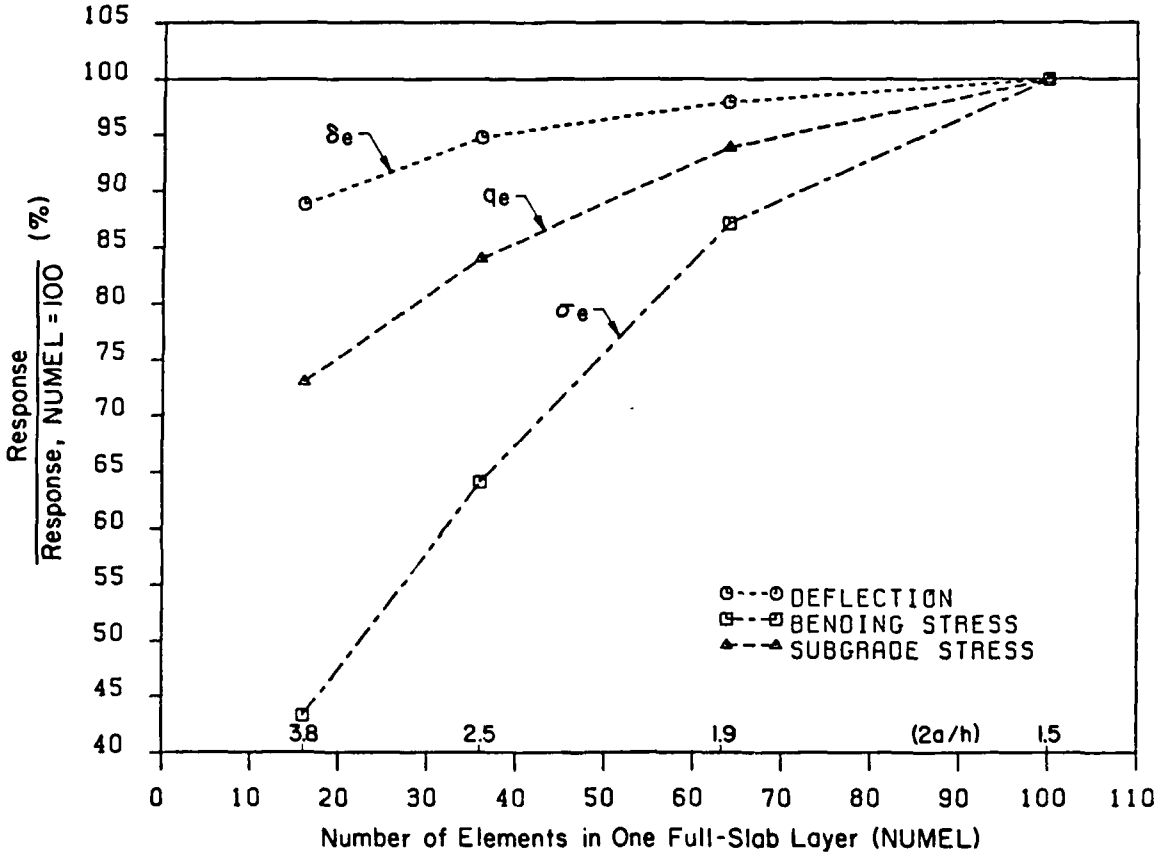

Fig. 2.29 Effect of Horizontal Slab Mesh Fineness (Edge Loading)

purposes of this study (which involves mainly relative rather than absolute response values) a value of (2a/h) below 1.5 was selected. The primary consideration for this is execution time, rather than per run costs, since most of the runs reported below have been performed on the HARRIS 800-2 virtual memory computer of the Department of Civil Engineering at the University of Illinois.

CHAPTER 3

THE INTERIOR LOAD CASE

3.1 ACCOUNTING FOR STRESS DEPENDENCE

To account for the stress dependent behavior of typical fine-grained subgrade soils, Thompson and Robnett [22] have proposed a resilient modulus characterization for the elastic solid foundation. This not only introduces soil nonlinearity but also, perhaps more importantly, accounts for the apparent increase in subgrade stiffness produced by rapidly moving, repeated loads. This loading condition is considered more appropriate for the type of moving loads applied by modern-day aircraft traffic.

The resilient modulus, E_R, of a subgrade may be defined as:

$$E_R = \sigma_D / \varepsilon_r$$

where:

σ_D : repeated deviator stress; and

ε_r : recoverable axial strain.

Extensive resilient laboratory testing, nondestructive testing, and pavement analysis and design studies at the University of Illinois [29; 30; 31] have confirmed that the E_R-deviator stress relations developed for Illinois soils are representative of soils exhibiting stress softening behavior. These are shown in Fig. 3.1, and are currently

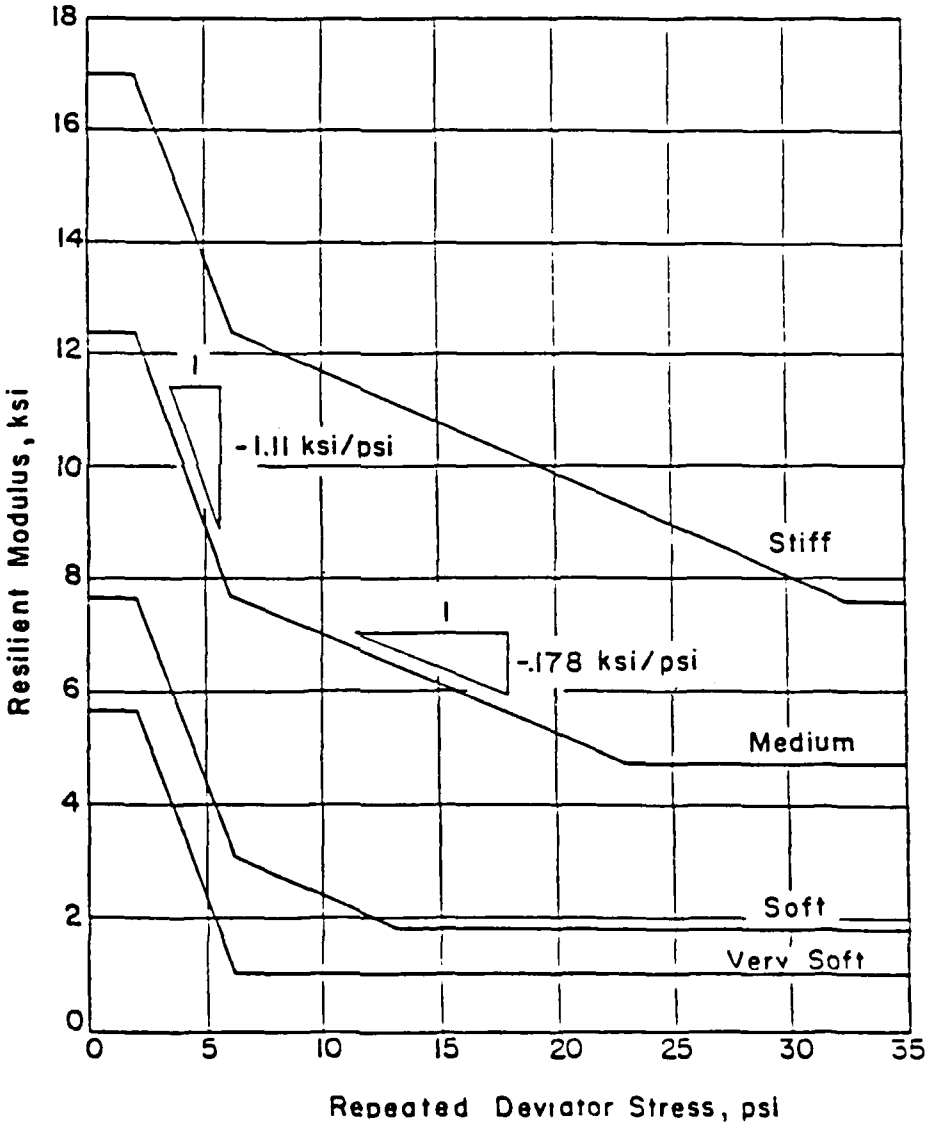

Fig. 3.1 Subgrade Soil Material Models for ILLI-PAVE Analyses

incorporated into finite element program ILLI-PAVE [21], which has been extensively used at the University of Illinois.

Simplified versions of the curves for stress dependent subgrades in Fig. 3.1 can be incorporated into the three-dimensional GEOSYS analysis. This is achieved through a post-processor, a program that receives as input results from GEOSYS (see section 1.6). A modified E_R v. σ_D relation for the 'SOFT' subgrade is employed in this study. This is shown in Fig. 3.2. The deviator stress has been defined in this case as the maximum difference between the three principal stresses determined by GEOSYS.

The process used to determine the resilient properties for each of the subgrade elements is an iterative one. First, assumed values of E_s and μ_s are provided as input to GEOSYS. The initial value of E_s is usually the value of E_R for $\sigma_D \leq 2.0$ psi, or 7682 psi for the 'SOFT' subgrade. Using these values, GEOSYS is executed and subgrade deviator stress is determined for each subgrade element. The post-processor receives these stresses which it separates, for practical reasons, into seven groups, depending on the level of σ_D. The range of σ_D in each group is given in Table 3.1. For the average value of σ_D in each group, a corresponding E_R value for the subgrade elements in that group is determined, using the relation in Fig. 3.2. Finally, the post-processor prepares a new input file for GEOSYS, which reflects the updated values of E_R in overstressed subgrade elements. A second GEOSYS run is performed, and the process is repeated until specified closure criteria are satisfied.

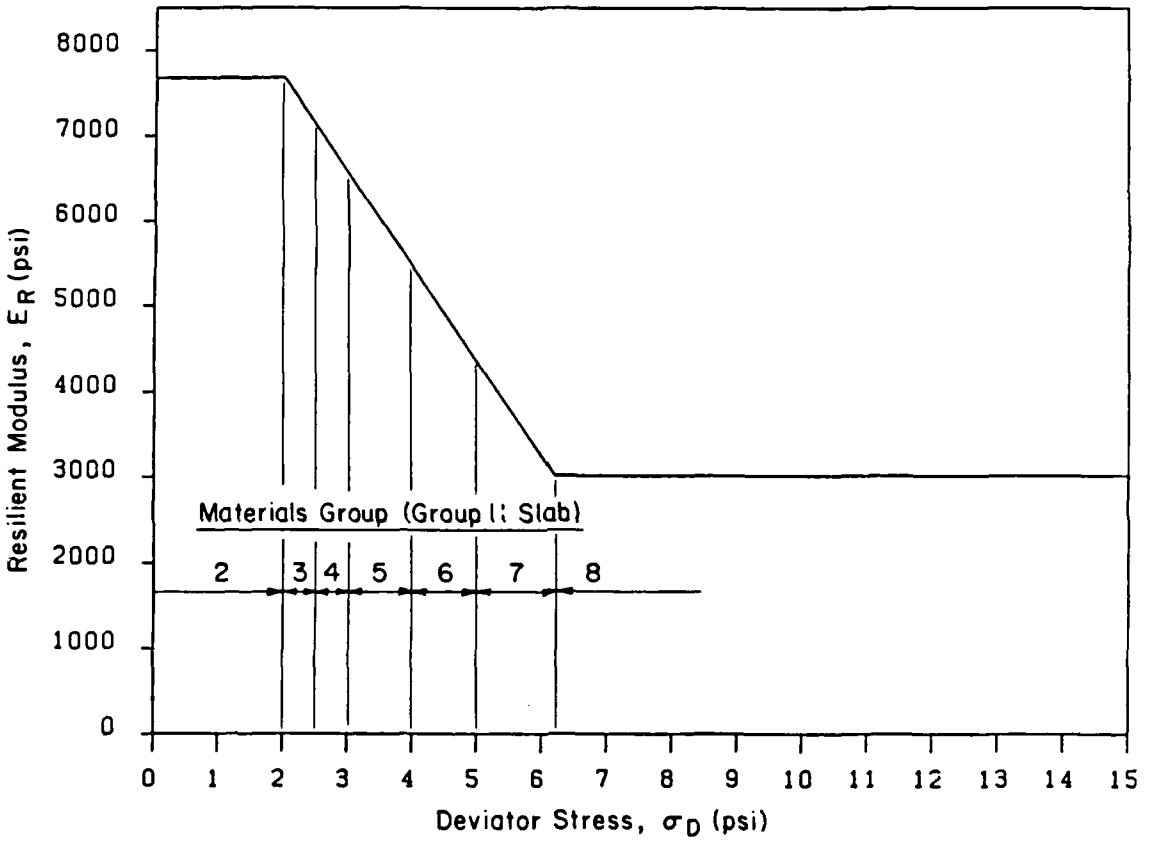

Fig. 3.2 Simplified E_R v. σ_D Relation for 'SOFT' Subgrade for Use in GEOSYS

TABLE 3.1

MATERIAL GROUP DEFINITIONS

(a) PAVEMENT SLAB GROUP

Group No.
1

(b) SUBGRADE GROUPS

Group No.	σ_D Range (psi)
2	≤2.0
3	2.0-2.5
4	2.5-3.0
5	3.0-4.0
6	4.0-5.0
7	5.0-6.2
8	≥6.2

Several possible closure criteria have been examined. The first was to demand that no elements change E_R subgrade group after the last iteration. The excessive cost of the large number of iterations required to achieve such a complete convergence, precludes the use of this criterion. An alternative was sought in specifying a small tolerance on the change in the values of maximum responses from two consecutive iterations. The method finally adopted consisted of performing three iterations, and using the average of the results from the second and third iterations. As shown in subsequent sections, these average values are indicative of the response obtained after several iterations, with adequate accuracy.

3.2 FINITE ELEMENT MODEL FOR SINGLE-WHEEL INTERIOR LOADING

In a previous study, the authors have shown that subgrade stress dependence is not important when slab-on-grade pavements are loaded by a single tire-print at the interior [14]. This conclusion was reached using the K_R or Resilient Subgrade model [12; 13], which is a variant of the conventional Winkler foundation characterization. Although stress dependence will probably not affect the interior loading behavior of a slab on an elastic solid either, completeness demands that this case be investigated, together with the edge and corner loading conditions.

To magnify any subgrade stress dependence effects, this study considered a relatively high load on a thin slab (8-in. thick), resting on the 'SOFT' subgrade. The load applied at the interior is an F-15

single-wheel load (SWL) of 30 kips at 355 psi. Other pertinent information for this run is given in Table 3.2. This Table also presents the maximum responses from GEOSYS, ILLI-SLAB [2; 6], and the closed-form solutions [26]. The mesh used for the GEOSYS run is shown in Fig. 3.3. In view of symmetry, only one-quarter of the system needs to be modeled.

3.3 DISCUSSION OF RESULTS FOR F-15 SWL AT THE INTERIOR

3.3.1 Effect of Subgrade Stress Dependence

A good indicator of the effect of subgrade stress dependence is the number of elements exceeding the 2 psi limit in σ_D, below which constant modulus behavior is assumed. For this GEOSYS run, only 5 out of 54 subgrade elements (or 9%) had a σ_D above 2 psi. The range of σ_D values in these elements was 2.059 to 2.270 psi, with an average of 2.135 psi. The five overstressed elements (which in a subsequent iteration would change subgrade group) were located in the upper 2.5 ft of the subgrade, underneath the applied load. The updated E_R value for these would be 7533 psi, a decrease of less than 2% from the initial 7682 psi assumed for the constant, low stress foundation modulus. It is evident that additional runs would not be very useful since such a small change cannot be expected to affect the system significantly.

The implications of these results, however, are of considerable value. For the interior loading case, the slab distributes the load effectively so that the subgrade is not subjected to high stresses.

TABLE 3.2

INVESTIGATION OF INTERIOR LOADING: F-15 SWL

SOLUTION	δ_i		q_i		σ_i	
	mils	%	psi	%	psi	%
GEOSYS-3D (Cycle 1)	32.15	90	5.031	104	609.55	96
ILLI-SLAB-2D	37.26	104	5.099	106	697.18	110
CLOSED-FORM	35.92	100	4.832	100	636.63	100

Notes:

$E = 4 \times 10^6$ psi $\mu = 0.15$ h = 8 in.
$E_s = 7682$ psi ('SOFT') $\mu_s = 0.45$ $\ell_e = 33.10$ in.
Slab: 15 ft x 15 ft ($L/\ell_e = 5.44$)
Load: 30 kips @ 355 psi, converted to 4 work equivalent loads
(c = 9.193 in.)

-GEOSYS Mesh: See Fig. 3.3 (double symmetry - slab extends between underlined coordinates);
x-coordinates: 0; 30; 35; 36.5; 38; 39; 40; 41; 41.75; 42.5 ft
y-coordinates: 42.5; 12.5; 7.5; 6; 4.5; 3.5; 2.5; 1.5; 0.75; 0 ft
z-coordinates: 0.6; 0.3; 0; -0.5; -1.0; -2.5; -6.5; -17.5; -40 ft
In slab: $(2a/h)_{min}$=1.125; χ=3.92; α_{max}=2.0; (c/2a)=0.511.

-All responses are at interior of slab, under load:
δ_i : at top of slab;
q_i : at surface of subgrade, by diagonal extrapolation;
σ_i : at bottom of slab, by orthogonal extrapolation of σ_x values.

-ILLI-SLAB-2D: (2a/h) = 0.75; square elements;
CLOSED-FORM: Equations by Losberg [26], for infinite slab.

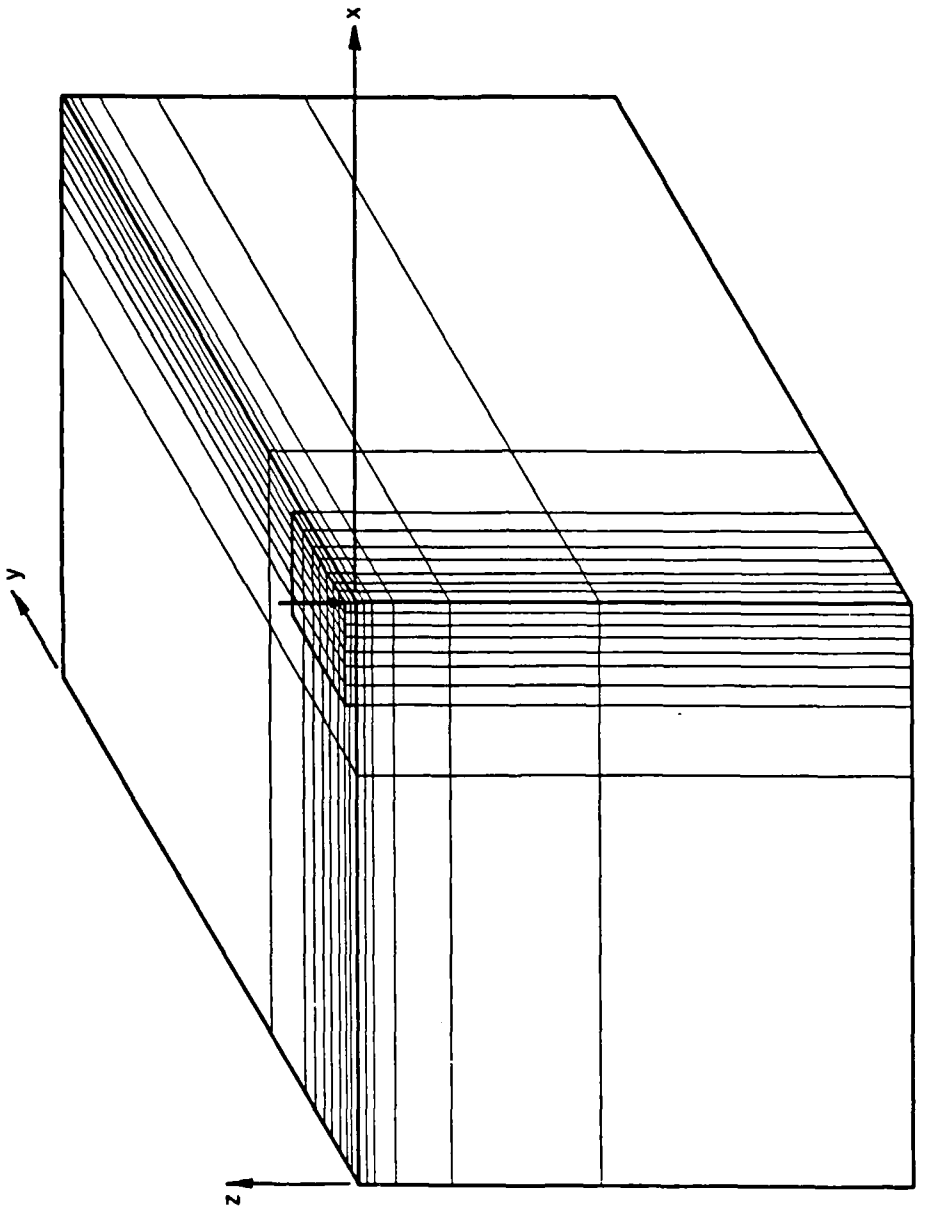

Fig. 3.3 Three-Dimensional Finite Element Mesh for F-15 Interior SWL Runs

This is especially true if, unlike the section employed here, a thicker slab is used to reduce bending stresses. This study confirms that subgrade stress dependence is not important for the interior loading case, and that additional iterations would not provide any benefits.

3.3.2 Comparison With Two-Dimensional Results

In Table 3.2, maximum responses from the three-dimensional GEOSYS run, are compared to those from a similar two-dimensional ILLI-SLAB run. Values predicted by the closed-form solutions [26] are also tabulated. The ILLI-SLAB run employed a rather fine mesh, with (2a/h) of 0.75. One-quarter of the slab was divided into 225 square elements, compared to only 49 elements used in the GEOSYS model. According to the results of extensive investigations using ILLI-SLAB [6; 2], such a fine mesh is necessary for results of adequate accuracy. The coarseness of the GEOSYS mesh is considered to be the prime source of the discrepancy between the finite element results and the closed-form solutions. For the value of (2a/h) of 1.125 used in the vicinity of the applied load in the GEOSYS mesh in Fig. 3.3, Fig. 2.20 indicates that a σ_i value about 5% too low, and a q_i value 2% too low may be expected, while δ_i should be accurately predicted. This would partly explain the discrepancy in the σ_i value from GEOSYS, but not those observed in the corresponding δ_i and q_i results. The latter are probably due to the fact that the mesh near the load needs to be even finer than elsewhere. In the mesh shown in Fig. 3.3 the load covers only partially the central element (c/2a = 0.51),

which leads to inaccuracies when the applied load is converted to four work equivalent nodal loads.

The necessity for an even finer mesh under the load than elsewhere was confirmed in a previous study [7]. This additional mesh fineness requirement over the area of applied load can also explain the high ILLI-SLAB results. All three responses may be expected to converge from above as the tire-print is subdivided into more elements. This assertion is reinforced by preliminary results obtained using the Cray X-MP/24 supercomputer. It is worth noting that convergence is ordinarily from below as the mesh (over the entire slab) is refined (Fig. 3.4).

Both GEOSYS and ILLI-SLAB results are also affected by the finite size of the slab in these analyses (compared to the infinite slab assumed in the closed-form solutions). This factor may partially explain why ILLI-SLAB δ_i and q_i are higher than the corresponding closed-form solutions, since these responses converge from above as slab size increases (Fig. 3.5). Bending stress, however, converges from below, so the relatively high σ_i obtained by ILLI-SLAB cannot be attributed to the slab size factor. The trends in Fig. 3.5 have been confirmed by studies using other two-dimensional models [7; 9].

It may, therefore, be concluded that the discrepancies between GEOSYS and ILLI-SLAB responses and the closed-form solutions are primarily the result of an effect related to the size of the loaded area. A useful measure of this size is the ratio (c/ℓ_e), in which c is the side-length of a square load, and ℓ_e is the radius of relative

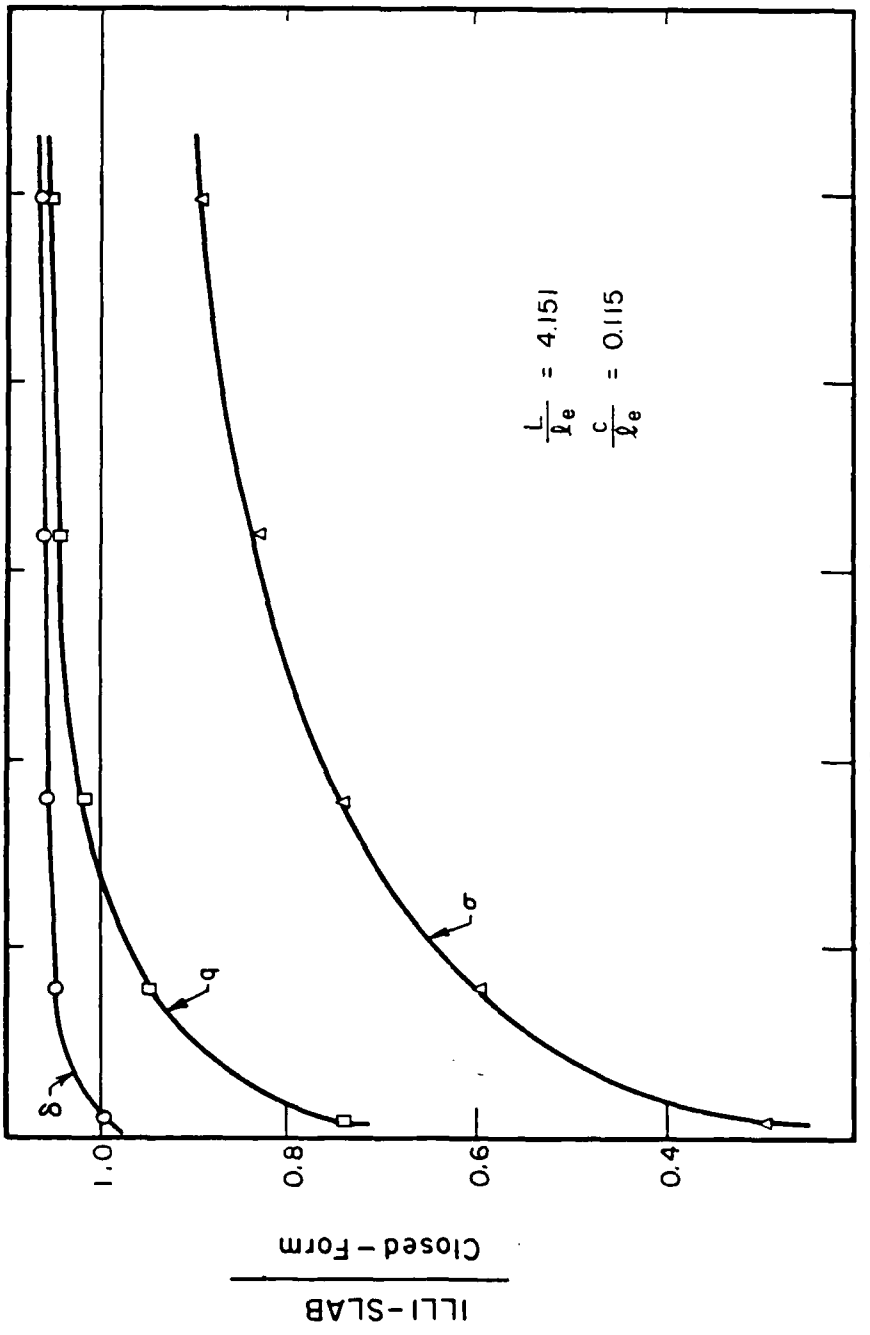

Fig. 3.4 Effect of Mesh Fineness on ILLI-SLAB Results (Interior Loading)

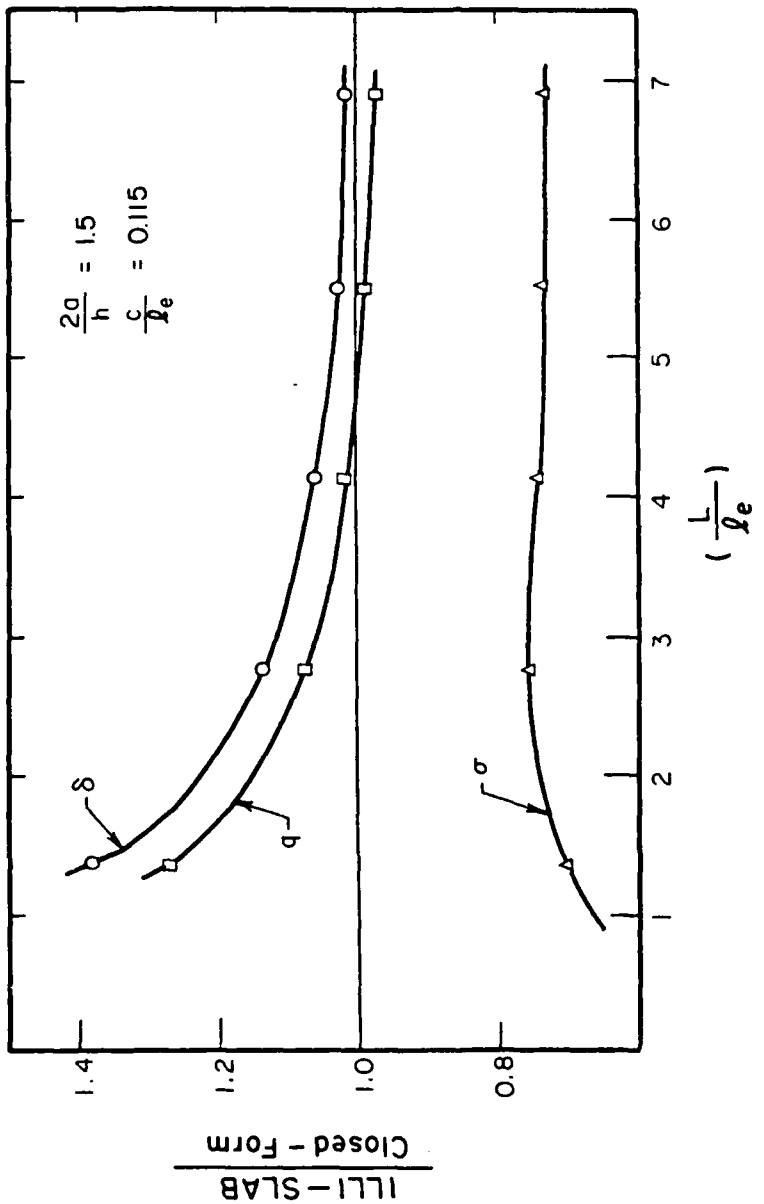

Fig. 3.5 Effect of Slab Size on ILLI-SLAB Results (Interior Loading)

stiffness of the slab-subgrade system. For the case considered in Table 3.2, (c/ℓ_e) is 0.278, which is on the high end of the spectrum of commonly used loaded areas. A discussion of the effect of loaded area size on finite element results using a dense liquid foundation [10; 2], identified two possible contributions to the discrepancies observed in Table 3.2:

(a) The fact that closed-form solutions [1; 26] are essentially truncated infinite series consisting of one or two terms only;

(b) The finite element discretization of externally applied loads and their conversion into a number of work equivalent nodal load components.

The aforementioned study using computer program CFES which employs the method of concordant deflections [7], as well as preliminary data from implementing ILLI-SLAB on a supercomputer with large memory core, indicates that (a) is probably much less important than (b). Upon further mesh refinement under the applied load, agreement between numerical results and closed-form solutions is excellent throughout the commonly used range of (c/ℓ_e) values.

CHAPTER 4

THE EDGE LOAD CASE

4.1 INTRODUCTION

Of the three fundamental loading conditions, the highest bending stress is produced by an edge load. The increase in bending stress as the load moves from the interior to the edge, is solely a function of a load size ratio, e.g. (a/ℓ_e), where a is the radius of the applied load (or some other measure of the size of the loaded area), and ℓ_e is the radius of relative stiffness of the slab-foundation system [32]. According to Westergaard's dense liquid theory, the ratio (σ_e/σ_i) of the edge loading bending stress ("New" formula) to that developing under an interior load, is typically around 1.9. Results from a previous study [2] indicate that for the elastic solid foundation the corresponding ratio is somewhat lower, typically about 1.6. In the latter subgrade idealization, the response of the system is affected significantly by the contribution of the soil adjacent to the slab. This factor will be investigated here in three dimensions. The effect of subgrade stress dependence, which is ignored in conventional linear (small strain) analysis, will also be considered. Analyses will be presented involving both single- and multi-wheel loads (SWL and MWL).

4.2 FINITE ELEMENT MODEL FOR SINGLE-WHEEL EDGE LOADING

In this investigation, an F-15 SWL is applied to a relatively thin slab on a weak subgrade. The same slab-and-subgrade system used in Chapter 3 for interior loading, is retained here for comparison. The pertinent characteristics of this system have been presented in Table 3.2. The finite element mesh used is shown in Fig. 4.1. Recommendations formulated in Chapter 2 are employed, with some gradation used to make the mesh finer in the critical area of the load and improve the accuracy of the results. Bending stresses developing in such a slab would be excessive in practice, and are only considered here so that the effect of subgrade stress dependence is magnified.

4.3 CONVERGENCE CRITERIA

The iterative scheme described in Chapter 3, may be used to introduce the stress dependent behavior of the subgrade. In evaluating the convergence of the system, two different methods were considered. The first method is based on the assumption that the maximum responses (δ_e, q_e and σ_e) are indicative of the behavior of the entire slab-foundation system. This is a reasonable assumption, since these responses occur in the critical areas of the mesh and are bound to be more sensitive to subgrade stress dependence than any other results.

Figure 4.2 shows maximum responses for each of the five cycles performed, normalized with respect to the results of the first

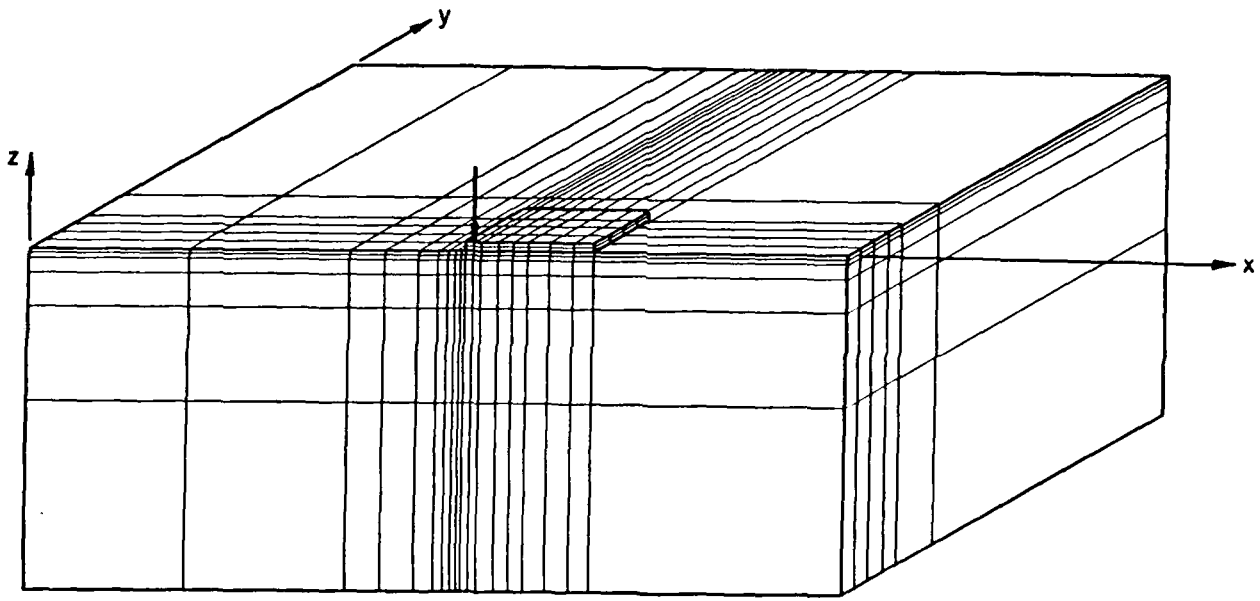

Fig. 4.1 Three-Dimensional Finite Element Mesh for F-15 Edge SWL Runs

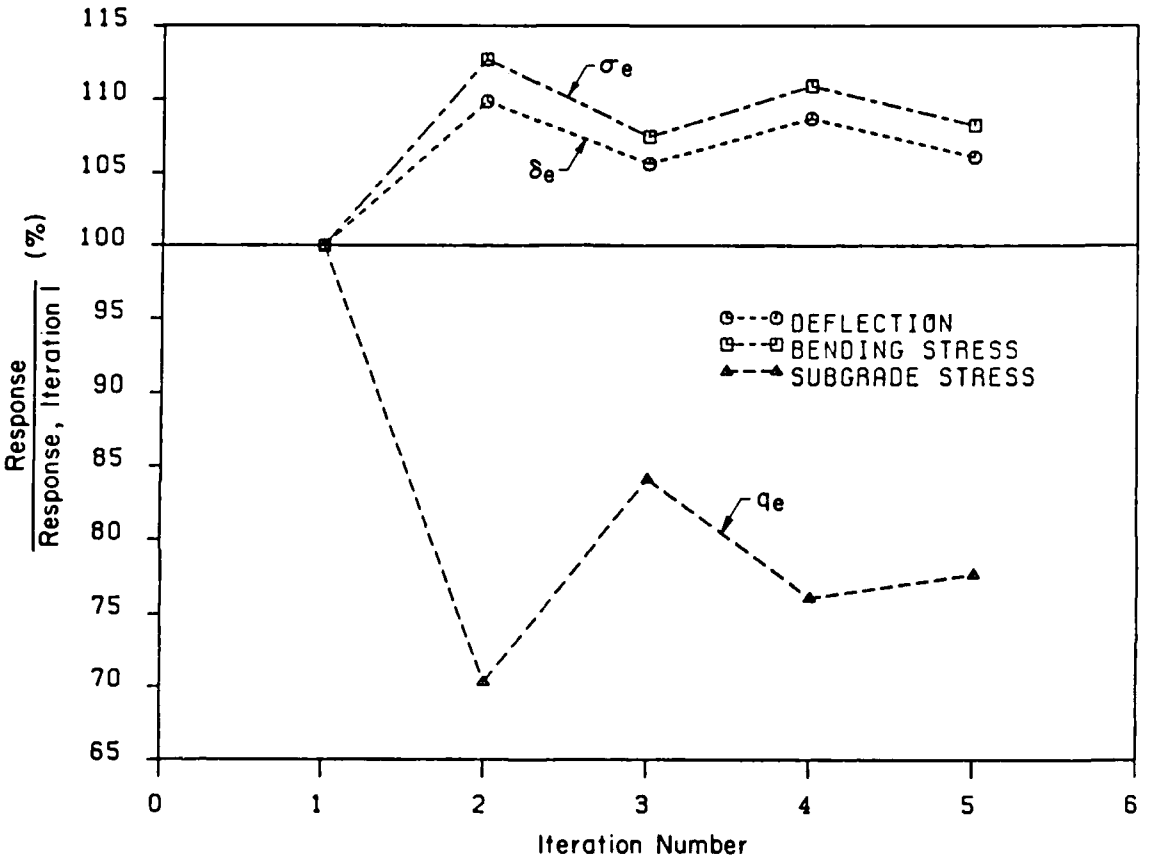

Fig. 4.2 Maximum Responses from Five Iterations

iteration. A uniform E_s of 7682 psi is assumed in the first iteration, and its results correspond to those from a conventional linear elastic analysis. It is observed that the maximum responses oscillate about a value to which, presumably, they would eventually converge, if enough cycles were conducted. The amplitude of oscillation becomes progressively smaller as more cycles are performed. The amplitude after a particular number of cycles depends on several factors, including the number of resilient modulus groups used to represent the complete E_R v. σ_D relation (see Fig. 3.2 and Table 3.1). If more than the seven groups used here (for practical reasons) are employed, convergence may be faster.

It is noted in Fig. 4.2 that the oscillation between maximum responses from the fourth and fifth iterations is only of the order 2%. This confirms that for most practical purposes, five cycles are more than adequate to achieve convergence. Furthermore, the average of the values of maximum responses obtained from the second and third iterations, consistently give an estimate within 2% of the projected converged values. This is demonstrated in Fig. 4.3, in which the maximum responses are re-plotted normalized with respect to the corresponding average value from the second and third iterations. It is, therefore, recommended that three iterations be performed, and the average of the responses from the second and third cycles be adopted.

A more direct measure of convergence may be obtained by comparing the resilient modulus, E_R, of each element, before and after a particular cycle. The absolute value of the change in modulus between

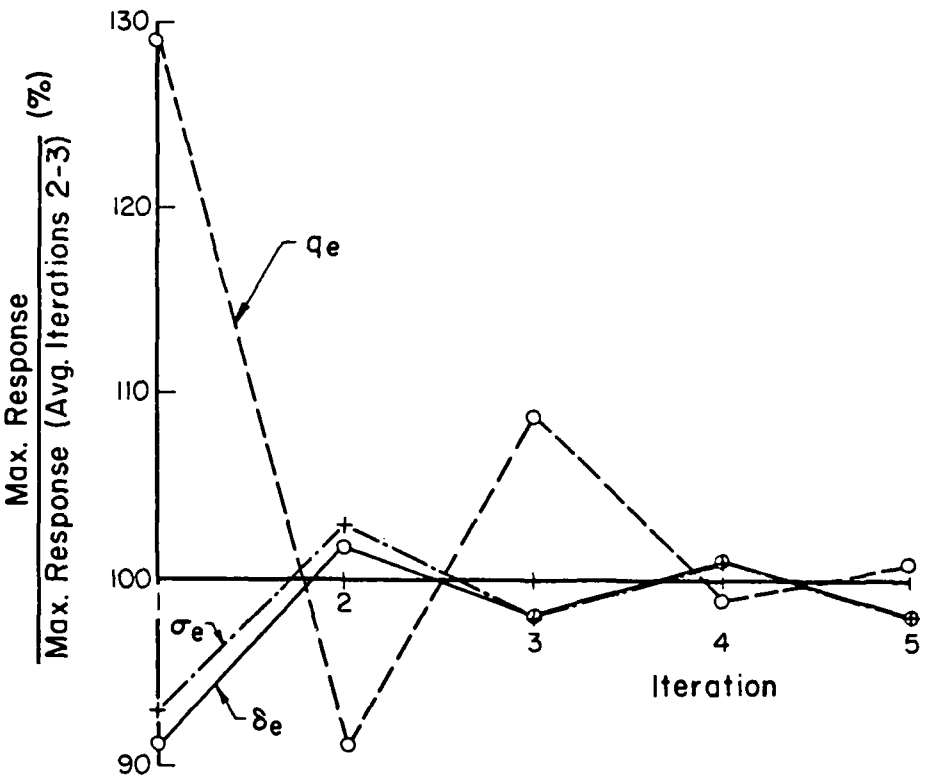

Fig. 4.3 Maximum Responses Normalized With Respect to Average of 2nd and 3rd Iterations

one cycle and the next shows how close a specific element is to its state of convergence. By summing this value over all subgrade elements, a measure of the total change in the system's properties is determined. Comparisons in Table 4.1 indicate that the average change in E_R, $\Delta^* E_R$, decreases from cycle to cycle. To define convergence as when this average change becomes zero, would require a very large number of iterations. In fact, the normalized plot in Fig. 4.4 suggests that for the case considered here, this may never be achieved. On the other hand, if the recommendation for three iterations is adopted, comparisons in Table 4.1 and Fig. 4.4 confirm that the largest portion of subgrade dependence will be accounted for.

It can be concluded that the oscillation of maximum responses adequately reflects the effect of additional iterations. Other parameters such as deflection basins, AREA [33], and variation of responses with depth, exhibit smaller oscillations, and generally follow the same convergence patterns as maximum responses. The latter are recommended as the closure criterion.

4.4 DISCUSSION OF RESULTS FOR F-15 SWL AT THE EDGE

4.4.1 Effect of Subgrade Stress Dependence

A direct way to evaluate the effect of subgrade stress dependence for the F-15 SWL at the slab edge, is to compare the maximum responses from the first iteration (which correspond to those from a conventional linear elastic analysis using a uniform, low σ_D soil modulus) to the

TABLE 4.1

CHANGES IN FOUNDATION MODULUS DURING ITERATIONS: F-15 EDGE SWL

SUBGRADE GROUP	ITERATION NO. 1		2		3		4		5	
	NEL	E_R*	NEL	E_R*	NEL	E_R*	NEL	E_R*	NEL	E_R*
2	648	7682	601	7682	598	7682	599	7682	598	7682
3	-	-	17	7423	16	7433	20	7431	17	7448
4	-	-	7	6919	10	6878	7	6909	9	6883
5	-	-	6	5889	16	6088	11	5947	15	5970
6	-	-	8	4883	6	5176	3	5038	7	4940
7	-	-	3	3776	1	3659	6	3589	0	3589
8	-	-	6	3020	1	3020	2	3020	2	3020
NCHNG	47		28		27		26		24	
Δ*E_R (psi)	1757		630		519		478		448	

Notes:

-For slab and subgrade characteristics, see Table 3.2.

-Mesh: See Fig. 4.1 (symmetry about x-axis employed - slab extends between underlined coordinates);
x-coordinates: 0; 18.5; 37; 41; 45; 47; 48; 49; 49.5; 50; 50.9375; 51.875; 53.750; 55.625; 57.5; 60; 62.5; 65; 95 ft
y-coordinates: 42.5; 12.5; 7.5; 5.625; 3.75; 1.875; 0 ft
z-coordinates: 0.6; 0.3; 0; -0.5; -1.0; -2.5; -6.7; -19.27; -40 ft
In slab: $(2a/h)_{min}$=2.81; χ=2.45; α_{max}=2.00; (c/2a)=0.20.

- NEL: Number of elements belonging to this subgrade group, during current iteration;
E_R*: Average E_R value (in psi) for this subgrade group;
NCHNG: Number of elements changing subgrade groups after current iteration;
Δ*E_R: Average change in E_R for the elements changing subgrade groups.

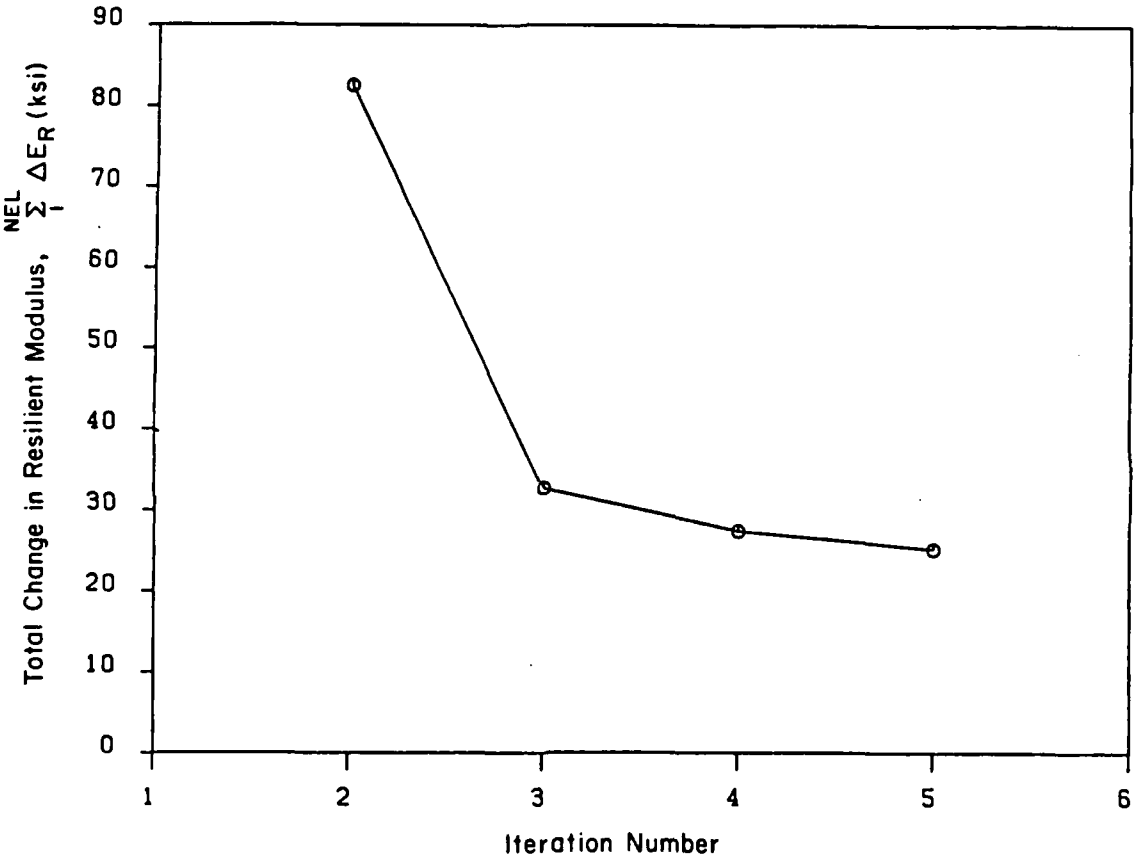

Fig. 4.4 Change in Foundation Modulus During Iterations

average of those from the second and third iterations. The latter were shown above to be adequately accurate estimates of the converged values. Such a comparison is shown in Table 4.2. Maximum deflection and bending stress increase by 10% and 8%, respectively. This change is comparable to that observed with the K_R model. For the F-111 edge SWL, for example, using a 12-in. slab resting on a 'SOFT' K_R foundation, deflection increased by 4%, while bending stress increased by 7% [12; 14].

On the other hand, maximum subgrade stress appears to be much more sensitive to stress dependence, decreasing by about 23%. It will be shown below that this is largely due to the development of high subgrade stress concentrations near the loaded edge. Subsequent iterations redistribute these stresses, thereby modeling local yielding, which would occur in a real soil subjected to these high stresses.

During this study, a large number of plots were prepared (most of which are not included in this Report), showing how distributions of various responses are affected by the use of a stress dependent subgrade. In these results, some important features have been identified. The first is that the overall behavior of the slab is quite similar for the constant modulus and the stress dependent subgrades. Furthermore, the differences in behavior that do exist, occur in and around the location of the subgrade elements with decreased resilient moduli. Table 4.1 indicates that about 8% of all the subgrade elements experience a decrease in E_R. These elements are located in the upper 6.5 ft of the subgrade. For the subgrade under the slab, additional bending stress and deflection accumulate in such elements as more

TABLE 4.2

EFFECT OF SUBGRADE STRESS DEPENDENCE: F-15 EDGE SWL

ITERATION	δ_e		q_e		σ_e	
	mils	%	psi	%	psi	%
1	60.32	100	24.63	100	826.0	100
2	68.00	113	17.32	70	907.6	110
3	64.84	107	20.72	84	872.3	106
4	66.91	111	18.74	76	898.1	109
5	65.30	108	19.13	78	876.2	106
Avg 2-3	66.42	110	19.02	77	890.0	108

Notes:

-For slab and subgrade characteristics, see Table 3.2.

-For mesh, see Fig. 4.1 and Table 4.1.

-All responses are at the intersection of loaded edge and centerline of load:
  δ_e : at top of slab;
  q_e : at surface of subgrade, by orthogonal extrapolation;
  σ_e : at bottom of slab, by orthogonal extrapolation of σ_y values.

iterations are performed, due to the decrease in subgrade support. This can be seen in the surface deflection profiles shown in Fig. 4.5, in which the basin observed after five iterations is deeper than the one obtained after the first iteration.

A different phenomenon is observed beyond the slab, in the subgrade adjacent to the loaded edge. There, the Cycle 5 profile is generally shallower than the Cycle 1 profile. This is illustrated in Fig. 4.6. Also note that deflection of the stress dependent subgrade (Cycle 5) is reduced to 50% of the maximum value within only 6 in. from the loaded slab edge. The constant modulus subgrade distributes the load better, experiencing a lower deflection at the loaded slab edge and a higher deflection away from the slab, compared to the stress dependent subgrade. Thus, a deeper but more localized basin is obtained using the stress dependent model. The structural contribution of the subgrade beyond the slab is less significant for the latter model, than for the constant modulus subgrade. This is reflected in the decreased deflections from Cycle 5 observed in Fig. 4.6, with the exception of the value at the loaded edge itself. At that location, the subgrade has a much lower modulus, which explains its high deflection. Therefore, it can be seen that stress dependence tends to move the elastic solid model toward the direction of the dense liquid idealization, in which the contribution of the subgrade adjacent to the slab edges is altogether neglected.

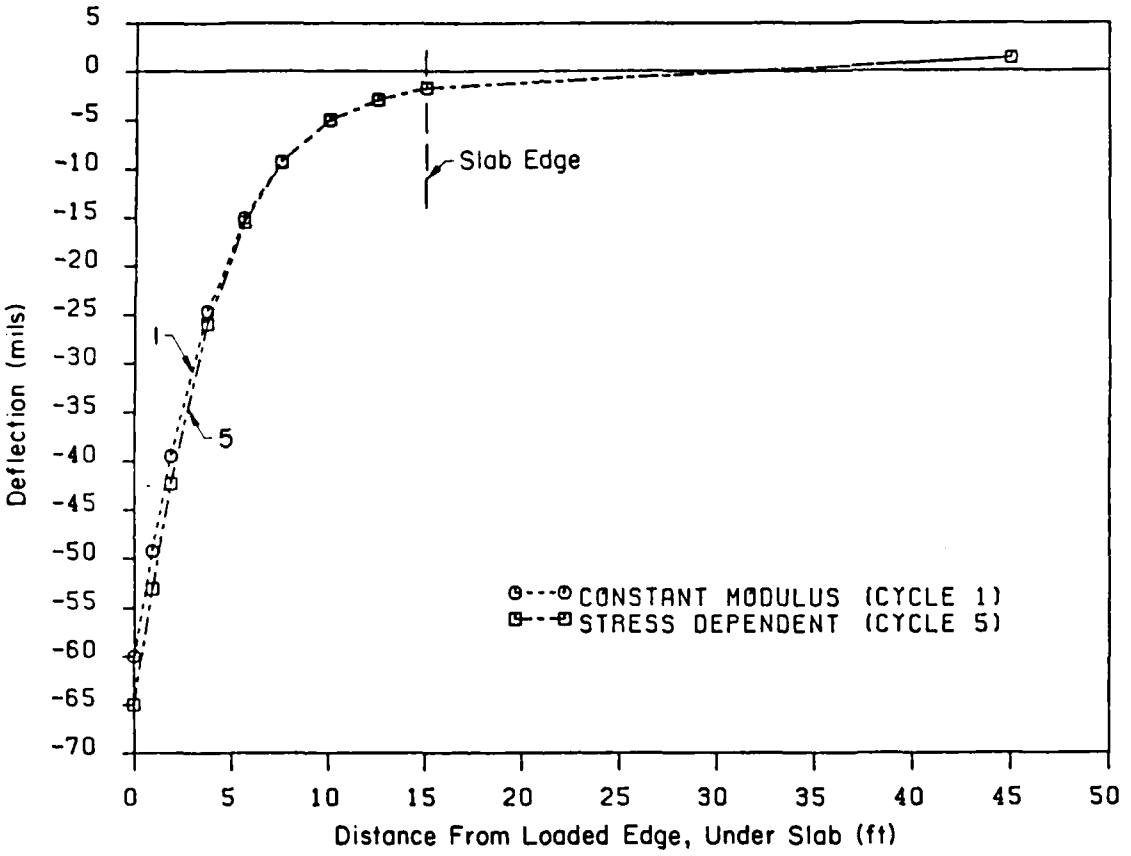

Fig. 4.5 Effect of Subgrade Stress Dependence on Subgrade Surface Deflection Profile, Under Slab, Along x-Axis in Positive Direction

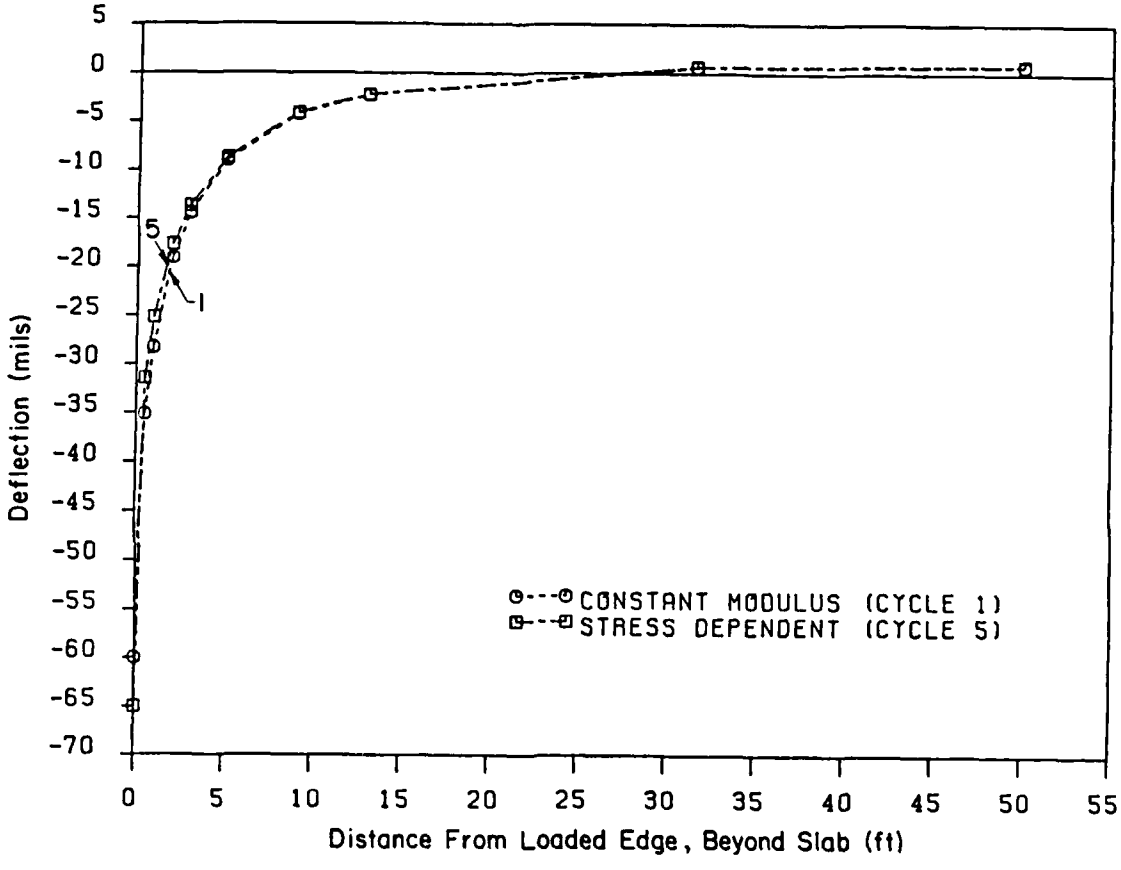

Fig. 4.6 Effect of Subgrade Stress Dependence on Subgrade Surface Deflection Profile, Beyond Slab, Along x-Axis in Negative Direction

4.4.2 Comparison With Two-Dimensional Results

Results obtained using GEOSYS may be compared to those from a number of two-dimensional models available, in order to establish the relative adequacy of the two approaches. In this section, results from programs FIDIES [9], H51ES [8] and ILLI-SLAB [6] will be considered. FIDIES is a two-dimensional finite difference solution, employing square elements throughout the slab. The external loads are converted to point loads, applied at the center of each element. Responses are calculated at these points alone. Thus, an extrapolation similar to that used with GEOSYS results, is necessary to obtain the edge responses. H51ES may only be used to calculate maximum bending stress at the edge, but its results are akin to a closed-form solution. Thus, they are not a function of user specified parameters such as mesh fineness, element aspect ratio, etc. These considerations can be crucial in the case of programs such as FIDIES and ILLI-SLAB. On the other hand, the latter can account for the finite size of the slab, and can determine the spatial distribution of all three responses, rather than just the maximum value of one of them.

Table 4.3 presents results obtained using these programs. The grid employed in the FIDIES run consisted of 441 square elements, giving a fineness ratio (Δ/h) of 1.07 (no symmetry capability exists in FIDIES at this time). Previous studies [9; 34; 2] suggest this grid may be slightly coarse, but it is dictated by computer memory limitations. In any case, the approximation involved in representing the applied load as a point load, located a few inches from the edge, is the overriding

TABLE 4.3

F-15 EDGE SWL: COMPARISON OF TWO-D AND THREE-D SOLUTIONS

SOLUTION	δ_e		q_e		σ_e	
	mils	%	psi	%	psi	%
GEOSYS-3D (Cycle 1)	60.32	91	24.63	42	826.0	70
FIDIES-2D (Linear extrap.)	73.21	111	30.93	53	1518.1	129
FIDIES-2D (Quadr. extrap.)	73.61	111	35.36	60	1605.8	136
H51ES	-	-	-	-	1055.9	89
ILLI-SLAB-2D (23x13 Mesh)	66.09	100	58.84	100	1180.8	100

Notes:

-For slab and subgrade characteristics, see Table 3.2.

-For GEOSYS mesh, see Fig. 4.1 and Table 4.2;
FIDIES mesh: $(\Delta/h) = 1.07$; 21x21 square elements;
ILLI-SLAB mesh: (symmetry about x-axis employed):
(23x13): $(2a/h)_{min}=0.575$; $\chi=3.0$; $\alpha_{max}=2.18$;
H51ES: 50 points used to define outline of applied load.

-All responses are at the intersection of loaded edge and centerline of load:
For extrapolation method used with GEOSYS results, see Table 4.2;
FIDIES results extrapolated using 2 (linear) or 3 (quadratic) elements along the slab centerline;
No extrapolation is involved in ILLI-SLAB and H51ES results.

consideration here. Unfortunately, this approximation cannot be avoided. The ILLI-SLAB run was conducted using a mesh fineness ratio (2a/h) of 0.575 in the vicinity of the load, a gradation, χ, of 3.0, and a maximum element aspect ratio, α_{max}, of 2.18. These parameters have been found to produce results of adequate accuracy, without exceeding the 500,000 words of memory available on the HARRIS 800-2 system [34]. The other results are normalized in Table 4.3 with respect to the ILLI-SLAB responses, all three of which are available and no extrapolation is involved in their determination.

The value of σ_e from ILLI-SLAB is about 11% higher than the "closed-form" solution from H51ES. This discrepancy cannot be explained by reference either to an inadequate mesh fineness or to the small slab size, since both these effects would tend to increase the ILLI-SLAB value of σ_e, and of the difference between this and the H51ES solution. A similar discrepancy was observed with the dense liquid foundation as well, and was related to the size of the loaded area. For the (c/ℓ_e) value of 0.28 used here, the discrepancy was 10% [2], which is close to that observed here. A number of comments on the sources of this discrepancy have been made in sub-section 3.3.2, above. Preliminary results using the Cray X-MP/24 indicated that this discrepancy disappears when the mesh under the loaded area is refined further.

On the other hand, FIDIES values of δ_e and σ_e are higher than the corresponding ILLI-SLAB ones, while q_e is lower. Again, overall grid fineness and slab size considerations cannot explain the discrepancy observed. It is considered that the major sources of this are:

(1) The conversion of the external load to a point load acting at the center of an edge element; and

(2) The extrapolation involved in obtaining the values in Table 4.3 from the FIDIES output.

In the case of the FIDIES edge subgrade stress, q_e, extrapolating leads to a considerable underestimation, because this technique is inadequate in areas of high stress gradients. The existence of such a stress concentration along the loaded slab edge, is confirmed by additional results presented below.

In Table 4.3, GEOSYS results from the first cycle are also presented. Comparison with those from ILLI-SLAB suggests that three-dimensional analysis gives q_e and σ_e values that are lower than those from ILLI-SLAB by about 60% and 30%, respectively. Maximum edge deflections are in relatively better agreement, the ILLI-SLAB value being only 9% higher than the corresponding one from GEOSYS. Part of this discrepancy may be attributed to the coarse mesh used with GEOSYS ($2a/h = 1.41$). The mesh fineness investigations in Chapter 2 (see Fig. 2.20) suggest that for the model used in this run, δ_e, q_e and σ_e may be underestimated by about 1, 3, and 12%, respectively. The remainder of the discrepancy is probably due to the fact that both GEOSYS σ_e and q_e are extrapolated from calculated values at the centroid of each brick element. This is particularly important in the case of subgrade stresses. The contour plots of subgrade stresses from two GEOSYS runs in Figures 4.7 and 4.8, indicate that the high stresses are limited to a narrow region along the loaded edge. Such a drastic

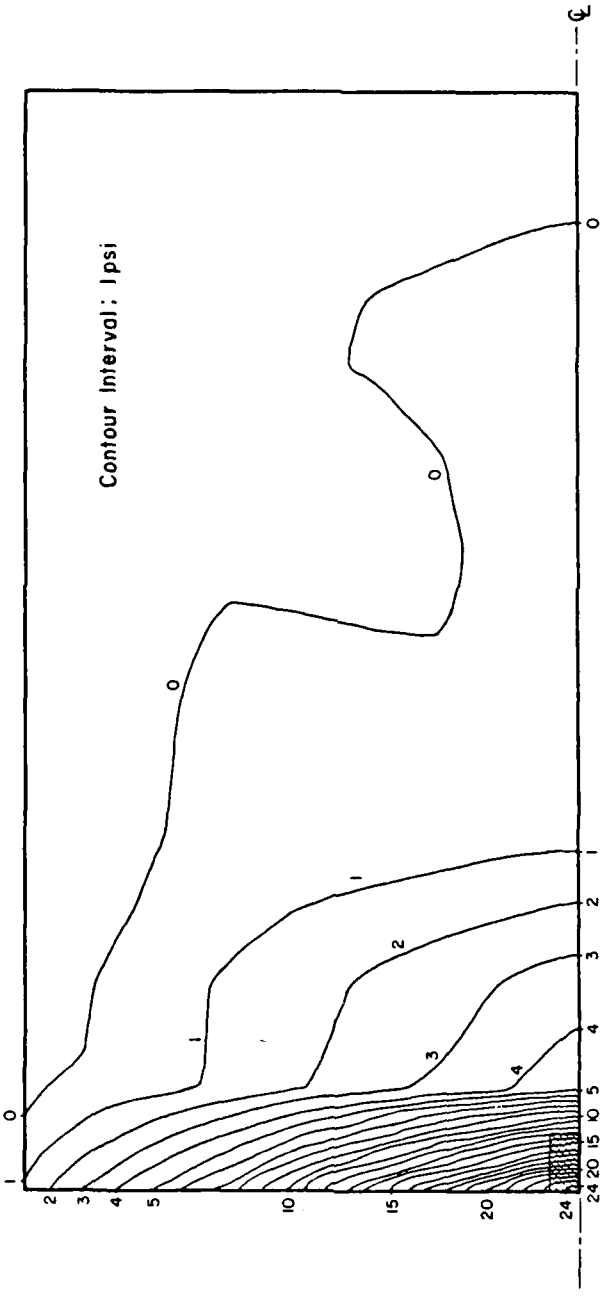

Fig. 4.7 Surface Subgrade Stress Contours from GEOSYS, Under Slab: Constant Modulus Subgrade (Cycle 1)

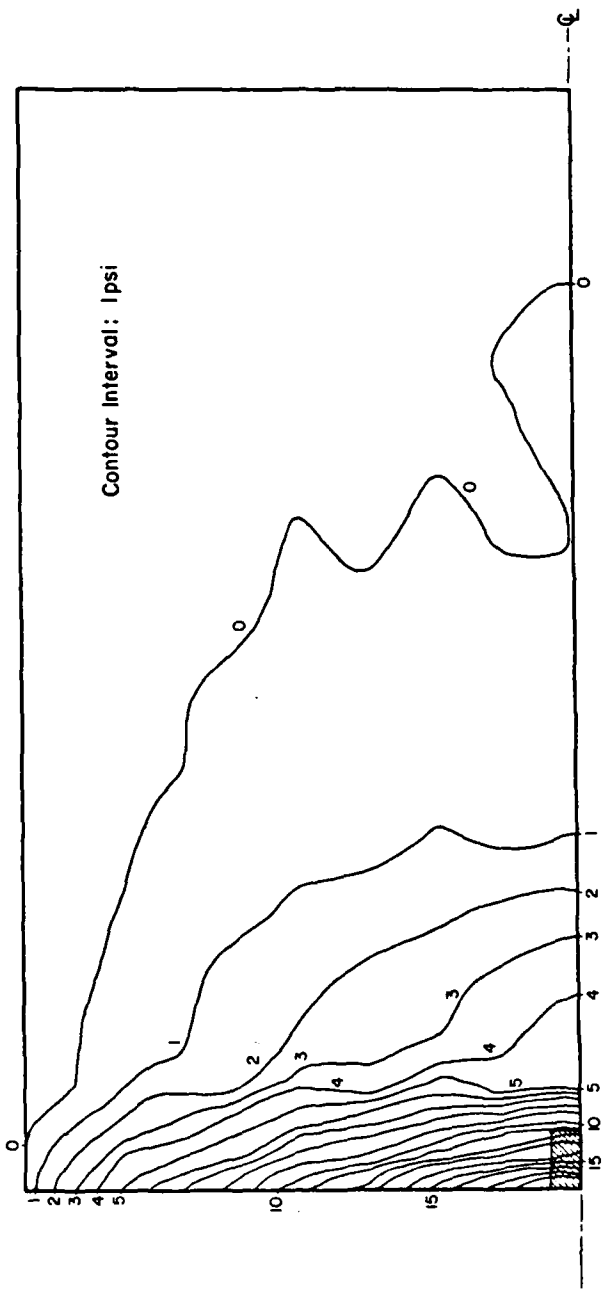

Fig. 4.8 Surface Subgrade Stress Contours from GEOSYS, Under Slab: Stress Dependent Subgrade (Cycle 5)

increase in subgrade stress right at the edge of the slab, has also been observed under interior loading [7], and is similar in nature to the infinite reactions predicted by theory at the edge of a rigid punch. The linear extrapolation used to determine q_e from GEOSYS results is unable to reproduce the high stress gradients at the slab edge.

In the narrow region immediately adjacent to the loaded edge, local yielding of the soil will occur under these high subgrade stresses. Thus, the theoretical value of the subgrade stress at the physical edge of the slab may not be of practical significance. A more meaningful value may be the subgrade stress developing a few inches inside from the edge, say at a distance of 0.2 ℓ_e. A previous study showed that this value is relatively insensitive to mesh fineness [7]. Additional iterations, such as presented in Table 4.2, have the effect of redistributing the stress away from highly stressed elements. Thus, introducing subgrade stress dependence enables the user to model local yielding which would occur in a real subgrade.

Notwithstanding the differences in their maximum responses, ILLI-SLAB and GEOSYS produce similar response distributions outside the critical edge region. The plots in Fig. 4.9 reinforce the validity of the comments made above.

4.5 FINITE ELEMENT MODEL FOR MULTI-WHEEL EDGE LOADING

In the previous section, an investigation of the edge loading condition due to a single-wheel load (SWL) was presented. Completeness

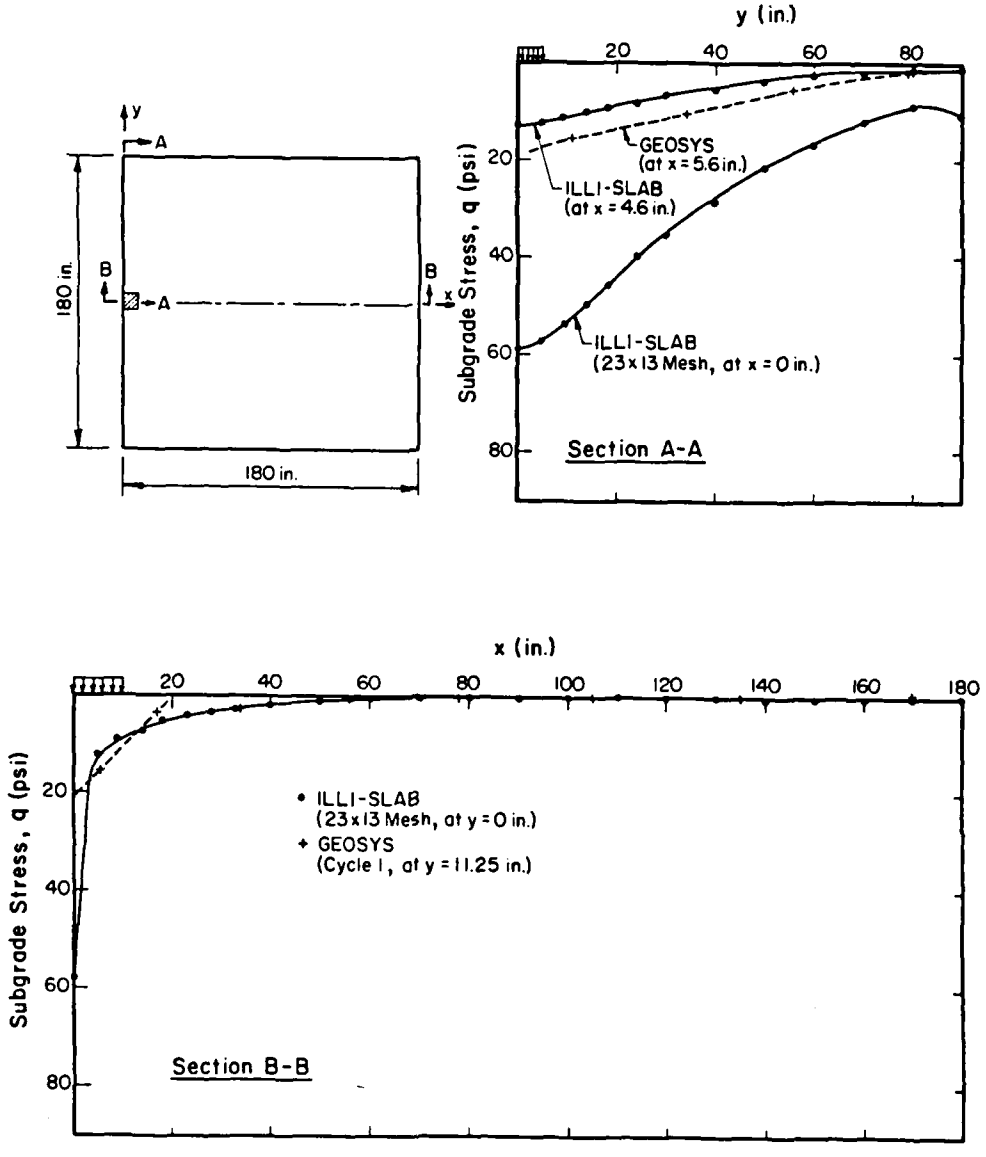

Fig. 4.9 Comparison of GEOSYS and ILLI-SLAB Surface Subgrade Stress Distributions for F-15 Edge SWL, Under Slab

now demands an examination of the corresponding effects due to a multi-wheel gear (MWL) placed adjacent to a slab edge. The majority of airplanes are equipped with landing gears consisting of more than one wheel. This allows them to carry a greater total load, but maintain the contact pressure reasonably low, by distributing the weight over a larger area of application. Depending on the size and spacing of the tire-prints and applied pressure intensity, the response of a slab-on-grade system under a MWL may be considerably different from what is observed under a SWL.

In the analyses described in this section, one landing gear from a C-141 aircraft is considered. This consists of four tire-prints, each loaded by 40.7 kips at 196 psi. The separation (center-to-center) between the wheels is 48 in. in the longitudinal direction, and 32.5 in. transversely. Because of the size of the load, a thicker slab is needed for this case, compared to that used earlier. A 12-in. thick slab was chosen because preliminary comparisons with ILLI-SLAB (two-dimensional) results indicated that a comparable maximum bending stress would be obtained in this case as for the previous F-15 studies. The finite element mesh used is shown in Fig. 4.10. The material properties for the slab-foundation system were identical to those used for the F-15 load (see Table 3.2) with the exception of slab thickness. Taking advantage of symmetry, only one-half of the system needs to be modeled.

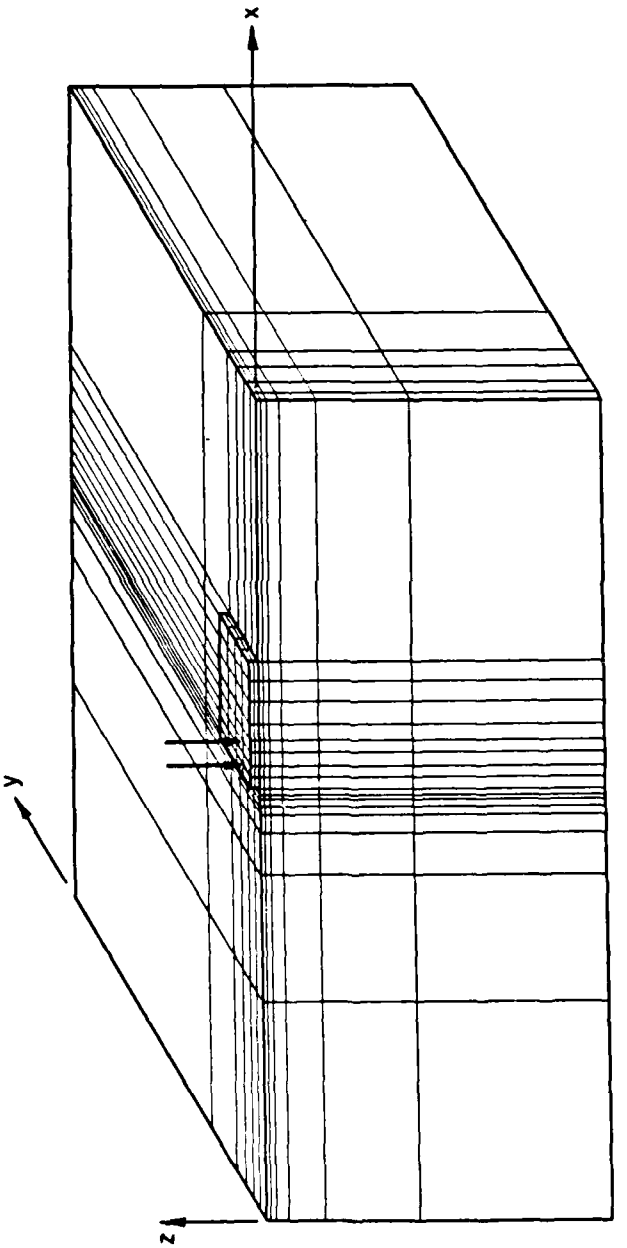

Fig. 4.10 Three-Dimensional Finite Element Mesh for C-141 Edge MWL Runs

4.6 DISCUSSION OF RESULTS FOR C-141 MWL AT THE EDGE

4.6.1 Effect of Subgrade Stress Dependence

A total of five iterations were performed for this case, using the procedure described above to account for subgrade stress dependence. The maximum responses from these runs are shown in Table 4.4. These confirm that the average responses from the second and third iterations provide adequate estimates of the values expected after a much larger number of iterations.

The effect of accounting for subgrade stress dependence is quite significant in this case. Maximum deflection increases by about 30% and maximum bending stress by more than 20%. On the other hand, maximum subgrade stress decreases by more than 30%. Maximum deflection and subgrade stress occur at the edge, on the system line of symmetry; maximum bending stress also occurs at the edge, but on the transverse axis of the two tire-prints. Both bending and subgrade stresses have been obtained by linear orthogonal extrapolation. Although these values are inevitably approximate, they indicate that subgrade stress dependence is more important in this case than for the F-15 load. This is further reflected in the much larger extent of the region of reduced resilient moduli obtained with the C-141 load.

4.6.2 Comparison With Two-Dimensional Results

Table 4.5 presents a comparison between maximum responses from the first cycle of GEOSYS, and the corresponding ones obtained using ILLI-

TABLE 4.4

EFFECT OF SUBGRADE STRESS DEPENDENCE: C-141 EDGE MWL

ITERATION	δ_e		q_e		σ_e	
	mils	%	psi	%	psi	%
1	159.7	100	41.25	100	684.1	100
2	215.9	135	26.91	65	865.9	127
3	203.6	127	28.39	69	812.6	119
4	211.3	132	26.99	65	849.7	124
5	205.6	129	28.37	69	822.5	120
Avg 2-3	209.8	131	27.65	67	839.3	123

Notes:

$E = 4 \times 10^6$ psi $\quad \mu = 0.15 \quad h = 12$ in.
$E_s = 7682$ psi ('SOFT') $\quad \mu_s = 0.45 \quad \ell_e = 49.64$ in.
Slab: 15 ft x 15 ft ($L/\ell_e = 3.63$)

-Load: Four tire prints, each 40.7 kips @ 196 psi, placed symmetrically along slab edge.

-Mesh: See Fig. 4.10 (symmetry about x-axis employed - slab extends between underlined coordinates):
x-coordinates: 0; 25; 40; 45; 47; 48; 49; 49.5; 50; 51.323; 52.647; 53.970; 55.735; 57.5; 60; 62.5; 65; 95 ft
y-coordinates: 42.5; 12.5; 7.5; 4.67; 2.67; 1.33; 0 ft
z-coordinates: 1; 0.5; 0; -0.5; -1; -2.5; -6.5; -17.5; -40 ft

In slab: $(2a/h)_{min}$=1.323; χ=1; α_{max}=1.239; (c/2a)=1.0.

-All responses occur at the loaded edge; δ_e and q_e occur on the system line of symmetry; σ_e occurs on the transverse axis of the two tire-prints:
δ_e : at top of slab;
q_e : at surface of subgrade, by orthogonal extrapolation;
σ_e : at bottom of slab, by orthogonal extrapolation of σ_y values.

TABLE 4.5

C-141 EDGE MWL: COMPARISON OF GEOSYS AND ILLI-SLAB RESULTS

SOLUTION	δ_e		q_e		σ_e	
	mils	%	psi	%	psi	%
GEOSYS (Cycle 1)	159.7	87	41.25	50	684.1	78
GEOSYS (Refined Mesh)	160.5	87	52.19	63	684.4	78
ILLI-SLAB (Mesh: 9x5)	175.4	95	55.55	68	850.0	97
ILLI-SLAB (Mesh: 12x8)	183.8	100	82.00	100	881.4	101
ILLI-SLAB (Mesh: 22x12)	184.1	100	82.20	100	872.6	100

Notes:

-For slab and subgrade characteristics, see Table 4.4.

-For GEOSYS mesh, see Fig. 4.10 and Table 4.4; in "Refined Mesh," a vertical nodal plane was added at x = 50.5 ft;
ILLI-SLAB meshes (symmetry about x-axis):
(9x5): $(2a/h)_{min}$=1.33; χ=3.0; α_{max}=2.12;
(12x8): $(2a/h)_{min}$=0.67; χ=6.0; α_{max}=3.75;
(22x12): $(2a/h)_{min}$=0.67; χ=9.0; α_{max}=1.13.

-For location of and extrapolation method for maximum responses, see Table 4.4;
No extrapolation is involved in ILLI-SLAB results, except in determining σ_e for the 9x5 mesh.

SLAB. Three different meshes were used for the ILLI-SLAB runs and two for the GEOSYS runs, to illustrate the effect of mesh fineness. The sensitivity of ILLI-SLAB results to this factor is easily demonstrated in Table 4.5, especially in the case of the subgrade stress. It should also be mentioned that the two finer ILLI-SLAB runs predict a very high subgrade stress at the slab corner as well (not included in Table 4.5).

Three-dimensional results are much lower than those from two-dimensional analysis, the biggest difference being exhibited by subgrade stress. This may be partly explained by reference to the mesh fineness requirements established in Chapter 2 (see Fig. 2.20). For the coarse mesh used in the GEOSYS runs ($2a/h = 1.323$), an underestimate of the order of 5% may be expected in the values of q_e and σ_e. This, however, is inadequate to explain the large differences observed here.

A large portion of the discrepancy between two- and three-dimensional results can be explained by reference to the high subgrade stress concentration which occurs at the edge of the slab. This phenomenon has also been observed under interior loading [7], as well as under the F-15 edge load in the previous section. Figure 4.11 shows the distributions of subgrade stress along the slab edge and the line of symmetry, obtained using the 22x12 ILLI-SLAB mesh and the somewhat refined GEOSYS mesh for Cycle 1. These indicate that agreement between the two models is very good, except in a narrow region, less than 8-in. wide (or $0.2\ \ell_e$), along the slab edge. Extrapolation of the GEOSYS subgrade stresses to obtain the maximum stress occurring at the edge, leads to an underestimate, being unable to account for the high stress

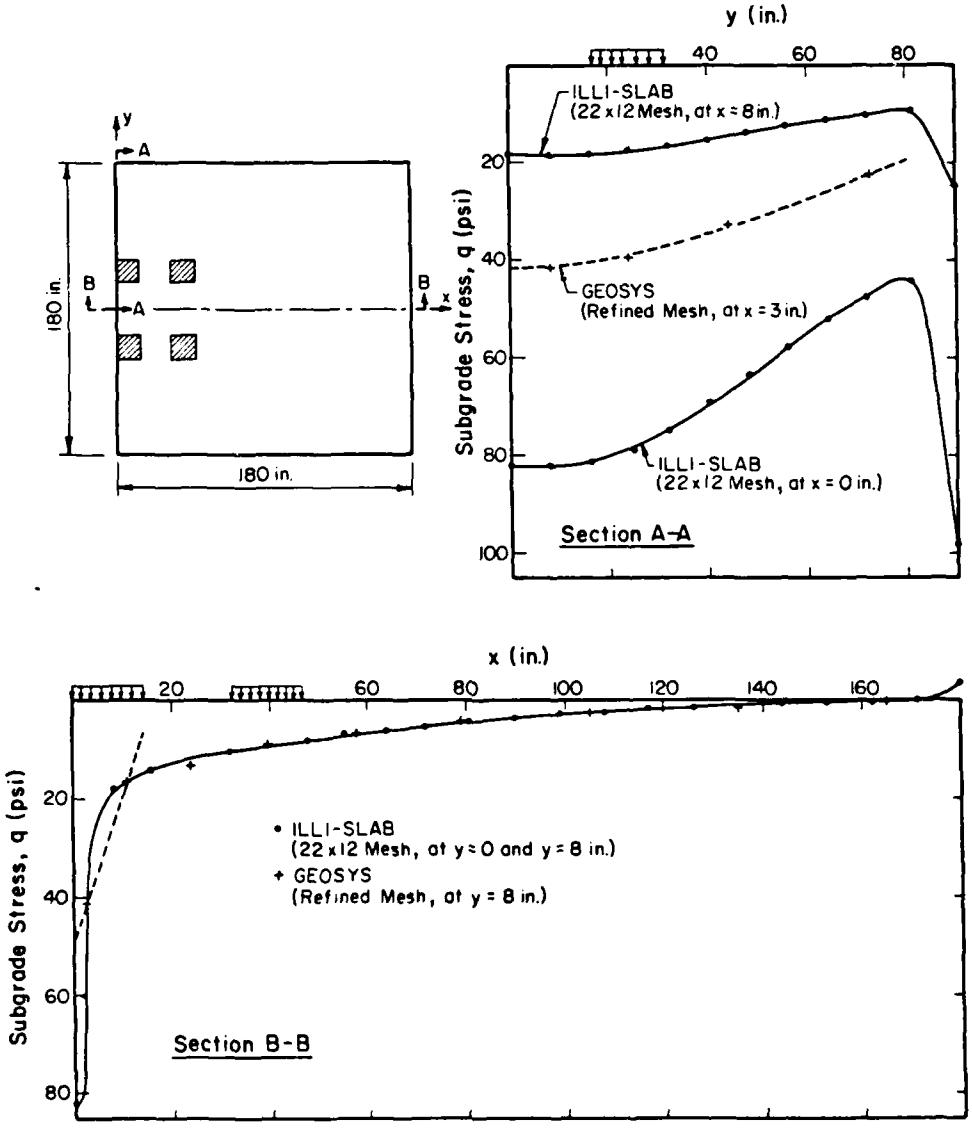

Fig. 4.11 Comparison of GEOSYS and ILLI-SLAB Surface Subgrade Stress Distributions for C-141 Edge MWL, Under Slab

gradients developing in the region immediately adjacent to the slab edge.

As mentioned in the previous section as well, local yielding in the soil will prevent the development of these high subgrade stresses. As a result, the subgrade stress predicted at a short distance from the edge is a more reliable value to use in design decisions. The subgrade stress distributions in Figures 4.9 and 4.11 indicate that comparing only the maximum q_e values from the two- and three-dimensional models may be misleading. The overall system responses are much closer to each other than the individual maximum values would suggest. This is especially true when fine meshes are used.

CHAPTER 5

THE CORNER LOAD CASE

5.1 INTRODUCTION

Two-dimensional analysis of a slab-on-grade indicates that corner loading produces the maximum deflection and subgrade stress. This has been confirmed for both the dense liquid and elastic solid foundations [2]. To complete the series of three-dimensional investigations using GEOSYS, the corner loading condition is examined in this Chapter, with an F-15 single-wheel load. Unfortunately, the lack of symmetry along either of the two major coordinate axes of the slab, dictates the use of a full mesh in the finite element idealization. This results in prolonged execution times (in excess of 12 CPU hours on the HARRIS 800-2) even using a rather coarse mesh, which gives rise to less accurate results. General trends, however, may still be observed and these can be useful despite any limitations in the accuracy of individual response values.

5.2 FINITE ELEMENT MODEL FOR SINGLE-WHEEL CORNER LOADING

The slab-subgrade system modeled in these runs is comparable to those assumed in the preceding Chapters. As noted earlier, the F-15 applies a load of 30 kips, at a pressure intensity of 355 psi. The finite element mesh used is shown in Fig. 5.1. To account for subgrade

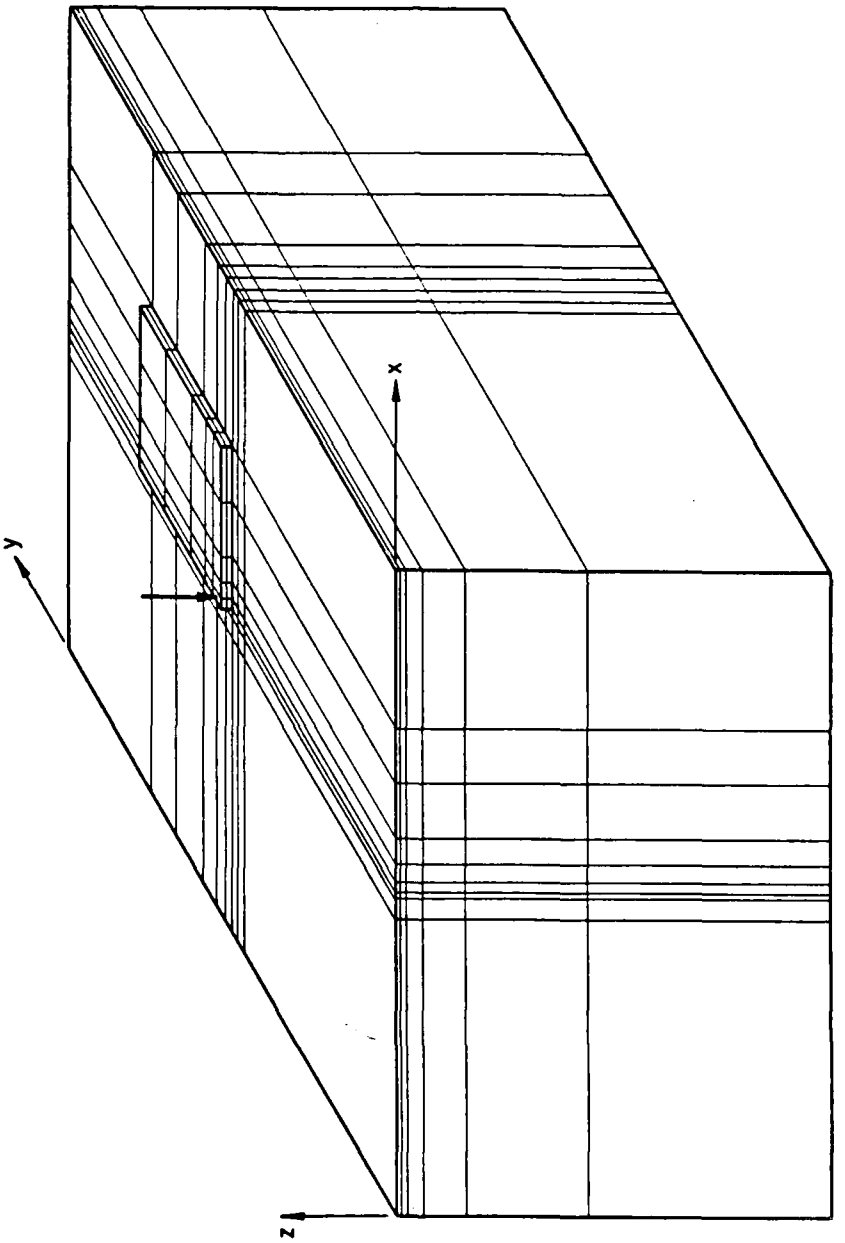

Fig. 5.1 Three-Dimensional Finite Element Mesh for F-15 Corner SWL Runs

stress dependence, the usual iterative scheme is employed, assuming a 'SOFT' subgrade, whose deviator stress-resilient modulus relation is as shown in Fig. 3.1. The material properties of slab and foundation are given in Table 5.1.

5.3 DISCUSSION OF RESULTS FOR F-15 SWL AT THE CORNER

5.3.1 Effect of Subgrade Stress Dependence

Table 5.1 presents a summary of maximum responses obtained from three iterations performed for this case. Maximum deflection, δ_c, and subgrade stress, q_c, occur at the corner of the slab. On the other hand, maximum (tensile) bending stress, σ_c, occurs at the top of the slab, some distance from the corner. Preliminary results using ILLI-SLAB [34], suggest that a slab resting on an elastic solid, also develops a high tensile bending stress at the bottom fiber under the load. This cannot be confirmed at this time using GEOSYS, however, since a much finer mesh would be required.

As noted earlier, the average responses from the second and third iterations provide an adequate estimate of the values that may be expected after a large number of cycles. Comparing these average values to those from Iteration 1 (which assumes a uniform, low σ_D, Young's modulus for the foundation), the effect of subgrade stress dependence may be observed. Subsequent iterations in Table 5.1 lead to a maximum deflection that is almost 20% higher than the value obtained from Cycle

TABLE 5.1

EFFECT OF SUBGRADE STRESS DEPENDENCE: F-15 CORNER SWL

ITERATION	δ_c		q_c		q_c^*		σ_c	
	mils	%	psi	%	psi	%	psi	%
1	72.42	100	42.93	100	31.27	100	312.1	100
2	87.67	121	28.16	66	19.95	64	358.5	115
3	82.99	115	22.16	52	19.86	64	343.1	110
Avg. 2-3	85.33	118	25.21	59	19.81	64	350.8	112

Notes:

$E = 4 \times 10^6$ psi $\quad \mu = 0.15 \quad h = 12$ in.
$E_s = 7682$ psi ('SOFT') $\quad \mu_s = 0.45 \quad \ell_e = 49.64$ in.
Slab: 15 ft x 15 ft $(L/\ell_e) = 3.63$
Load: 30 kips @ 355 psi, converted to four work equivalent loads
(c = 9.193 in.)

-Mesh: See Fig. 5.1 (slab extends between underlined coordinates):
x-coordinates = 0; 27.5; 29.167; 30; 30.833; 32.5; 35; 40; 45; 60 ft
y-coordinates = 60; 45; 40; 35; 32.5; 30.833; 30; 29.167; 27.5; 0 ft
z-coordinates = 1; 0.5; 0; -0.5; -1; -2.5; -6.5; -17.5; 40 ft

In slab: $(2a/h)_{min}=0.833$; $\chi=1.09$; $\alpha_{max}=6.0$; $(c/2a)=0.92$.

-Location and method of extrapolation of responses:
δ_c : at slab corner, at top of the slab;
σ_c : tension at top of slab, at some distance from corner:
$\sigma_c = \sigma_1$, from values of σ_x, σ_y, τ_{xy}, extrapolated to the top, using linear orthogonal extrapolation;
q_c : compressive, at surface of subgrade under corner of slab: extrapolated up to surface of subgrade from values under corner region of slab, using linear orthogonal extrapolation.
q_c^* : compressive, at surface of subgrade, at x=5 in., y=5 in. from corner, under slab, extrapolated like q_c.

1. Similarly, an increase of more than 10% is observed in the maximum bending stress developing in the slab.

On the other hand, a dramatic decrease in the value of the maximum subgrade stress predicted by the first iteration is obtained as subgrade stress dependence is considered. This reflects the redistribution of high subgrade stresses concentrated at the slab edges, observed earlier as well. Local yielding of soil in the corner region prevents these high stresses from developing, and this is accounted for by the iterative procedure used with GEOSYS. The maximum subgrade stress occurring at the slab corner itself, therefore, may not be a meaningful response to seek. The subgrade stress developing under the center of the load, q_c^* say, may be a more realistic indication of subgrade response. This will be substantially lower than the value at the corner and, therefore, less sensitive to stress dependence. The oscillation of q_c^* in Table 5.1 is of considerably smaller amplitude than that of q_c itself.

Table 5.2 presents the results of an analysis of the changes in foundation modulus, E_R, occurring after each of the three iterations performed. It is observed that about 20% of the subgrade elements are affected by stress dependence, compared to only 8% for the F-15 edge load. Subgrade stress dependence is predictably a more serious consideration under corner than under edge loading.

Figure 5.2 shows the distribution of deviator stress, σ_D, with depth at the center of the critical element, as obtained from Cycle 1. This element is located outside the slab, adjacent to the slab corner. It is

TABLE 5.2

CHANGES DURING ITERATIONS: F-15 CORNER SWL

GROUP	NEL AFTER CYCLE			E_R^* (psi) AFTER CYCLE			σ_D (psi) AFTER CYCLE		
	1	2	3	1	2	3	1	2	3
2	402	396	399	7682.	7682.	7682.	0.319	0.341	0.340
3	19	31	24	7390.	7374.	7381.	2.250	2.265	2.258
4	15	14	20	6911.	6883.	6904.	2.661	2.685	2.668
5	14	21	13	5814.	5856.	5870.	3.603	3.567	3.555
6	7	12	2	4951.	4888.	4754.	4.343	4.398	4.513
7	3	1	15	3702.	3348.	3458.	5.415	5.719	5.624
8	26	11	13	3020.	3020.	3020.	9.205	7.225	6.971

Notes:

-For slab and subgrade characteristics, see Table 5.1.

-Mesh: See Fig. 5.1 and Table 5.1.

-NEL: Number of elements belonging to this subgrade group;
E_R^*: Average E_R value (in psi) for this subgrade group;
σ_D^*: Average σ_D value (in psi) for this subgrade group.

-Total Number of Subgrade Elements = 486.

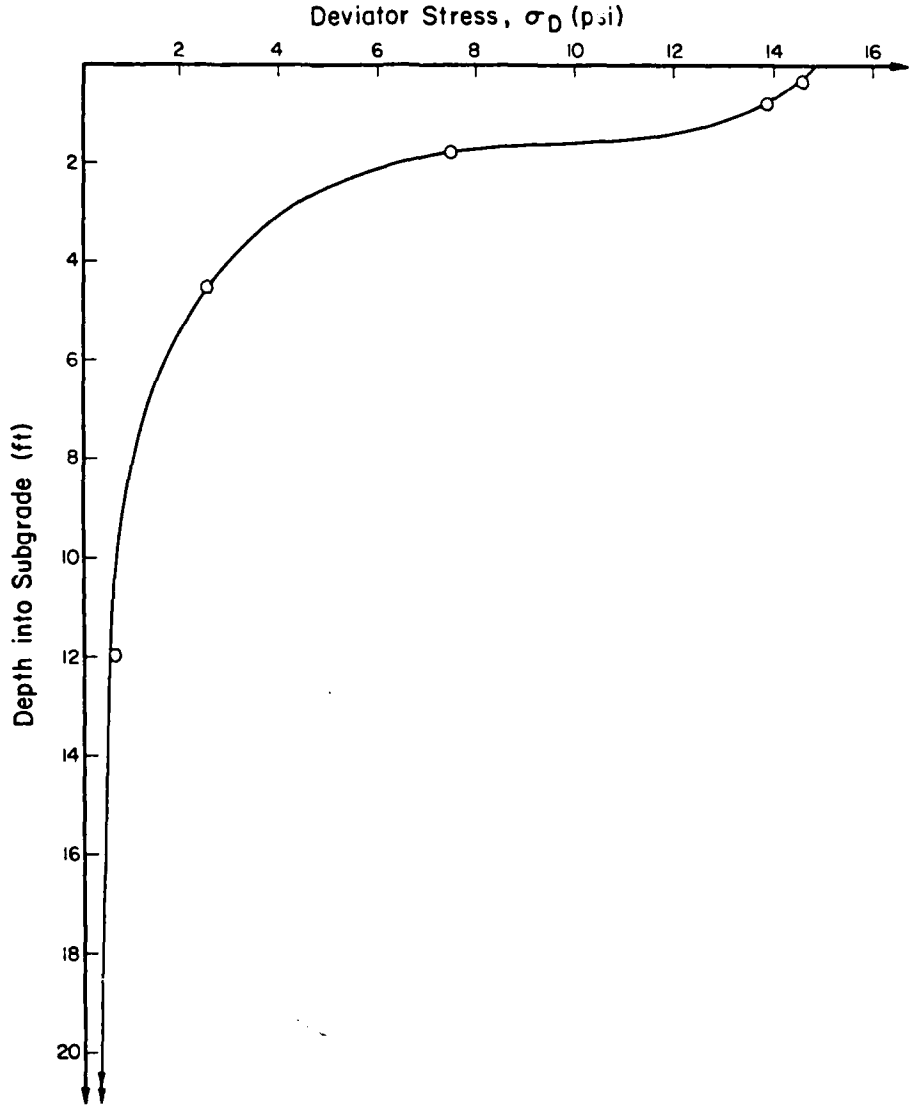

Fig. 5.2 Deviator Stress Distribution with Depth, Under Element Adjacent to Slab Corner: F-15 Corner SWL (Cycle 1)

observed that the high values of σ_D are limited to the upper 5.5 ft of the subgrade, below which σ_D is less than 2 psi.

5.3.2 Comparison With Two-Dimensional Results

In view of the relatively coarse mesh employed in the GEOSYS runs [$(2a/h)_{min}$ = 0.833; χ = 1.0], considerable discrepancies exist between three- and two-dimensional responses presented in Table 5.3. According to the criteria developed in Chapter 2 (see Fig. 2.20), GEOSYS results in Table 5.3 may be expected to be too low, by the following amounts:

Max. deflection:	1%
Max. bending stress:	5%
Max. subgrade stress:	2%

These would reduce slightly the discrepancies in deflection and subgrade stress values in Table 5.3, but would increase the disagreement in the bending stress values. Possible causes of the gap between the two- and three-dimensional results were identified above as the coarseness of the GEOSYS mesh in the area of the load, and the extrapolation involved in obtaining maximum stress values from the GEOSYS output. The latter is more important in the case of subgrade stress, in view of the high stress gradients existing near loaded slab edges and corners. The sensitivity of q_c from ILLI-SLAB to mesh fineness is also noted in Table 5.3.

Figure 5.3 shows the distribution of subgrade stresses predicted by ILLI-SLAB and GEOSYS. These confirm that the two models are in good agreement, except in a region about 8-in. wide (or 0.2 ℓ_e), along the

TABLE 5.3

F-15 CORNER SWL: COMPARISON OF GEOSYS AND ILLI-SLAB RESPONSES

SOLUTION	δ_c		q_c		q_c^*		σ_c	
	mils	%	psi	%	psi	%	psi	%
GEOSYS (Cycle 1)	72.42	91	42.93	28	31.27	55	312.1	108
ILLI-SLAB (Mesh:6x6)	77.93	98	129.13	85	53.73	94	285.6	99
ILLI-SLAB (Mesh:12x12)	79.84	100	151.43	100	57.13	100	288.9	100

Notes:

-For slab and subgrade characteristics, see Table 5.1.

-For GEOSYS mesh, see Fig. 5.1 and Table 5.1;
ILLI-SLAB meshes:
(6x6) : $(2a/h)_{min}$=0.83; χ=1.0; α_{max}=6.0;
(12x12) : $(2a/h)_{min}$=0.77; χ=4.0; α_{max}=2.2.

-For location of and extrapolation method for responses, see Table 5.1;
No extrapolation is involved in ILLI-SLAB results.

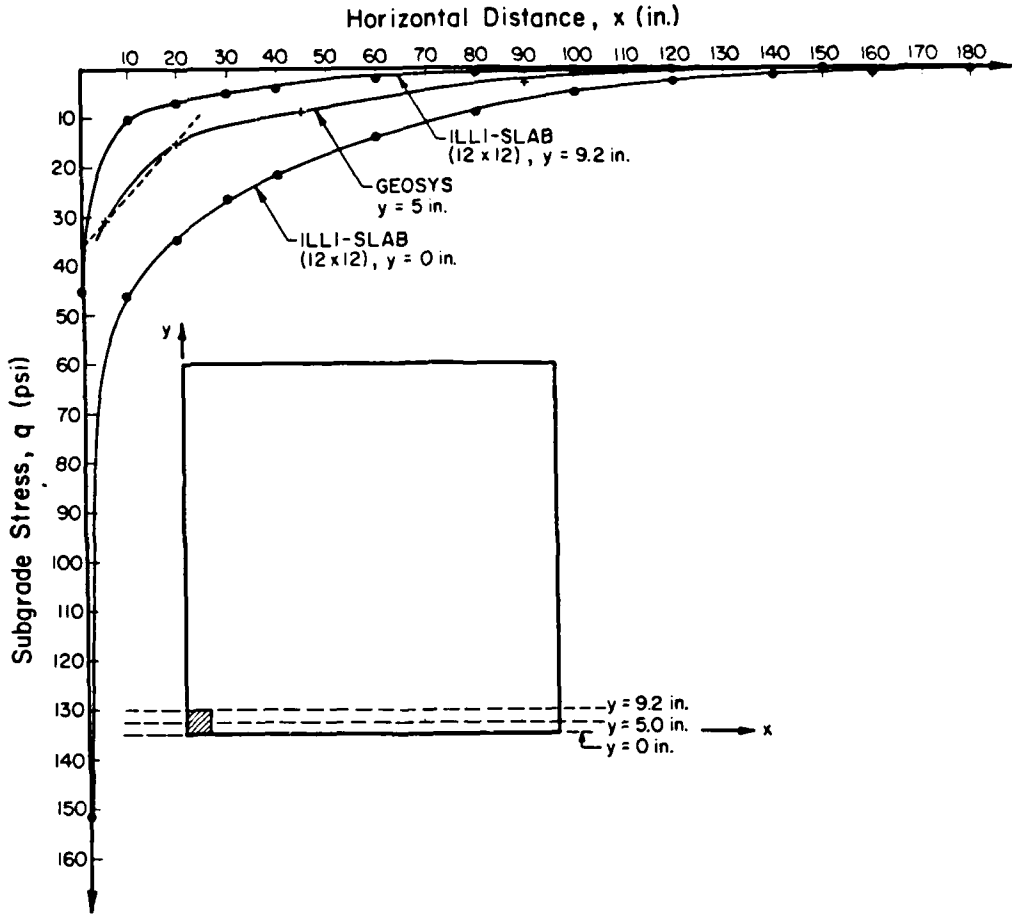

Fig. 5.3 Comparison of GEOSYS and ILLI-SLAB Surface Subgrade Stress Distributions for F-15 Corner SWL, Under Slab

slab edges. Similar observations are also made in Ref. 7 with respect to interior loading, and in the preceding Chapter with reference to the edge loading condition. Pronounced subgrade stress gradients develop very close to the edges of the slab under all three fundamental loading conditions.

CHAPTER 6

SUMMARY AND CONCLUSIONS

6.1 RESEARCH ACCOMPLISHMENTS

Research described in this Report comprises the final stage of a multi-component project, which examined current computerized analysis techniques for slabs-on-grade. Two earlier Reports submitted by the investigators to the U.S. Air Force Office of Scientific Research (AFOSR) [12; 2] have presented progress accomplished in the application of two-dimensional medium-thick plate theory for the slab, and a variety of subgrade models (including the dense liquid [10]; stress dependent resilient [13; 14]; elastic solid [6; 7; 8; 9]; and two-parameter Vlasov [6] foundations).

The main focus of investigations discussed herein has been the application of the three-dimensional finite element program GEOSYS [24] to the solution of the slab-on-grade problem. The program uses an elastic solid foundation. Through an iterative procedure, this has been modified to a stress dependent resilient subgrade. The following two fundamental questions have been addressed:

1. How do three-dimensional analysis results compare with those from two-dimensional programs, such as ILLI-SLAB [6], FIDIES [9], H5IES [8], CFES [7], etc.? A corollary to this is whether three-dimensional finite element analysis is necessary, and

what the implications of its results are on the routine application of two-dimensional models.

2. How important is the effect of introducing the stress dependent resilient subgrade (characterized by E_R, the resilient elastic modulus)? This effect was found earlier to depend on the placement and severity of the applied loads, using the two-dimensional resilient (K_R) subgrade in ILLI-SLAB [14].

Results presented in this Report provide an adequate, if not complete, answer to both questions. The major findings from research conducted are summarized in subsequent sections of this Chapter.

Other factors have also been examined using the GEOSYS program. These include:

a. The extent of slab and subgrade; and

b. Mesh fineness.

Naturally, three-dimensional analysis presents several problems, such as: prolonged execution times (especially when the iterative scheme is used to introduce subgrade stress dependence); the use of relatively coarse meshes; the need for stress extrapolation to determine critical responses; the restriction to a single slab; the difficulty in manipulating a long program code developed elsewhere, etc. Nonetheless, considerable progress has been made in establishing user guidelines for the application of this finite element slab-on-grade model. These are also presented in a precis below.

On a more practical level, a number of useful conclusions have been reached, with immediate bearing on current analysis and design

methodologies, as well as future research directions. One of these conclusions is that persistent problems facing pavement engineers for several decades now, can be solved if the fundamental parameters entering the analysis are isolated and are expressed in a non-dimensional, lumped form. The most important such ratio in the analysis of slabs-on-grade has been identified as (a/ℓ_e), where a is the radius of the applied load (or some other measure of the loaded area), and ℓ_e is the radius of relative stiffness of the slab-foundation system [32; 35]. This simple ratio is the governing parameter in determine the responses of a slab-on-grade under a single, contiguous loaded area. It incorporates the properties of both the pavement slab (E, μ, h), and of the supporting soil (k or E_s, μ_s), as well as the characteristics of the applied load [$a = \sqrt{(P/\pi p)}$].

It is reasonable to seek a similar lumped parameter for cases involving multi-wheel loads, multi-layer pavements and multi-panel systems. Three-dimensional finite element analysis is shown in this Report to be a feasible and viable tool in this direction. Although it is unlikely to become a routine procedure in the near future, results presented herein indicate that it is possible to use a three-dimensional model to account for subgrade stress dependence, soil yielding, etc., as well as to accommodate multi-wheel gears situated anywhere on the pavement surface.

6.2 USER GUIDELINES FOR THREE-DIMENSIONAL FINITE ELEMENT MODELING

Investigations conducted during this study have shown that several important decisions must be made with respect to the design of the finite element mesh used for three-dimensional slab-on-grade analysis. To provide the data-base for establishing some user guidelines for this purpose, 108 GEOSYS runs have been conducted. Despite the tremendous amount of information accumulated from these results, the present study cannot be considered exhaustive. It is merely a substantial effort to provide answers to very complex questions.

For example, the loading assumed for the mesh investigation runs was almost always a point load. This is simple and easy to apply at a node, compared to a uniformly distributed load covering, in general, only part of an element. The latter must be converted into work equivalent nodal load components. The point load, however, conceals a mesh fineness effect related to the size of the loaded area.

The overriding importance of mesh fineness was first identified and quantified by the authors in previous studies, using two-dimensional models [10; 6]. A major conclusion reached was that a more stringent mesh fineness criterion is required under the loaded area, than elsewhere in the finite element mesh [7]. This counterbalances the approximation involved in discretizing applied distributed loads. A corollary of this, which has serious implications with respect to recent efforts to model non-uniform pressure distributions [36; 37], may be stated as follows:

In view of the conversion of external distributed loads into nodal components (which inevitably leads to at least some approximation, especially in the case of partially loaded elements), refinement of the applied pressure distribution, for the purpose of simulating observed deviations from simplistic uniformity, without due consideration and reciprocal improvement of mesh fineness, will be self-defeating, leading only to an illusion of improved accuracy.

Notwithstanding the limited scope of the mesh investigations conducted in this study, a number of useful guidelines have been established. They can assist the user of the three-dimensional GEOSYS model in setting up a reasonable finite element mesh and interpreting results therefrom. These are summarized below:

(a) In extrapolating stresses to obtain the responses at critical locations, linear orthogonal extrapolation may be used, for both bending and subgrade stresses. For axisymmetric stress distributions (e.g. subgrade stresses under interior loading) diagonal linear extrapolation should be used.

(b) In selecting the total depth, Z, of subgrade to be modeled, due consideration must be given to the constant vertical strain depth, z_{cvs}. This is a function of the lateral extent of the subgrade, X, beyond the slab edges. If z_{cvs} is exceeded, it can lead to an overestimate of vertical directions. Typically, the subgrade should extend to a depth of about 10 ℓ_e (on the order of 40 ft).

(c) The lateral extent of the subgrade, X, beyond the slab edges should be between 7 and 10 ℓ_e (or about 25-35 ft).

(d) Roller boundary conditions should be used at both the horizontal and vertical boundaries. For the GEOSYS model used

in this study, this is also the boundary condition for a plane of symmetry.

(e) The slab in GEOSYS should be modeled by two layers, and linear bending stress distribution within its depth may be assumed.

(f) For the purpose of subdividing the subgrade into vertical layers, it is useful to consider the total depth, Z, as consisting of an upper, a middle and a lower portion. The lower portion should start below 0.5 z_{cvs}, and may be divided into one or more layers. The upper portion is typically about 1.0 ℓ_e (or 4 ft) deep, and should consist of layers no thicker than 0.25-0.50 ℓ_e (or 1 to 2 ft). Finally, for the middle portion, which typically comprises the subgrade between 1 and 4 ℓ_e (4-15 ft), two layers are usually enough.

(g) The lateral extent of the subgrade, X, beyond the slab edges should generally be subdivided into two or more elements, in the horizontal direction. For the subgrade adjacent to a loaded edge or corner, more stringent requirements apply. For such cases, the following recommendations may be adhered to:

Zone	Width (ft)	(Width/ℓ_e)	Element Size, 2a (ft)	(2a/h)
Inner	3.0	0.75	1.0	1.0
Transition	6.0	1.75	3.0	3.0
Outer	40.0	10.00	20.0	20.0

(h) With respect to the horizontal slab mesh fineness, a ratio (2a/h) of about 0.8 is required for the three- as well as for the two-dimensional finite element models. Mesh gradation may be used outside the loaded and critical areas, always keeping maximum element aspect ratio below 3.

(i) With respect to the iterative scheme, introduced to account for subgrade stress dependence, maximum responses are good indicators of overall behavior. The average of the values from Iterations 2 and 3 may be used for this purpose.

6.3 CONCLUSIONS REGARDING THE USE OF A THREE-DIMENSIONAL STRESS DEPENDENT FINITE ELEMENT MODEL

In addition to the 108 mesh investigation runs discussed above, several runs have been conducted to examine the behavior of a slab-on-grade system under an interior, edge and corner single-wheel load. For the edge loading condition, a multi-wheel gear was also considered. An iterative scheme was used to model subgrade stress dependence. Thus, observations made in this study may be broadly divided into two groups:

1. Those related to the effect of the transition from a two- to a three-dimensional model; and
2. Those associated with subgrade stress dependence.

The most significant of conclusions reached is, perhaps, that the three-dimensional investigations reinforce the validity and desirability of conventional two-dimensional analysis. In view of the relatively

limited amount of three-dimensional results generated during this investigation, the accuracy of these results was often assessed by reference to the corresponding two-dimensional values. Where these disagreed, probable causes were considered and were usually found to be due to the coarse three-dimensional mesh used in these analyses.

This is not to deny the desirability of three-dimensional analysis as a tool for checking and validating two-dimensional results. It merely suggests that for meaningful utilization of the much more complex and demanding three-dimensional approach, adequate computer resources must be available. The rapid advances of computer technology in general, and the introduction of supercomputers in particular, provide reasons for optimism in this respect. Results from this study will be invaluable when considering the implementation of such a model on the mammoth machines anticipated in the near future. Based on this experience, the following features are considered important in any future application of the three-dimensional slab-on-grade model:

(a) Adequate mesh fineness must be used. This problem may be best addressed with due consideration to both the software (i.e. the program itself), and the hardware (i.e. the machine on which it is implemented) involved.

(b) Simultaneously, CPU and exposures (i.e. real) execution times must be reduced. A typical run on the HARRIS 800-2 computer using a rather coarse mesh, required between 12 and 15 CPU hours. The average exposure time was about 3 days, and the

probability of system breakdown during that time (which necessitated restarting from scratch) was roughly 1 in 4.

(c) Since a tremendous amount of information is generated by each run, a wide range of suitable post-processors is required. These will perform manipulation of the results (e.g. extrapolation, statistical analysis, input data preparation for the next run, etc.), as well as produce graphic displays of the results. Considerable effort was expended in creating the first type of post-processors during this study. Unfortunately, the non-existent graphics capability of the HARRIS 800-2 system used, precluded any attempt at the latter.

(d) This study demonstrated the flexibility of three-dimensional finite element modeling. The possibility of extending the model to include jointed pavements with load transfer devices, as well as multi- layered systems, should be examined further.

From a more practical viewpoint, comparisons between two- and three-dimensional results have led to a number of interesting conclusions with respect to the use of the elastic solid foundation. One of the most important ones is the confirmation of the existence of very high subgrade stress gradients along the edges and at the corners of the slab. These gradients become even steeper when these locations are loaded. This realization provides a probable explanation for the discrepancies between GEOSYS and ILLI-SLAB results, since the extrapolation used in conjunction with the first, fails to reproduce the high stress concentrations that exist at the slab edges and corners.

Furthermore, it suggests that attempting to define a maximum edge and corner subgrade stress (as Westergaard did using the dense liquid foundation [1]) may be futile, and certainly meaningless in terms of a practical design criterion. Finally, it illustrates the ability of the subgrade stress dependent iterative scheme to model local soil yielding, which will undoubtedly occur in reality under these extreme subgrade stresses along the slab edges.

Another interesting observation made is that for corner loading, two-dimensional results (using ILLI-SLAB and FIDIES) suggest that a tensile stress occurs under the center of the load, at the slab bottom fiber. This is usually of the same order as, and may sometimes even exceed, the tensile stress occurring along the slab diagonal at the top fiber. The existence of a tensile stress at the bottom is readily explained by the support provided by the soil beyond the slab edges, a contribution ignored in dense liquid theory. In view of the coarse mesh employed, this phenomenon has not been conclusively established yet using the three-dimensional model.

Turning now to subgrade stress dependence, it must be stated that the investigations conducted have been of very restricted scope. This does not only refer to the coarseness of the mesh used, dictated by limited computer resources. The slab-on-grade systems and loading conditions selected were very limited in number, and were designed to magnify any stress dependence effects. Nonetheless, this study has shown that, at least under some conditions, subgrade stress dependence may be important, primarily when considering heavy edge and corner

loads. The following is a summary of observations made with regard to maximum responses for the cases considered:

		Stress Dependent Response (% of Iter. 1)		
Loading	ℓ_e (in.)	Max. δ	Max. q	Max. σ
F-15 Edge	33.1	110	77	108
C-141 Edge	49.6	131	67	123
F-15 Corner	49.6	118	64	112

These results suggest that subgrade stress dependence affects the maximum subgrade stress to a much greater extent than the other two responses. They also confirm that when the load becomes more severe, as, for example, when it is placed near a corner rather than near an edge, the difference between the first and last iterations becomes much greater. These conclusions are similar to those reached using the two-dimensional K_R model [14]. Although the effect of subgrade stress dependence is sometimes quite pronounced, establishing the desirability of such a model for general use (considering its high cost in terms of execution time) would require additional investigations involving typical pavement and loading systems.

Some other observations have also been made, based on the cases examined during this research. These include:

(a) Only a small fraction of subgrade elements are affected by subgrade stress dependence. This fraction ranges from less than 10 to almost 20%. Overstressed elements generally occur

in the upper 5 to 7 ft of the subgrade (1 to 2 ℓ_e). This observation can be very useful in a future attempt to incorporate stress dependence by lowering a priori the E_s of critical elements and performing only one iteration. Note that the extent of the overstressed region will also depend, of course, on the applied loading (P, p, a, gear configuration).

(b) The behavior of the stress dependent and constant modulus subgrades is generally similar. Stress dependence effects are mostly localized phenomena.

(c) Concerning the contribution of the subgrade beyond the slab edges, introduction of subgrade stress dependence tends, if only slightly, to move the response of the elastic solid foundation toward that of the dense liquid model. The latter seems, therefore, to be closer to real (stress dependent) subgrades, than is often assumed.

6.4 FUTURE RESEARCH DIRECTIONS

6.4.1 Development of a Generalized Mechanistic Design Procedure

The three-dimensional finite element model for the problem of slab-on-grade described in this Report, may be used in several ways in future research, due to its flexibility and general nature. Two such potential areas of research are outlined in the remainder of this Chapter.

Recent investigations at the University of Illinois have confirmed the feasibility of developing a mechanistic design procedure for a

variety of pavement types and aircraft loadings, using results from numerical computerized analyses [30; 31]. The main tools used for this purpose have been the finite element computer programs ILLI-PAVE [21] (for flexible pavements) and ILLI-SLAB [6] (for rigid pavements). Both these programs have been developed at the University of Illinois, and have been extensively used over the last decade.

The development of a mechanistic design procedure for a given aircraft and pavement type consists of two basic steps:

(i) A data-base of structural responses is generated using the appropriate finite element computer code.

(ii) The data are fitted with engineering design algorithms using statistical analyses, which can then be used to predict the response of a given pavement section, without recourse to the finite element computer program itself.

The advantage of this approach is that it makes available to the engineer a set of simple formulae which can be applied using a desk-top calculator. These formulae incorporate the effect of sophisticated procedures to account for such phenomena as subgrade stress dependence, the dynamic nature of fast-moving wheel loads, soil yielding in accordance with the Mohr-Coulomb criterion, etc. To include these effects would otherwise require executing the complex finite element computer programs with relatively high demands on computer resources, and a high probability of misuse. This, in turn, would call for a computer system with large memory, not currently available in design offices or on site. Furthermore, the algorithms can be extrapolated

within reasonable ranges of the independent variables, to cover cases not included in the original data base used to develop the algorithms.

The application of the mechanistic design method described above suffers from two fundamental limitations:

(i) If subgrade stress dependence is to be accounted for using ILLI-PAVE, analyses are necessarily restricted to single-wheel interior loading only. On the other hand, if ILLI-SLAB is used, single- or multi-wheel edge and corner loading conditions may be accommodated, but subgrade stress dependence and soil yielding cannot be considered effectively.

(ii) The algorithms developed up to now have been applicable only to one particular aircraft type. The process must be repeated for each aircraft with different total load, applied pressure and gear configurations.

Further research is required to address these two problems, using tools that have recently become available to engineers. The three-dimensional finite element model presented in this Report can be used to establish a methodology for the development of a mechanistic design procedure applicable to multi-wheel loads placed at the interior, edge or corner of a pavement. This method will be based on a data-base developed from multiple executions of the three-dimensional computer code, that will account for the following effects (in addition to the conventional linear elastic analysis):

(a) Subgrade stress dependence (stress softening for cohesive materials and stress stiffening for granular soils).

(b) Local yielding of the subgrade (Mohr-Coulomb criterion).

(c) The finite size of a pavement system panel.

(d) Multi-wheel gears.

(e) Interior, edge or corner loading conditions.

The procedure described in this Report for rigid pavements (three-dimensional finite element program GEOSYS and associated pre- and post-processors, implemented on the HARRIS 800-2 virtual memory computer) can be modified for this purpose. This program will soon be implemented on the Cray X-MP/24 supercomputer at the University of Illinois. Implementation of the proposed procedure on such a system will enhance its capabilities and ease-of-application tremendously.

Such a study would provide a synthesis of several years of research activities at the University of Illinois involving both rigid and flexible pavements. It will put previously developed mechanistic design procedures in a broader context, expanding their scope of applicability to include more than one aircraft type. The investigation will also quantify the effects of multi-wheel gears placed anywhere on the pavement system surface. At the same time, it will generate a large data-base from three-dimensional finite element analysis, incorporating advanced materials characterization procedures, and will take advantage of major recent breakthroughs in numerical analysis methods and computer technology.

6.4.2 Establishment of a Comprehensive Engineering Procedure for the Analysis and Design of Both Rigid and Flexible Pavements

Current methodologies nearly always treat the pavement system either as "rigid" or as "flexible". A rigid pavement owes the bulk of its strength to its capacity to develop and resist bending stresses through plate or slab action, while a flexible system distributes the applied load through its depth primarily in the form of direct compression or tension. Conceptually, the use of the terms rigid and flexible has often led to the impression that a flexible pavement should respond in the manner prescribed by the layered elastic theory, while a rigid pavement should follow the rules of plate theory. This is reflected in the existence of two distinct design approaches, and more recently in the development of two separate categories of computer programs.

There has been an effort in recent years to remedy this situation, through the development of a comprehensive procedure, that would bridge the gap between rigid and flexible pavements. Unfortunately, more often than not, this extremely ambitious, philosophically sound and practically desirable undertaking has been reduced to the mere elimination of one of the two distinct categories, depending on the personal preferences and expertise of each individual investigator.

The theoretical shortcomings of analyzing both flexible and rigid pavements using layered elastic theory (ordinarily restricted to the former only) have recently been pointed out [35]. Comparisons to date between plate and layered elastic theories, have been restricted, however, to the interior loading condition, within a prescribed range

of (a/ℓ_e) values, using a semi-infinite elastic solid foundation. The feasibility of similar comparisons for the multi-layered foundation can be examined using the three-dimensional finite element model presented herein, as well as currently available programs (e.g. WESLAYER [38], RISC [39]). The possibility of applying a similar approach to multi-wheel loads (e.g. by coupling ILLI-SLAB and a layered elastic model, such as BISAR [40]) can also be investigated. The three-dimensional finite element model described in this Report, would be an indispensable tool in the context of such a study, whose main objectives would be:

(i) Analytical investigation of the similarities and differences of available design tools as applied to flexible and rigid pavements.

(ii) Critical review and theoretical examination of attempts to date to develop a comprehensive procedure.

(iii) Selection and evaluation of current design methodologies and computer codes that could be used in establishing the feasibility, and eventually developing a comprehensive engineering procedure for the analysis and design of both rigid and flexible pavements.

Such a study would contribute significantly in establishing a common approach for rigid and flexible pavements. At the same time, it would point out the theoretical pitfalls to be avoided when developing new design procedures for each of these two broad categories, for as long as such a comprehensive procedure does not exist. In addition, the

following products are envisaged, which will be useful on their own right:

(i) Improvement of analysis techniques for multi-wheel loads (for flexible pavements) and multi-layer systems (for rigid pavements).

(ii) Quantifying the effect of multi-wheel loads (applied load, gear configuration, pressure intensity, etc.).

(iii) Improvement of modeling approaches used for load transfer systems.

APPENDIX

DIRECTORY OF GEOSYS RUNS FOR PRELIMINARY MESH INVESTIGATIONS (Chapter 2)

RUN	GENERAL PURPOSE	DESCRITION
	STRESS EXTRAPOLATION	
1		No Symmetry - 4x4 for Full Slab
2		Symmetry - 2x2 for Quarter-Slab
3		- 3x3
4		- 4x4
5		- 5x5
6		- 6x6
	VERTICAL SUBGRADE EXTENT	
7		5 Vertical ft of Soil
8		10
9		15
10		20
11		25
12		30
13		35
	NUMBER OF SLAB LAYERS	
14		3 Slab Layers
15		4 Slab Layers
	LATERAL SUBGRADE EXTENT	
16		4.0 ft Lateral Extent
17		7.5
18		12.0
	VERTICAL SUBGRADE DIVISION	
19		4 Elements in Lower Layer
20		3
21		2
22		1
23		3 Elements in Upper Layer
24		4
	NUMBER OF SLAB LAYERS	
25		5 Slab Layers
	LATERAL SUBGRADE EXTENT	
26		18 ft Lateral Extent
	VERTICAL SUBGRADE DIVISION	
27		5 Elements in Upper Layer
	NUMBER OF SLAB LAYERS	
28		6 Slab Layers
	LATERAL SUBGRADE EXTENT	
29		24 ft Lateral Extent
	VERTICAL SUBGRADE DIVISION	
30		4 Elements in Lower Layer: Study 2
31		3

AD-A174 987 THREE-DIMENSIONAL FINITE ELEMENT ANALYSIS OF A SLAB ON STRESS DEPENDENT E..(U) ILLINOIS UNIV AT URBANA DEPT OF CIVIL ENGINEERING A M IOANNIDES ET AL. 31 OCT 86 3/3

UNCLASSIFIED AFOSR-TR-86-2108 AFOSR-82-0143 F/G 13/13 NL

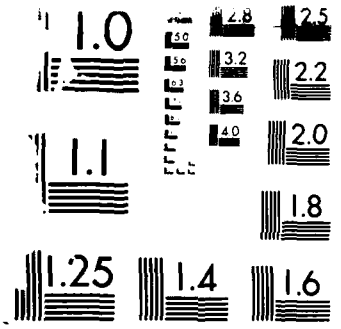
1.0
1.1
1.25
1.4
1.6
1.8
2.0
2.2
2.5
2.8
3.2
3.6
4.0

RUN	GENERAL PURPOSE	DESCRITION
32		2 Elements in Lower Layer: Study 2
33		1
34		4 Elements in Upper Layer: Study 2
35		3
36		1
	LATERAL SUBGRADE EXTENT	
37		30 ft Lateral Extent - 3@10'
	HORIZ. SUBGR. MESH FINENESS	
38		30 ft - 2@15'
39		30 ft - 1@30'
40		30 ft - 0; 26'; 30'
41		35 ft - 0; 30'; 35'
42		Run Missing
	HORIZ. SLAB MESH FINENESS	
43		3x3 Mesh for Quarter-Slab
44		4x4
45		5x5
46		6x6
	POISSON'S RATIO	
47		30 ft Lateral - μ_s = 0.3
48		= 0.1
49		35 ft Vertical - μ_s = 0.3
50		= 0.1
	LATERAL SUBGRADE EXTENT	
51		36 ft Lateral Extent
	VERTICAL SUBGRADE EXTENT	
52		Revised (2@1'; 1@7')
53		(2@1'; 2@7')
54		(2@1'; 3@7')
55		(2@1'; 4@7')
56		(2@1'; 5@7')
	BOUNDARY CONDITIONS	
57		Free at 7.5 ft
58		Free at 30.0 ft
	HORIZ. SLAB MESH FINENESS	
59		14x14 Mesh for Quarter-Slab
60		16x16
	HORIZ. SUBGR. MESH FINENESS	
61		30 ft - 4@7.5'
	VERTICAL SUBGRADE EXTENT	
62		Revised (2@1'; 6@7')
	SLAB MAX. ELEMENT ASPECT RATIO	
63		5x5 Mesh - Max. α = 1.33
64		4x4 Mesh - Max. α = 2.00
65		3x3 Mesh - Max. α = 4.00

RUN	GENERAL PURPOSE	DESCRITION
	EDGE LOADING	
	HORIZ. SLAB MESH FINENESS	
66		4x2 for Half-Slab
67		6x3
68		8x4
69		10x5
	ADJACENT SOIL EXTENT	
70		X_a = 30 ft
71		= 35 ft
72		= 40 ft
73		= 45 ft
74		0 ft Beyond Slab
75		15 ft Beyond Slab
76		X_a = 50 ft
77		= 55 ft
78		22.5 ft Beyond Slab
79		20.0
80		Revised, X_a = 40 ft
81		= 30 ft
82		Revised, 10 ft Beyond Slab
83		Revised, X_a = 50 ft
84		Revised, 30 ft Beyond Slab
	HORIZ. SUBGR. MESH FINENESS	
85		Adjacent - 3@2.5'; 1@42.5'
86		- 3@2.5'; 2@21.25'
87		Beyond - 1@30'
88		- 3@10'
89		Adjacent - 2@2.50'; 2@22.5'
90		- 4@1.25'; 2@22.5'
91		- 5@1.00'; 2@22.5'
92		- 2@3' in Middle Region
93		- 3@2' in Middle Region
	HORIZ. SLAB MESH FINENESS	
94		7x7 Slab Mesh - 1 Point Load
95		7x7 - 4 Work Eqvt Loads
96		6x6
97		5x5
98		4x4
99		3x3
100		8x8
	VERTICAL SUBGRADE EXTENT	
101		Revised, 2@1'; 7@7'
	VERTICAL SUBGRADE DIVISION	
102		2 Elements in Middle Region
103		3

RUN	GENERAL PURPOSE	DESCRITION
104		4
105		1 Element in Middle Region
106		4 Elements in Lower Region
107		3
108		1

REFERENCES

1. Westergaard, H.M., "Stresses in Concrete Pavements Computed by Theoretical Analysis," Public Roads, Vol. 7, No. 2, April, 1926. Also in Highway Research Board, Proceedings, 5th Annual Meeting (1925, published 1926), Part I, under title "Computation of Stresses in Concrete Roads."

2. Ioannides, A.M., "Analysis of Slabs-On-Grade for a Variety of Loading and Support Conditions," Ph.D. Thesis, University of Illinois, Urbana, 1984. Also published by U.S. Air Force Office of Scientific Research, Report No. TR-85-0083, Air Force Systems Command, USAF, Bolling AFB, D.C. 20332, September, 1984.

3. Winkler, E., "Die Lehre von der Elastizitat und Festigkeit," (The Theory of Elasticity and Stiffness), H. Dominicus, Prague, 1867.

4. Boussinesq, M.J., "Application des Potentiels a l'etude de l'equilibre et du mouvement des solides elastiques, principalement au calcul des deformations et des pressions que produisent, dans ces solides, des efforts quelconques exerces sur une petite partie de leur surface ou de leur interieur: Memoire suivi de notes etendues sur divers points de physique mathematique et d'analyse," (Application of Potential to the Study of the Equilibrium and Movement of Elastic Solids, Particularly the Calculation of Deformations and Stresses Produced within Such Solids, by Some Load Applied upon a Small Portion of Their Surface or Their Interior: Continuous Paper from Extensive Notes on Diverse Points of Physical Mathematics and Analysis), Gauthier-Villars, Paris, 1885.

5. Vlasov, V.Z., and Leont'ev, N.N., "Beams, Plates and Shells on Elastic Foundations," translated from the Russian (date of original: 1960), NASA-NSF, NASA TT F-357, TT 65-50135, Israel Program for Scientific Translations, 1966.

6. Ioannides, A.M., Thompson, M.R., and Barenberg, E.J., "Finite Element Analysis of Slabs-On-Grade Using a Variety of Support Models," Proceedings, Third International Conference on Concrete Pavement Design and Rehabilitation, Purdue University, April, 1985.

7. Ioannides, A.M., "Axisymmetric Slabs of Finite Extent on Elastic Solid," submitted for publication, Transportation Engineering Journal, ASCE, March, 1986.

8. Ioannides, A.M., "Chart for Edge Stress in Plate on Elastic Solid," submitted for presentation and publication, 67th Annual Meeting of the Transportation Research Board, Washington, D.C., January, 1988.

9. Ioannides, A.M., "Finite Difference Solution for Plate on Elastic Solid," submitted for publication, Transportation Engineering Journal, ASCE, October, 1986.

10. Ioannides, A.M., Thompson, M.R., and Barenberg, E.J., "Westergaard Solutions Reconsidered," Transportation Research Record 1043, Transportation Research Board, National Research Council, Washington, D.C., 1985.

11. Westergaard, H.M., "New Formulas for Stresses in Concrete Pavements of Airfields," ASCE, Transactions, Vol. 113, 1948. Also in ASCE Proceedings, Vol. 73, No. 5, May, 1947.

12. Thompson, M.R., Ioannides, A.M., Barenberg, E.J., and Fischer, J.A., "Development of a Stress Dependent Finite Element Slab Model," U.S. Air Force Office of Scientific Research, Report No. TR-83-1061, Air Force Systems Command, USAF, Bolling AFB, D.C. 20332, May, 1983.

13. Fischer, J.A., Thompson, M.R., Ioannides, A.M., and Barenberg, E.J., "K_R - The Resilient Modulus of Subgrade Reaction," Transportation Research Record 954, Transportation Research Board, National Research Council, Washington, D.C., 1984.

14. Ioannides, A.M., Barenberg, E.J., and Thompson, M.R., "Finite Element Model with Stress Dependent Support," Transportation Research Record 954, Transportation Research Board, National Research Council, Washington, D.C., 1984.

15. Tabatabaie-Raissi, A.M., "Structural Analysis of Concrete Pavement Joints," Ph.D. Thesis, University of Illinois, Urbana, 1977.

16. Timoshenko, S., and Woinowsky-Krieger, S., "Theory of Plates and Shells," Second Edition, McGraw-Hill, 1959.

17. Zienkiewicz, O.C., "The Finite Element Method," Third Edition, McGraw-Hill, 1977.

18. Dawe, D.J., "A Finite Element Approach to Plate Vibration Problems," Journal of Mechanical Engineering Science, Vol. 7, No. 1, 1965.

19. Tabatabaie, A.M., Barenberg, E.J., and Smith, R.E., "Longitudinal Joint Systems in Slip-Formed Rigid Pavements, Volume II--

Analysis of Load Transfer Systems for Concrete Pavements," U.S. Department of Transportation, Report No. FAA-RD-79-4, II, November, 1979.

20. Tabatabaie, A.M., and Barenberg, E.J., "Structural Analysis of Concrete Pavement Systems," Transportation Engineering Journal, ASCE, Vol. 106, No. TE5, September, 1980.

21. Raad, L. and Figueroa, J.L., "Load Response of Transportation Support Systems," Transportation Engineering Journal, ASCE, Vol. 106, No. TE1, January, 1980.

22. Thompson, M.R. and Robnett, Q.L., "Resilient Properties of Subgrade Soils," Transportation Engineering Journal, ASCE, Vol. 105, No. TE1, January, 1979.

23. Lopez, L.A., "FINITE: An Approach to Structural Mechanics Systems," International Journal for Numerical Methods in Engineering, Vol. 11, 1977.

24. Agbabian Associates, "Analytic Modeling of Rock-Structure Interaction," Volumes 1-3, prepared for Advanced Research Projects Agency of U.S. Department of Defense, and U.S. Bureau of Mines, Report No. AD-761-648, 649, 650, 1973.

25. Cook, R.D., "Concepts and Applications of Finite Element Analysis," Second Edition, John Wiley and Sons, 1981.

26. Losberg, A., "Structurally Reinforced Concrete Pavements," Doktorsavhandlingar Vid Chalmers Tekniska Hogskola, Goteborg, Sweden, 1960.

27. Michelow, J., "Analysis of Stresses and Displacements in an N-Layered Elastic System under a Load Uniformly Distributed on a Circular Area," California Research Corporation, Richmond, CA, 1963.

28. Carrier, W.D. and Christian, J.T., "Rigid Circular Plate Resting on a Non-Homogenous Elastic Half-Space," Geotechnique, Vol. 23, No. 1, 1973.

29. Hoffman, M.S. and Thompson, M.R., "Nondestructive Testing of Flexible Pavements-Field Testing Program Summary," Civil Engineering Studies, Transportation Engineering Series No. 31, Illinois Cooperative Highway and Transportation Research Program Series No. 188, University of Illinois at Urbana-Champaign, June, 1981.

30. Costigan, R.R., and Thompson, M.R., "Response and Performance of Alternate Launch and Recovery Surfaces (ALRS) Containing

Stabilized-Material Layers," presented at the 65th Annual Meeting of the Transportation Research Board, Washington, D.C., January, 1986.

31. Kelly, IV, H.F., "Development of Mechanistic Flexible Pavement Design Concepts for the Heavyweight F-15 Aircraft," Ph.D. Thesis, University of Illinois, Urbana, 1986.

32. Ioannides, A.M., Discussion of "Response and Performance of Alternate Launch and Recovery Surfaces (ALRS) Containing Stabilized-Material Layers," by R.R. Costigan and M.R. Thompson, submitted for publication, Transportation Research Board, February, 1986.

33. Hoffman, M.S. and Thompson, M.R., "Mechanistic Interpretation of Nondestructive Pavement Testing Deflections," Civil Engineering Studies, Transportation Engineering Series No. 32, Illinois Cooperative Highway and Transportation Research Program Series No. 190, University of Illinois at Urbana-Champaign, June, 1981.

34. Ioannides, A.M., "Recent Findings Using Advanced Analysis Methods for Slabs-On-Grade," Informal Presentation, Committee on Rigid Pavements (A2B02), 65th Annual Meeting of the Transportation Research Board, Washington, D.C., January, 1986.

35. Ioannides, A.M., Discussion of "Rigid Bottom Considerations for Nondestructive Evaluation of Pavements," by W. Uddin, A.H. Meyer, and W.R. Hudson, submitted for publication, Transportation Research Board, February, 1986.

36. Marshek, K.M., Chen, H.H., Connell, R.B., and Saraf, C.L., "The Effect of Truck Tire Inflation Pressure and Axle Load on Flexible and Rigid Pavement Performance," presented at the 65th Annual Meeting of the Transportation Research Board, Washington, D.C., January, 1986.

37. Chen, H.H., Marshek, K.M., and Saraf, C.L., "The Effects of Truck Tire Contact Pressure Distribution on the Design of Flexible Pavements -- A 3D Finite Element Approach," presented at the 65th Annual Meeting of the Transportation Research Board, Washington, D.C., January, 1986.

38. Chou, Y.T., "Structural Analysis Computer Programs for Rigid Multicomponent Pavement Structures with Discontinuities-WESLIQID and WESLAYER; Report 1: Program Development and Numerical Presentations; Report 2: Manual for the WESLIQID Finite Element Program; Report 3: Manual for the WESLAYER Finite Element Program," Technical Report GL-81-6, U.S. Army Engineer Waterways Experiment Station, May, 1981.

39. Majidzadeh, K., Ilves, G.J., and Sklyut, H., "RISC - A Mechanistic Method of Rigid Pavement Design," Proceedings, Third International Conference on Concrete Pavement Design and Rehabilitation, Purdue University, April, 1985.

40. SHELL OIL Co., "BISAR: Bitumen Structures Analysis in Roads, User's Manual," Koninklijke/Shell - Laboratorium, Shell Research N.V., Amsterdam, 1978.

END

1-87

DTIC